



Politecnico di Torino

Department of Environment, Land and Infrastructure Engineering (DIATI)

Master's Degree in Environmental and Land Engineering

Flexible Climate Adaptation with Nature-Based Solutions

Applying the DAPP Approach in the Sømose Å Catchment

Supervisors: Candidate:

Prof. Francesco Laio

Prof. Peter Steen Mikkelsen

Co-supervisors:

Steffen Davidsen Rick Pieter Kool Pierluigi De Carlo

Abstract

As climate change increases the frequency and severity of extreme rainfall events, urban areas face growing challenges related to surface flooding. This thesis investigates whether Nature-Based Solutions (NBS) offer a flexible approach to addressing urban flooding under climate-related uncertainty, and how the Dynamic Adaptive Policy Pathways (DAPP) framework can support their effective implementation.

The study focuses on the Sømose Å catchment near Copenhagen, Denmark—an urbanizing area with limited infiltration capacity and heightened flood risk due to the presence of a stream (Sømose Å) crossing densely built environments. Using RCP-based climate projections, the Curve Number method, and geospatial tools such as SCALGO Live and QGIS, the analysis evaluates the potential of four NBS (green roofs, porous asphalt, bioswales, and rain gardens) to reduce flood impacts over time. The DAPP approach is applied to identify tipping points, explore adaptation pathways, and design flexible strategies that remain robust across uncertain future scenarios.

The results show that NBS can provide adaptable and effective flood mitigation in the context of climate uncertainty, particularly when integrated into a DAPP-informed planning process. This combined approach supports resilient, long-term decision-making and contributes to the Harrestrup Å Capacity Plan through tailored recommendations for the Sømose Å subcatchment.

Preface

This thesis represents the final project of my Master's degree in Environmental Engineering, with a specialization in Climate Change. It has been carried out as part of an Erasmus+ program in collaboration between my home university, Polytechnic of Turin, and the Technical University of Denmark (DTU). The project corresponds to 30 ECTS credits and is due on 10 July 2025. The work has been developed at DTU in collaboration with the consultancy company NIRAS, an international multidisciplinary engineering firm based in Denmark.

Acknowledgements

I would like to express my deepest gratitude to my main supervisor, Peter Steen Mikkelsen, for his continuous support, valuable guidance, and encouragement throughout this project. His expertise and patience have been fundamental for the successful completion of this thesis. A big acknowledgement also goes to my co-supervisors: Steffen Davidsen from NIRAS, who provided essential help with the modelling, consultancy, various practical matters, and showed great patience during the process; and Rick Kool, an expert in the DAPP approach, whose insights and advice greatly enriched this work. I would also like to thank Prof. Francesco Laio of Politecnico di Torino, my supervisor at my home university, for his constant support, valuable feedback, and guidance throughout the project.

I thank my friends at DTU, especially Paolo and Alessandra, whose presence and support were incredibly important during difficult moments. A special thank you to Leonard, whose support and valuable advice were fundamental. Sharing a similar path made me feel less alone and more confident in facing the challenges of this thesis.

I also want to express my heartfelt thanks to my flatmates in Copenhagen — in particular Riccardo, for his daily cheerfulness and unwavering support. It is difficult to find the right words to express my gratitude to you. I also thank Solèn for her precious words of support and encouragement, and Franca, whose expertise in the field was extremely helpful throughout the development of this thesis.

To my family, thank you for always being there and for never letting me feel alone. Your curiosity, enthusiasm, and the way you engaged with what I was doing have always motivated me to keep going. A special thanks to Francesco, whose ability to support and lighten my mood in difficult times was of great help.

I am grateful to all my friends at Politecnico — especially Giulio, Francesca, Elena, Camilla, Arianna, Francesca, and Giovanni — for being there, trying to understand my difficulties, helping me, and making sure I never felt alone. I know I can always count on you, regardless of the distance.

To my friends from my hometown, Copertino — especially Andrea, whose constant presence, companionship, and interest have always made me feel appreciated and supported. A special thanks to Simona, the two Federicos, Alessandro, Sofia, and Serena: your closeness, a phone call, or a simple message has always made me feel connected and close to you, even from afar.

In my bachelor's thesis, I concluded by stating that determination and perseverance always pay off. With this master's thesis, I can add that the courage to step out of one's comfort zone, especially in a context like this, leads to greater rewards and enrichment from multiple perspectives, both academically and, above all, personally.

Italian version follows

Vorrei esprimere la mia più profonda gratitudine al mio relatore principale, Peter Steen Mikkelsen, per il suo continuo supporto, preziosa guida e incoraggiamento durante tutto il progetto. La sua esperienza e pazienza sono state fondamentali per il successo di questa tesi.

Un grande ringraziamento va anche ai miei co-relatori: Steffen Davidsen di NIRAS, che ha fornito un aiuto essenziale con la modellazione, la consulenza e varie questioni pratiche, dimostrando grande pazienza durante il processo; e Rick Kool, esperto nell'approccio DAPP, i cui suggerimenti e consigli hanno arricchito molto questo lavoro.

Vorrei inoltre ringraziare il Prof. Francesco Laio del Politecnico di Torino, mio relatore presso l'università di origine, per il suo costante supporto, i preziosi feedback e la guida fornita durante tutto il progetto.

Ringrazio i miei amici della DTU, in particolare Paolo e Alessandra, la cui presenza e il cui supporto sono stati incredibilmente importanti nei momenti difficili. Un ringraziamento speciale a Leonard, il cui supporto e i suoi preziosi pareri sono stati fondamentali. Condividere un percorso simile mi ha fatto sentire meno solo e più sicuro nell'affrontare le sfide di questa tesi.

Desidero inoltre esprimere un sentito ringraziamento ai miei coinquilini di Copenaghen — in particolare Riccardo, per la sua allegria quotidiana e il suo supporto costante. È difficile trovare le parole giuste per esprimere la mia gratitudine nei tuoi confronti.Ringrazio Solèn per le preziose parole di sostegno e incoraggiamento, e Franca, la cui esperienza nel campo è stata di grande aiuto durante lo sviluppo di questa tesi.

Alla mia famiglia, grazie per esserci sempre stati e per non avermi mai fatto sentire solo. La vostra curiosità, entusiasmo e il modo in cui vi siete appassionati a ciò che facevo mi hanno sempre spronato. Un ringraziamento speciale a Francesco, la cui capacità di sostenermi e alleggerirmi nei momenti più difficili mi è stata di grande aiuto.

Sono grato a tutti i miei amici del Politecnico — in particolare Giulio, Francesca, Elena, Camilla, Arianna, Francesca e Giovanni — per esserci stati, cercando di capire le mie difficoltà, aiutandomi e facendo in modo che non mi sentissi mai solo. So di poter sempre contare su di voi, indipendentemente dalla distanza.

Ai miei amici della mia città natale, Copertino, in particolare Andrea, la cui presenza costante, compagnia e interesse mi hanno sempre fatto sentire apprezzato e supportato. Un ringraziamento speciale va a Simona, a Federico, ad Alessandro, Federico, Serena e Sofia: la vostra vicinanza, una telefonata o un semplice messaggio mi hanno sempre fatto sentire connesso.

Nella mia tesi triennale concludevo affermando che la determinazione e la perseveranza ripagano sempre. Con questa tesi magistrale posso aggiungere che il coraggio di uscire dalla propria zona di comfort, soprattutto in un contesto come questo, porta a una ricompensa maggiore, un arricchimento sotto diversi punti di vista, sia accademico che, soprattutto, personale.

Contents

1	Intr	oduction		1
	1.1	Climate	Change:Impacts and Attribution	1
	1.2	Climate	Change Mitigation and Adaptation	3
		1.2.1	Nature Based Solutions (NBS)	3
	1.3	Goal of	the thesis	4
2	Tool	s		5
	2.1	SCALG	O Live	5
	2.2	QGIS		5
3	Sou	rces		6
	3.1	Data .		6
	3.2	Literatu	re	6
4	The	ory		7
	4.1	The Dy	namic Adaptive Policy Pathways (DAPP) Approach	7
	4.2	Climate	scenarios	11
	4.3	Nature 1	Based Solutions (NBS)	13
		4.3.1	Definition	13
		4.3.2	Challenges addressed	13
		4.3.3	Cost	16
		4.3.4	NBS in Denmark	17
		4.3.5	Directives	18
	4.4	Curve N	Number Method	18
5	Bacl	kground	and Analysis	21
	5.1	The cate	chment area	21
		5.1.1	Land cover	25
		5.1.2	Soil, Groundwater, and Contamination Conditions	26
		5.1.3	Vulnerabilities	28
			Extreme flood map	28
			Elevated groundwater levels	30
		5.1.4	Uncertainties	32
	5.2	Harrestr	rup Å - Capacity Plan	33
		5.2.1	Subproject-Sømose Å	35
			Delineation of the context	35
			Into the project:hydraulic aspects	36
			Current Urban Water System	39
	5 3	Natura 1	Rased Solutions (NRS) selected	30

		5.3.1	Permeable Pavements	40
		5.3.2	Bioswale	41
		5.3.3	Rain garden	43
		5.3.4	Green roofs	44
		5.3.5	Summary of the NBS selected	46
6	Met	hodolog	y	48
	6.1	Catchn	ment Climate Scenarios	48
			5 year event	48
		6.1.1	Tipping point	53
	6.2	Applic	eation areas	54
	6.3	Curve	Number Method for NBS	59
	6.4	Investi	gated outcome	65
7	Resu	ults		66
	7.1	RCP 2	.6	66
	7.2	RCP 4	.5	67
		7.2.1	Adaptation Pathway	68
	7.3	RCP 8	.5	70
		7.3.1	Adaptation Pathway	72
	7.4	Water	balance	73
		7.4.1	Before NBS	74
		7.4.2	After NBS	74
8	Disc	cussion		76
	8.1	Unkno	own Scenario	76
	8.2	Cost .		77
	8.3	Trigge	r point	77
	8.4	Floodi	ng Contribution Analysis	83
		8.4.1	SCALGO Live Artificial Categories	83
		8.4.2	Influence of the areas selected on the Tipping point	84
	8.5	Limita	tions	84
		8.5.1	Monitoring Phase	84
		8.5.2	Uncertainties and Vulnerabilities	84
		8.5.3	SCALGO Live	85
		8.5.4	Curve Number for NBS	85
		8.5.5	Spatial extent of NBS application	85
		8.5.6	Data on NBS	86
9	Con	clusion		87
A	Bacl	kground	d and Analysis	89
	A.1	Harres	trup Å - Capacity Plan	89
		A.1.1	Solutions	89

	Green floodplains	89
	Cloudburst pools	90
	Widening the river	90
	Removing bottlenecks	91
	Centralised risk based management of reservoirs and pumps	91
A.1.2	Subproject-Sømose Å	94
	Lowland restoration and biodiversity	94

1 Introduction

1.1 Climate Change:Impacts and Attribution

Nowadays, the world is experiencing numerous extreme climate events, such as glacier melting, floods, droughts, and cyclones. We are living in a period of continuous and extreme changes that make life increasingly difficult. Millions of people are losing their families and homes, making it crucial to find mitigation and adaptation solutions in this rapidly changing context.

On 2nd July 2011, Copenhagen, the capital of Denmark, experienced the most destructive cloudburst in its history. The event had return period of 100 years and, in the worst affected areas, up to 200 mm of rain was recorded in just two hours. Within the first 30 minutes, several critical infrastructures began to flood and the water level rose dangerously close to the point where evacuation was necessary. The total damage was estimated at around EUR 1.6 billion, making it the most expensive natural disaster of that year [1].



Figure 1.1: Cloudburst in Copenhagen in 2011 [1]

This event left an unforgettable mark on the city, pushing it to act against future water challenges. As a result, Copenhagen has become a global leader in urban water management through the implementation of a cloudburst management plan [1]. On the other hand, in recent years, many countries have faced long periods of drought. A significant example is the city of Turin, traditionally known as the "rainy city", which experienced a 110-day drought in 2022. As a result, a state of emergency was declared in June 2022, with various restrictions on water use, including a ban on irrigation and outdoor watering, car washing and filling swimming pools and fountains [2]. The effects are clearly visible in the Po (Figure 1.2), the main river that flows through Turin. In fact, the drought of 2022 was by far the worst in the last two centuries, with the average river flow 30 % lower than the second worst. Statistically, this is an event that occurs only once every 600 years [3].



Figure 1.2: Po drought in 2022 [3]

The Intergovernmental Panel on Climate Change (IPCC) defines an extreme weather event as 'a rare event at a specific location and time of year', and an extreme climate event as 'a pattern of extreme weather events that persists over a certain period of time, such as a season' [4].

Extreme events are becoming increasingly frequent around the world and, according to the IPCC, this trend is largely due to anthropogenic climate change. Focusing on precipitation, which is the primary aspect analyzed in this study as explained in Section 6.1, global temperatures rise due to increased greenhouse gas concentrations, increasing the atmosphere's capacity to hold moisture and intensifying the hydrological cycle. This leads to more frequent and intense precipitation events [5].

As illustrated in Figure 1.3, the IPCC's Sixth Assessment Report (AR6) - Synthesis Report: Climate Change 2023 - reveals that the observed increases in heat waves, intense precipitation, droughts and tropical cyclones can now be attributed to human influence with a high level of confidence [6]. This conclusion comes from the previous report (AR5), which already identified greenhouse gas (GHG) emissions, mainly produced by human activities, as the main cause of the increase in heat extremes and the decrease in cold extremes.

	Observed	Attributed	Projected at GWL (°C)			
Change in Indicator	(since 1950)	(since 1950)	+1.5			
Warm/hot extremes: Frequency or intensity	↑	✓ Main driver	↑	↑	1	
Cold extremes: Frequency or intensity	V	✓ Main driver	V	V	Ψ.	
Heavy precipitation events: Frequency, intensity and/or amount	Over majority of land regions with good observational coverage	Main driver of the observed intensification of heavy precipitation in land regions	↑ in most lad	↑ nd regions	↑ in most land regions	
Agricultural and ecological droughts: Intensity and/or frequency	† in some regions	in some regions	in more regions compared to observed changes	in more regions compared to 1.5°C of global warming	in more regions compared to 2°C of global warming	
Precipitation associated with tropical cyclones	↑	1	↑ Rate +11%	↑ Rate +14%	↑ Rate +28%	
Tropical cyclones: Proportion of intense cyclones	↑	√	+10%	↑ +13%	+20%	
Compound events: Co-occurrent heatwaves and droughts	↑ (Frequency)	✓ (Frequency)	(Frequency and intensity increases with warming)			
Marine heatwaves: Intensity & frequency	↑ (since 1900)	✓ (since 2006)	Strongest in tropical and Arctic Ocean		cean	
Extreme sea levels: Frequency	(since 1960)	1	(Scenari	o-based assessment for 21st	century)	

Figure 1.3: Summary table presenting observed changes in extreme weather events since 1950 (unless otherwise noted), their attribution to human influence, and projections for future changes under 1.5°C, 2°C, and 4°C global warming scenarios, analyzed at both global and continental levels [6]

1.2 Climate Change Mitigation and Adaptation

Globally, two fundamental concepts have emerged to address the challenges derived from climate change: climate change adaptation and climate change mitigation.

The European Environment Agency defines Adaptation as "anticipating the adverse effects of climate change and taking appropriate action to prevent or minimize the damage they can cause, or taking advantage of opportunities that may arise." Adaptation measures include large-scale infrastructure interventions, such as building defenses against sea level rise, but also behavioral changes, such as reducing personal exposure to high temperatures and caring for vulnerable family members or neighbors during heat waves. In essence, adaptation is about preparing for and adjusting to the current and future effects of climate change [7].

Mitigation, on the other hand, is defined as "making the impacts of climate change less severe by preventing or reducing the emission of greenhouse gases (GHG) into the atmosphere." This can be achieved by reducing emissions-for example, by increasing the use of renewable energy or creating a cleaner mobility system-or by enhancing natural absorbers of greenhouse gases, such as forest extension. In short, mitigation is about human interventions to reduce sources of GHG emissions and/or increase their removal from the atmosphere [7].

1.2.1 Nature Based Solutions (NBS)

In the context of climate change adaptation, the increase in the frequency and intensity of rainfall events presents an opportunity to rethink urban development strategies. Nature-Based Solutions (NBS) are effective in this context, as they contribute to creating greener and more pleasant urban environments. NBS are measures that tackle urban environmental challenges by integrating natural elements into planning and design strategies.

Importantly, NBS contribute to both climate change mitigation and adaptation. On one hand, they support adaptation by addressing key urban challenges such as flooding, water scarcity, and the urban heat island effect. On the other hand, they also contribute to mitigation by promoting carbon sequestration and reducing energy demand, for instance through urban greening and increased vegetation cover.

These solutions also offer a wide range of co-benefits, including increased property values, enhanced biodiversity, and new recreational opportunities for residents. In this sense, NBS make a significant contribution to the creation of more liveable and resilient cities [8]. Furthermore, NBS is in line with the International Water Association's Principles for Water Wise Cities, which focuses Water Sensitive Urban Design, that not only reduces the risk of flooding, but also improves urban livability through the integration of visible water into the urban landscape [8].

At the same time, many cities are facing a rapid process of urbanization, in which green areas are often replaced by artificial surfaces, such as buildings and asphalt roads. This reduces the natural capacity of the soil to absorb water, increasing the risk of flooding. It is therefore necessary to adopt alternative solutions that can adapt to this accelerated population growth. NBS, such as green roofs - vegetated roofs - are an effective response: they mitigate heat island effect, store water addressing water scarcity, and in the same time delay and reduce rainwater runoff.

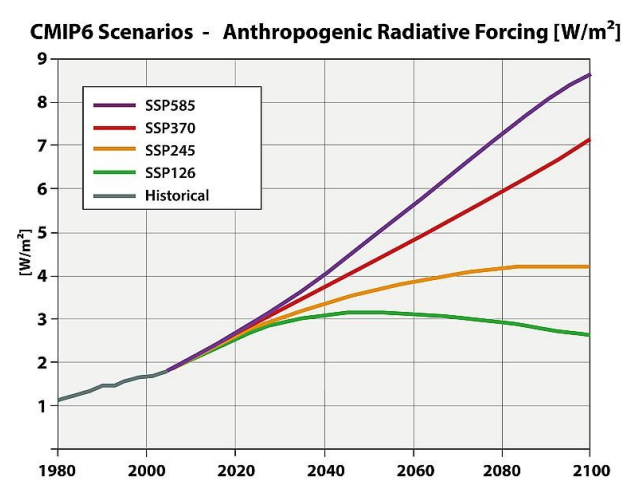


Figure 1.4: CMIP6 projections of Anthropogenic Radiative Forcing (in W/m²) from 1980 to 2100 under different Shared Socioeconomic Pathways (SSPs): SSP585 (high emissions), SSP370 (medium-high), SSP245 (medium), and SSP126 (low emissions), along with historical data [9].

In the process of developing future urban planning strategies, such as including NBS, one of the main challenges is related to uncertainty. that could be related to climate change but also to evolving regulations. For this reason, it is crucial to design flexible solutions that ensure resilience over time.

In this context, the Dynamic Adaptive Policy Pathways (DAPP) approach offers a flexible framework to support decision-making in evolving and uncertain scenarios.

1.3 Goal of the thesis

This thesis aims to understand whether Nature-Based Solutions (NBS) can offer flexible responses to climate-related water challenges—specifically, surface flooding—and how the Dynamic Adaptive Policy Pathways (DAPP) approach can support their implementation under future uncertainty related to climate change. The study focuses on a catchment area in Denmark, where flood risk is driven by increasing urbanization, limited infiltration capacity, and the presence of the Sømose Å stream, which crosses the area and contributes to flooding in the municipalities of Herlev and Ballerup. By combining hydrological modeling, climate projections, and adaptive planning, the thesis investigates how NBS can be effectively integrated into long-term flood management strategies.

2 Tools

2.1 SCALGO Live

In this study, SCALGO Live is used as a practical tool to explore both current and future conditions of the area. It provides valuable insights into flooding, groundwater levels, land cover, and lithology. The platform also supports scenario modeling by allowing modifications of input parameters—such as rainfall—and setting output conditions like water depth thresholds to better visualize the extent and severity of flooding.

Although a more detailed hydrodynamic analysis was initially planned using MIKE+—a modeling tool designed for simulating complex water systems such as drainage networks, urban flooding, and surface—subsurface interactions—time constraints led to relying exclusively on SCALGO Live for this study. Nevertheless, SCALGO proved to be an effective tool for preliminary assessment and scenario exploration.

SCALGO Live was also employed to simulate the implementation of Nature-Based Solutions (NBS) by adjusting the Curve Number (CN) to reflect increased infiltration capacity. This was done through the "Infiltration and Drainage" mode in the "Flash Flood Mapping" section, applied specifically to the flooded areas.

The catchment area was defined in the workspace by uploading a dedicated shapefile. This allowed the platform to isolate and analyze the selected area in more detail—such as visualizing land cover and flood-prone zones—and to simulate how infiltration improvements affect water distribution across the catchment.

These differences are determined by parameters such as the Curve Number (CN), which estimates the potential for surface runoff based on land use, soil type, and moisture conditions. This concept will be explained in the next section.

2.2 QGIS

QGIS (Quantum Geographic Information System) is a free and open-source software used for geographic information system (GIS) tasks. It allows users to create, edit, visualize, analyze, and publish spatial data, supporting a wide range of formats and tools for effective geospatial analysis.

In particular, for the development of this thesis, it provides significant support in obtaining land cover information of the catchment area and offers important insights into the flooding situation of the catchment, once the related raster files from SCALGO Live and the shapefile of the catchment area are imported.

3 Sources

3.1 Data

In order to achieve a better delineation of the catchment—including its background and related ongoing projects—NIRAS, a multidisciplinary engineering and consultancy firm, provided support by supplying reports, technical files (such as shapefiles), and other relevant data.

3.2 Literature

The literature review was conducted through systematic searches in scientific databases such as Google Scholar. Keywords, for example Nature-Based Solutions (NBS), Curve Number (CN), DAPP approach, Representative Concentration Pathways (RCP), and flood risk assessment, were used to guide the search and identify relevant literature.

The search focused on recent peer-reviewed articles, technical reports, and official guidelines relevant to the research objectives. Selection criteria included relevance, publication date, and source credibility. Additionally, references within key papers were examined to uncover further pertinent studies.

4 Theory

4.1 The Dynamic Adaptive Policy Pathways (DAPP) Approach

To achieve these goals mentioned in the section 1.3, significant support is provided from the Dynamic Adaptive Policy Pathways (DAPP) approach. In the DAPP approach, a plan is conceptualized as a sequence of actions over time (pathways), including initial measures and long-term options. The core idea is proactive planning for flexible adaptation over time, responding to how the future actually unfolds. The approach is based on the premise that policies and decisions have a limited lifespan and may fail when operating conditions change. When actions fail, additional or alternative measures are needed to ensure that the original objectives are still achieved, leading to the emergence of multiple potential pathways. Depending on how the future develops, the course can be adjusted when predetermined conditions occur, ensuring that objectives remain attainable. Central to this approach is the concept of Adaptation Tipping Points (ATP), which identify critical thresholds where a system may experience a rapid and irreversible shift. The recognition of these tipping points helps to define when adjustments to the plan are necessary, guiding the process of adapting policies and actions in real-time to avoid crossing these thresholds and ensure the continued success of the original goals [10].

The preference for specific pathways varies among stakeholders and depends on trade-offs, such as costs (including negative externalities) and benefits associated with different options. Based on an evaluation of the various possible pathways, an adaptive plan can be developed, integrating both initial actions and long-term options. The plan is continuously monitored for signals indicating when the next step in a pathway should be implemented or if a comprehensive reassessment is necessary.

A (policy) pathway consists of a sequence of policy actions, where a new action is triggered when the previous one is no longer able to achieve the specified objectives. Pathways may focus on adapting to changing conditions (adaptation pathways), enabling socio-economic developments (development pathways), or transitioning toward a desired future (transition pathways).

Figure 4.1 illustrates the DAPP approach, including its phases, which are explained in more detail in the following sections.

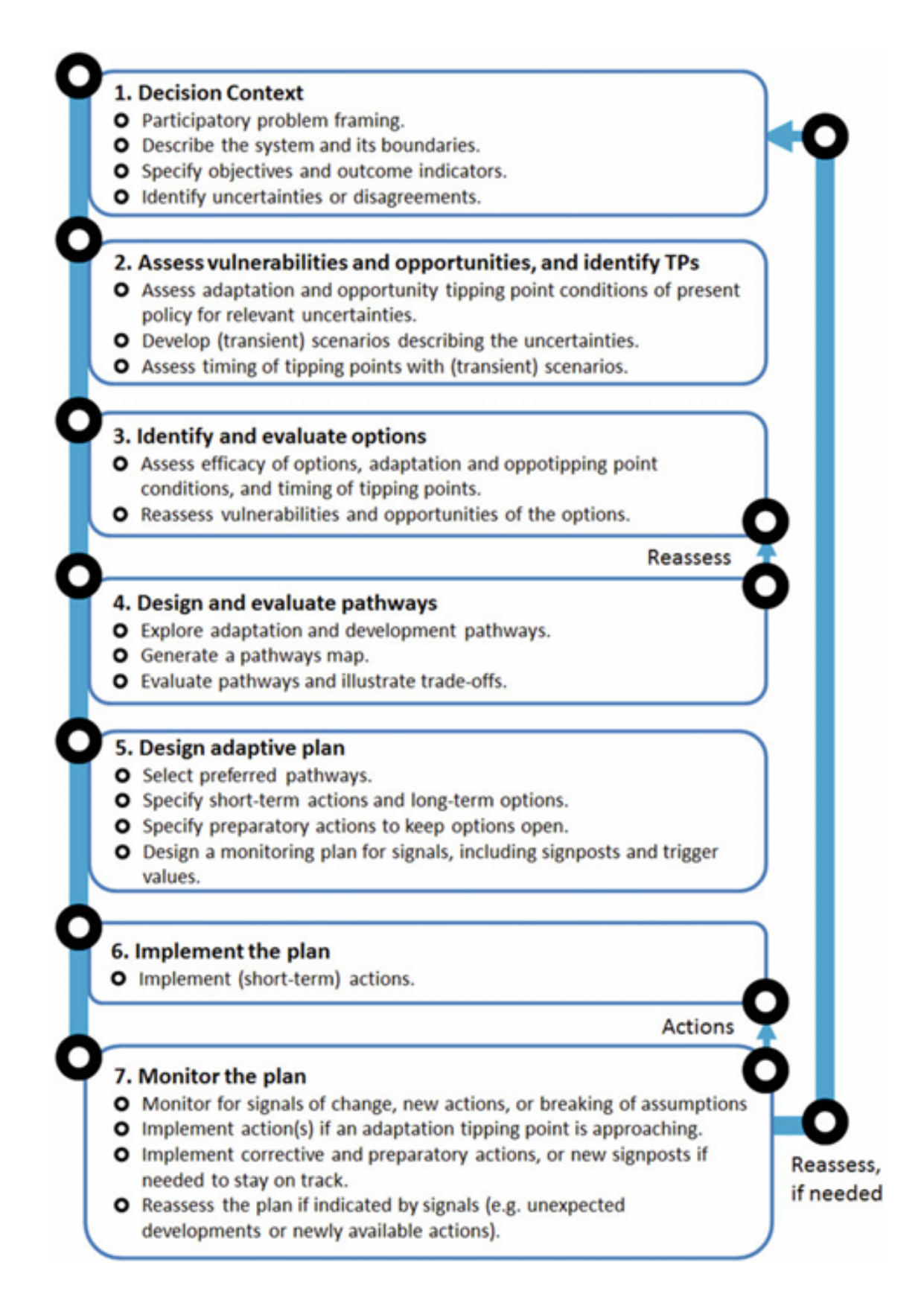


Figure 4.1: Phases in the DAPP approach [11].

Phase 1: Decision context The first step involves describing the context, including the system's charac-

teristics, objectives, current constraints, and potential future constraints. The result is a clear definition of success, which specifies the desired outcomes in terms of indicators and objectives. These are then used in subsequent phases to evaluate the performance of actions and pathways, as well as to assess the conditions and timing of the ATPs. This phase also includes specifying the main uncertainties or disagreements that play a role in the decision-making process, such as (changes in) external forces, system structure, and outcome assessment. The identified uncertainties are used to generate a set of plausible futures in the form of scenarios. These scenarios can be either static (describing a final point in the future) or dynamic over time (describing developments over time) [11].

Phase 2: Assess vulnerabilities and opportunities, and identify TPs

The second step focuses on evaluating the current state in relation to various plausible future scenarios, using predefined indicators and objectives to determine when the system begins to perform unacceptably (ATP). This occurs when a specified indicator fails to meet its intended target. Each plausible future is analyzed as a "reference case", assuming that no new policies are introduced. These reference cases consist of transitory scenarios that capture the uncertainties outlined in Phase 1. It is essential to take into account both opportunities and vulnerabilities: opportunities refer to developments that can support achieving the defined objectives, while vulnerabilities are those developments that may hinder or prevent reaching those objectives [11]

Phase 3: Identify and evaluate options

Alternative policy measures are found to alleviate vulnerabilities and take advantage of opportunities, building on the issue analysis conducted in Phases 1 and 2. The same methodology as in Phase 2 is used to evaluate the timing and circumstances of the ATP for each action according to how well they accomplish the intended results over time or under different situations. Only promising activities are continued into the following phases to act as building blocks for putting together adaptation pathways, whereas ineffective actions are eliminated [11].

Phase 4: Design and evaluate pathways

Once the set of policy actions is deemed appropriate, the next step is to design and evaluate the pathways. It is important to note that alternatives may not only consist of individual actions but can also include portfolios of actions implemented simultaneously. The outcome is a pathway map (Figure 4.2), which summarizes all the policy actions and the potential logical pathways through which the specified objectives can be achieved under changing conditions [11].

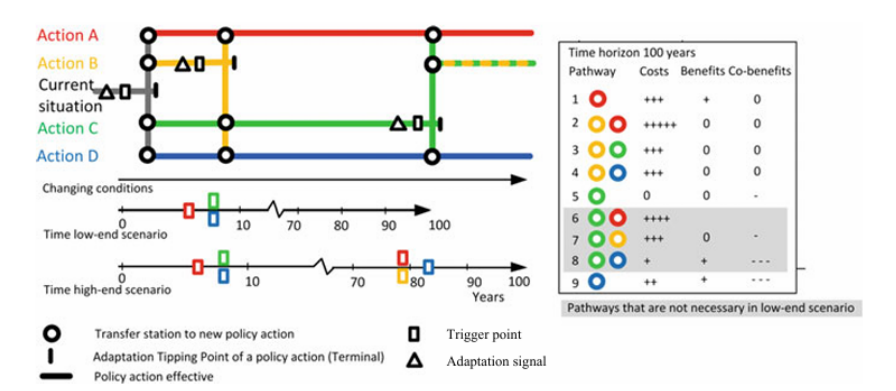


Figure 4.2: A pathways map along with a scorecard that outlines the costs and benefits of the pathways shown in the map [11].

The map illustrates various axes, such as (multiple) changing conditions and the assessed timing of these conditions for different scenarios. With this map, it is possible to identify opportunities, no-regret actions, bottlenecks, and the timing of actions. This supports decision-making in a dynamic environment. Some action sequences may be impossible, undesirable, or less likely (for example, when they exclude a transition to other actions or when it is very costly to add or shift actions), while other sequences will align well and allow for an adaptive response to changing conditions. Each pathway is then evaluated—using methods such as scorecards, cost-benefit analysis, multi-criteria analysis, or engineering options analysis—based on its performance as well as other key criteria. These include the urgency of actions, the severity of impacts, uncertainty, path dependency, and the willingness to keep future options open [11].

Phase 5: Design adaptive plan

The fifth phase involves identifying the initial actions and long-term options for a set of preferred pathways selected based on trade-offs. The robustness of the preferred pathways is strengthened through contingency planning. This requires specifying enabling, corrective, defensive, and capitalizing actions to stay on track, as well as a series of preparatory actions to keep the long-term preferred options open for as long as possible [11]. The adaptive plan also requires an associated monitoring system, which describes the signals to monitor and the related activation points that indicate when to implement subsequent actions. Ideally, the monitoring system provides signals before a decision needs to be made to take action (i.e., before a decision point) [11].

The specification of the right signaling variables and how to analyze the information is crucial to ensure that the pathways do not result in maladaptation or that preparation for subsequent actions is not delayed. The signal may differ from the related ATP, which is linked to objectives (impacts). Signals might be correlated not only with impacts but also with driving forces, such as trends and events in the physical environment, human-induced impacts on the system, technological developments, or changes in societal values and perspectives. After producing the final pathway map, an action plan is developed that specifies the immediate actions to be taken (initial actions), as well as an overview of long-term options, the enabling measures necessary to keep them open, developments to monitor, and the conditions under which subsequent actions should be taken to stay aligned with the preferred pathway or pathways. The plan should essentially summarize the outcomes of all previous phases, including all objectives, issues,

potential and preferred pathways, enabling actions, and the monitoring system [11].

Phases 6 and 7: Implement and monitor the plan

Afterwards, the initial actions and the enabling measures needed to keep the long-term options open are implemented, and the monitoring system is established to track low flows in the region. From that point on, time progresses, signpost information related to the predefined trigger points is collected, and actions may be initiated, adjusted, postponed, or expanded accordingly. Once monitoring confirms prevailing climate trends and a trigger point is reached, the preferred policy can be activated. In the meantime, the strategy is periodically reviewed and revised in light of new data [11].

4.2 Climate scenarios

In recent years, the climate change research community has developed an updated suite of scenarios aimed at improving our understanding of future climate trajectories and the complex interactions between climate systems and human societies. These scenarios are designed to reflect a broad spectrum of plausible futures by considering not only changes in the Earth's climate system but also concurrent shifts in socioeconomic, technological, and policy dimensions. They incorporate variations in key factors such as population growth, economic development, energy use, technological innovation, and emissions of greenhouse gases and aerosols, offering a comprehensive framework for assessing both risks and response strategies [12].

A central component of this framework is the Coupled Model Intercomparison Project Phase 6 (CMIP6), which integrates two key scenario families: the Shared Socioeconomic Pathways (SSPs) and the Representative Concentration Pathways (RCPs). SSPs describe possible global socio-economic developments in the absence of climate policies, while RCPs represent different trajectories of greenhouse gas concentrations based on varying levels of climate policy and mitigation. Each RCP corresponds to a specific level of radiative forcing, which refers to the change in the Earth's energy balance due to factors like greenhouse gas concentrations and aerosols. Radiative forcing is measured in watts per square meter (W/m²), and higher values, such as 8.5 W/m², indicate more energy being trapped in the Earth's atmosphere, leading to greater global warming. By combining these two dimensions, CMIP6 enables researchers to explore a wide range of potential futures that account for both human-driven and climate-driven uncertainties [12].

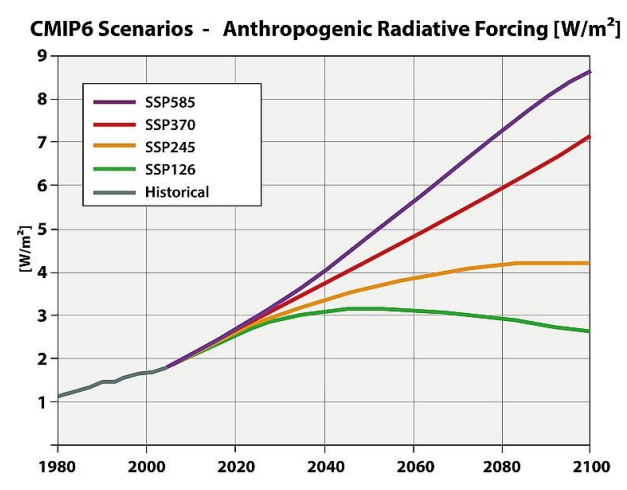


Figure 4.3: CMIP6 projections of Anthropogenic Radiative Forcing (in W/m²) from 1980 to 2100 under different Shared Socioeconomic Pathways (SSPs): SSP585 (high emissions), SSP370 (medium-high), SSP245 (medium), and SSP126 (low emissions), along with historical data [9].

.

This integrated approach allows for more detailed and policy-relevant climate modelling, supporting better-informed decisions regarding climate mitigation and adaptation. It also facilitates cross-disciplinary collaboration by linking social science insights with physical climate modeling, thereby enhancing the relevance and usability of climate projections for governments, institutions, and other stakeholders involved in long-term planning and sustainability efforts [12].

For this case study, the focus has been placed on three CMIP6 scenarios — SSP1-2.6, SSP2-4.5, and SSP5-8.5 — which are classified as "high priority" pathways according to the IPCC Sixth Assessment Report [6]. The analysis is specifically limited to the corresponding levels of radiative forcing (i.e., the "RCP" components 2.6, 4.5, and 8.5) embedded within these scenarios, in order to assess the climate impacts associated with different emissions trajectories.

The first one, SSP1-2.6,represents a *sustainable future* scenario where global actions limit radiative forcing to 2.6 W/m² by 2100, resulting in approximately 1.5–2 °C global temperature rise [6] . It assumes strong climate policies and eventual net-zero carbon emissions, reflecting a balanced mix of socioeconomic development and effective climate action.

[12]. SSP2-4.5 combines the "middle-of-the-road" socioeconomic pathway (SSP2) with a moderate radiative forcing level (4.5 W/m²) by the end of the century [6]. It assumes that historical trends continue without major disruptions or trasformative policies. Population growth is moderate, economic development proceeds unevenly, and technological change is gradual. While moderate mitigation efforts are implemented, this pathway leads to a medium level of global warming, with a stabilization of emissions at an intermediate level [12].

SSP5-8.5, on the other hand, pairs a high economic growth scenario (SSP5) with a high radiative forcing level (8.5 W/m²) [6]. This scenario represents a future with rapid technological advancements, especially in energy production, along with high levels of industrialization and energy consumption. Population growth is relatively moderate, but the emphasis is on increased economic development and fossil fuel-driven energy production. As a result, it leads to very high greenhouse gas emissions and significant global warming, reflecting a pathway with minimal climate mitigation efforts [12].

4.3 Nature Based Solutions (NBS)

As introduced in the chapter 1.2.1, Nature Based Solutions (NBS) are implemented in this thesis, to address challenges that come from the catchment area, with a particular focus on flooding caused by rainfall events.

4.3.1 Definition

The European Commission defines Nature-Based Solutions (NBS) as "Solutions that are inspired and supported by nature, which are cost-effective, simultaneously provide environmental, social and economic benefits and help build resilience. Such solutions bring more, and more diverse, nature and natural features and processes into cities, landscapes and seascapes, through locally adapted, resource-efficient and systemic interventions". NBS aim to address relevant societal challenges, foster resource recovery, contribute to climate change mitigation and adaptation, promote human well-being, ecosystem restoration and enhance biodiversity in urban environments [13].

Nature-Based Solutions (NBS) are systems that use ecosystem services to manage water resources and lower the risks that come with them. These solutions take different forms and can be applied in a wide range of contexts. For example, green roofs (as visible in the upper right of the Figure 4.4) can help reduce urban flooding while offering multiple co-benefits, including improving air quality, reducing the urban heat island effect and creating space for social or recreational activities. Another example of NBS are artificial wetlands, which allow natural wastewater treatment at landscape level, reduce carbon emissions and provide habitats for wildlife [14]. More generally, NBS improve the infiltration and water retention capacity of soils, helping to reduce the impacts of floods, purify polluted water, mitigate droughts through the gradual release of naturally stored water, and increase in value over time through the regeneration of nature and associated ecosystem services [14].



Figure 4.4: Examples of Nature Based Solution (NBS) [15].

4.3.2 Challenges addressed

Although there is growing evidence that states that NBS can be more cost-effective than grey infrastructure or traditional approaches [16], their implementation is still hindered by several barriers. Among the most relevant barriers are financial constraints and considerable difficulties in developing effective governance models capable of designing and implementing efficient interventions that ensure the active

participation of all relevant stakeholders. Such models must promote shared responsibility and collaboration. In this context, it is crucial to identify appropriate tools to communicate the benefits of NBS and to foster involvement and cooperation among stakeholders in order to promote more effective dissemination and adoption.

Indeed, it would be a pity not to exploit the potential of NBS, as they can offer significant benefits in many areas, particularly in water management.

NBS can contribute both to regulating water supply and to improving water quality. With regard to supply, their high infiltration capacity favours groundwater recharge, increasing the water retention capacity of soils and wetlands. Moreover, during dry periods, they are able to release water stored in natural reservoirs such as soil, groundwater and surface water. They also help extend the life of reservoirs by reducing siltation. With regard to water quality, NBS can treat polluted water by trapping and retaining contaminants in sediments. Removing heavy metals, They help protect groundwater from pollution; additionally they reduce pressure on existing water infrastructure through processes such as bioretention and infiltration [17]. In this thesis, NBS are of particular importance, especially in light of the major challenges posed by extreme climate scenarios. Numerous studies have shown that NBS can play a significant role in the management of such events. In particular, they are able to increase water storage capacity in both catchment areas and urban areas, thus helping to reduce downstream flooding. NBS delay and reduce peak runoff, which, in the majority of cases, minimizes the risk of flooding. In addition, NBS help slow the velocity of floodwaters, reduce the vulnerability of crops to drought and mitigate the impacts of droughts by maximizing groundwater recharge and retention [17]. Figure 4.5 provides an overview of the different types of Nature-Based Solutions (NBS), evaluated according to their effectiveness in responding to four main water services: water supply, moderation of extreme events, erosion control and water purification, as previously introduced.

	Water services				
Nature-based solution	Water supply	Moderate extreme events	Erosion control	Water purification	
Flood bypass					
Green spaces (bioretention and infiltration)					
Permeable pavements					
Farming practices (contour ridging, crop rotation, low till, grazing pressure, etc.)					
Green roofs					

Figure 4.5: Assessment of some NBS addressing four water services. The color of the cells indicate the level of contribution to water service(white-insificant contribution, dark-significant contribution) (adapted from UNEP,2014)

The analysis shows that agricultural practices (including techniques such as crop rotation and contour farming) offer the most comprehensive coverage of all services considered. This is followed by permeable pavements-such as porous asphalt-that, due to their porosity, allow infiltration and temporary water storage. Green spaces, such as rain gardens, are also effective in promoting infiltration, purification and water retention through the use of selected vegetation. Flood bypass systems and green roofs rank lower in the ranking, contributing mainly to the moderation of extreme events [17]. Going

more in deep in this context, Figure 5.24 shows the total score given to each NBS, assessing their effectiveness with respect to flood risk reduction, mitigation of the heat island effect and environmental co-benefits (such as biodiversity conservation and recreational opportunities). In this context, the solutions with the highest scores are floodplains—low-relief Earth surfaces positioned adjacent to freshwaters and subject to flooding (including fringing floodplains of lakes and rivers, internal and river deltas)—and riparian forests, which are transitional semi-terrestrial areas extending from the edge of permanent water bodies to the edge of uplands and influenced by freshwater [18]—followed by green forest areas (particularly effective in reducing the heat island effect), and finally roadside trees and green paths.

Code	Name	Effectiveness against Flood Risk	Heat Island Effect Reduction	Environmental Co-Benefits	Total Score
1	Forested green areas	1.9	3	2.3	7.2
2	Rain gardens	1.6	1.5	1.7	4.8
3	Urban gardens	1.2	2	1.6	4.8
4	Green roofs	1	1.5	1	3.5
5	Green facades	0.1	1	0.7	1.8
6	Roadside trees and green paths	1.6	3	2.2	6.8
7	Green rails	1	2	1	4
8	Green urban furniture	1	2	1	4
9	Permeable surfaces	0.7	0	0.7	1.4
10	Rainwater harvesting	0.1	0	0.5	0.6
11	Infiltration basins	1.6	1.5	2	5.1
12	Infiltration trenches	1	0	1.2	2.2
13	Retention ponds	1.6	1.5	2.1	5.2
14	Restoration of rivers for the control of infiltrations	1.2	0	1.6	2.8
15	Creation of floodplains and riparian forests	2.8	2	3	7.8

Figure 4.6: Evaluation of NBS addressing flooding, heat island effect and taking into account their environmental co-benefits [19]

With particular focus on the ability of NBS to reduce flood risk, special attention is given to their capacity to reduce runoff. The table shown in Figure 4.7 presents the runoff reduction—expressed as a percentage—associated with stormwater Best Management Practices (BMPs), which include some NBS.

	Runoff Reduction			
Practice	(percent) *			
Green Roof	45-60			
Rooftop Disconnection	25-50			
Raintanks and Cisterns	40			
Permeable Pavement	45-75			
Grass Channel	10-20			
Bioretention	40-80			
Dry Swale	40-60			
Wet Swale	0			
Infiltration	50-90			
ED Pond	0-15			
Soil Amendments	50-75			
Sheetflow to Open Space	50-75			
Filtering Practice	0			
Constructed Wetland	0			
Wet Pond	0			
*Range of values is for median (Level 1) and 75th percentile (Level 2) designs.				

Figure 4.7: Range of values of runoff reduction (%) for different BMPs(Best Management Practices) [20].

As noted from the Figure above, permeable pavements have a high capacity to reduce runoff, with an average reduction of around 60% within the reported range. On the other hand, green roofs achieve a slightly lower average value, approximately 52%. Some of these nature-based solutions will be analyzed in more detail in the section 5.3.

4.3.3 Cost

Figure 4.8 presents cost estimates, including both installation and maintenance costs. Values for each NBS were averaged and converted into annual costs, assuming two different discount rates (3% and 5%) and a time horizon up to 2030. Among the analysed solutions, green roofs are the most expensive option, with an annualized cost of 65.04 EUR/m² assuming a 5% discount rate, followed by green rails and infiltration trenches [19].

		Costs					
Code	Name	Installation (EUR/m ²)	Maintenance (EUR/m²)	Average Annual Cost by 2030 (EUR/m²) r = 3%	Average Annual Cost by 2030 (EUR/m ²) r = 5%		
1	Forested green areas	1.32	2.49	0.47	0.49		
2	Rain gardens	1.08	0.3	0.43	0.44		
3	Urban gardens	3.85	3.85	4.3	4.35		
4	Green roofs	77.5	55	64.09	65.04		
5	Green facades	100	3.5	15.22	16.45		
6	Roadside trees and green paths	33.78	34.22	10.57	10.41		
7	Green rails	210	2.4	27.05	29.63		
8	Green urban furniture	80	(n/a)	9.38	10.36		
9	Permeable surfaces	65	3	10.62	11.42		
10	Rainwater harvesting	32.5	0.63	4.44	4.84		
11	Infiltration basins	26.25	2.83	5.9	6.22		
12	Infiltration trenches	80	2.12	11.5	12.48		
13	Retention ponds	14	3	4.64	4.81		
14	Restoration of rivers for the control of infiltrations	3.8	1.7	2.16	2.19		
15	Creation of floodplains and riparian forests	0.75	0.05	0.14	0.15		

Figure 4.8: Cost of NBS [19]

However, assessing the economic value of NBS and their indirect positive effects comparing to conventional solutions such as sewer systems and traditional basing is often complex. In Denmark, there aren't currently official guidelines for calculating the benefits and added value of green solutions such as NBS [8].

4.3.4 NBS in Denmark

In Copenhagen, the capital of Denmark, the district of Skt. Kjelds has been transfromed to a resilient neighbourhood. Since 2014, the area has been the focus of a major project aimed at increasing its ability to cope with the effects of climate change, in particular heavy rainfall [14].

Located in the northeastern part of the city, Skt. Kjelds is located on a natural slope that descends towards the harbour. This conformation has defined the main objective of the project: to retain surface water within the neighbourhood and promote its infiltration into the groundwater as much as possible. The storage capacity is used to manage water during heavy rain and cloudbursts [14].

In the event of extreme events, such as cloudbursts, excess rainwater is channeled to specially identified low-risk areas, minimizing potential damage. The overall objective is to implement flexible solutions based on surface management that can locally cope with daily rainfall. During extreme events, these surface solutions are supplemented with a separate stormwater sewer system, ensuring safe and controlled runoff to the nearest port [14].

As shown in Figure 8.1a, before 2013 the neighborhood was in a state of marked decay, completely devoid of green areas. Today, as shown in Figure 8.1b, the main square-Taasinge Plads-completed in 2014-has been transformed into a green pocket park that is an example of integrated surface water management. The area demonstrates how three different types of stormwater are managed: rainwater from roofs is reused for recreational and play purposes; rainwater from low-traffic areas is channeled to local infiltration into the ground; while road runoff is filtered through special filter materials [14]. Due to the use of de-icing salt during winter, water from roads is not infiltrated into the groundwater, but is conveyed directly to the harbour. During heavy rain events (cloudbursts), the open-air storage capacity built into the park comes into operation, allowing the temporary storage of excess water, creating a dynamic 'blue' element within the urban green space[14].





(a) Taasinge Plads in 2013

(b) Taasinge Plads in 2014

Figure 4.9: Taasinge Plads:before and after be transoformed in resilient [21]

The transformation was finished in 2019, substituing asphalt and pavements with green spaces, urban nature and integrated surface water management solutions. The natural elements included are inspired by the wet/dry biotopes typical of Copenhagen, adapting their ecological processes to efficiently retain and treat rainwater [14].

Surface runoff from the streets is managed through a 'first-flush' system: the first, more polluted flow, generated by heavy rainfall, is conveyed into the existing sewer system, while the second, cleaner flow is directed to green infrastructure for infiltration and purification. This system can be switched off in the winter months to avoid salt contamination of vegetated areas[14].

4.3.5 Directives

According to the European Union's Water Framework Directive and the Danish Environmental Protection Law, Danish municipalities must assess whether it is necessary to treat runoff water when using NBS. This decision depends on the pollution level of the runoff and the sensitivity of the receiving water body in order to meet its quality requirements [8].

A key aspect is infiltration: when it occurs, it must not contaminate the groundwater. If runoff is discharged into a lake or watercourse, it must not compromise its ecological or biological status. If the water is used for recreational purposes, the general guideline is that rainwater may be stored for a maximum of 24 hours, due to the risk of pathogens. If treated runoff is sprayed or pumped for play (e.g. in playgrounds), UV disinfection is often necessary [8].

There are various solutions for treating runoff, often already integrated in NBS. These include basic treatment mechanisms such as sedimentation, filtration, adsorption, biological degradation and flocculation, that are often combined [8].

4.4 Curve Number Method

As briefly mentioned in the previous section, the Curve Number is an important parameter that, in the context of this thesis, allows the implementation of different Nature-Based Solutions (NBS), taking into account their varying water infiltration capacities.

As a rainfall-runoff model, the Runoff Curve Number Method, often referred to as the CN method, was developed by the US Soil Conservation Service (now Natural Resources Conservation Service). This method

Parameter	Maximum Permissible Value
рН	6–9
Suspended Solids	< 0.1 mg/L
Iron	< 0.5 mg/L
Total Nitrogen	4 mg tot-N/L
Ammonium (NH ₄ -N)	1 mg/L
BOD_5	$3 \text{ mg O}_2/L$
Oxygen	6 mg/L (50% saturation)

Table 4.1: Maximum permissible values for water quality parameters [8]

provides an empirical relationship (Equation 4.1) between rainfall and runoff, primarily relying on the Curve Number (CN) and the proportionality factor (λ) to characterize runoff behavior [22].

$$Q = \begin{cases} 0, & \text{if } P \le I_a \\ \frac{(P - I_a)^2}{(P - I_a) + S}, & \text{if } P > I_a \end{cases}$$
 (4.1)

 $Q = \text{Runoff} \quad [\text{mm}]$

P = Precipitation [mm]

 $I_a = \text{Initial loss} \quad [\text{mm}]$

S =Potential maximum retention after runoff begins [mm]

The initial loss I_a can be approximated as a fraction of the potential maximum retention S after runoff begins:

$$I_a = \lambda * S \tag{4.2}$$

where λ , the proportionality factor, is commonly recommended to be 0.2; however, several later studies suggest alternative values (that range between 0.05 and 0.2 [23].

The potential maximum retention S is related to the Curve Number (CN) by the following equation:

$$S = \frac{25400}{CN} - 254\tag{4.3}$$

Curve Number (CN) values typically range from 30 for permeable soils with high infiltration rates to 100 for water bodies and soils with very low infiltration capacity [23]. The CN is generally determined from standard tables (such as that one shown in Figure 4.10), based on a combination of factors, including the hydrologic soil group, land cover type, soil hydrologic condition, and land treatment. The hydrologic soil group is classified according to the soil's ability to infiltrate, evaporate, and percolate water [23].

Land Use Description	Hydro	logic So	il Group	
Residential	Α	В	С	D
Average Lot Size				
1/8 acre or less	77	85	90	92
1/4 acre	61	75	83	87
1/3 acre	57	72	81	86
1/2 acre	54	70	80	85
1 acre	51	68	79	84
2 acre	46	65	77	82
Paved parking, roofs	98	98	98	98
Streets and Roads				
Paved with curbs	98	98	98	98
Gravel	76	85	89	91
Dirt	72	82	87	89
Commercial and business areas	89	92	94	95
Industrial districts	81	88	91	93
Open spaces, lawns, parks				
good condition	39	61	74	80
fair condition	49	69	79	84
Fallow	77	86	91	94
Row Crops	72	81	88	91

Figure 4.10: Curve Number for different types of land use [24]

However, nowadays there are no established values of CN for Nature-Based Solutions, so this method represents an important starting point to determine them, which will be explained in the section 6.3in detail.

5 Background and Analysis

5.1 The catchment area

The catchment area, called Sømose is located between Ballerup and Herlev, two municipalities located approximately 20 km from Copenhagen, the capital of Denmark. It can be identified on the map shown in Figure A.5, where the catchment area is marked in purple, while the black lines indicate the borders of the two municipalities.

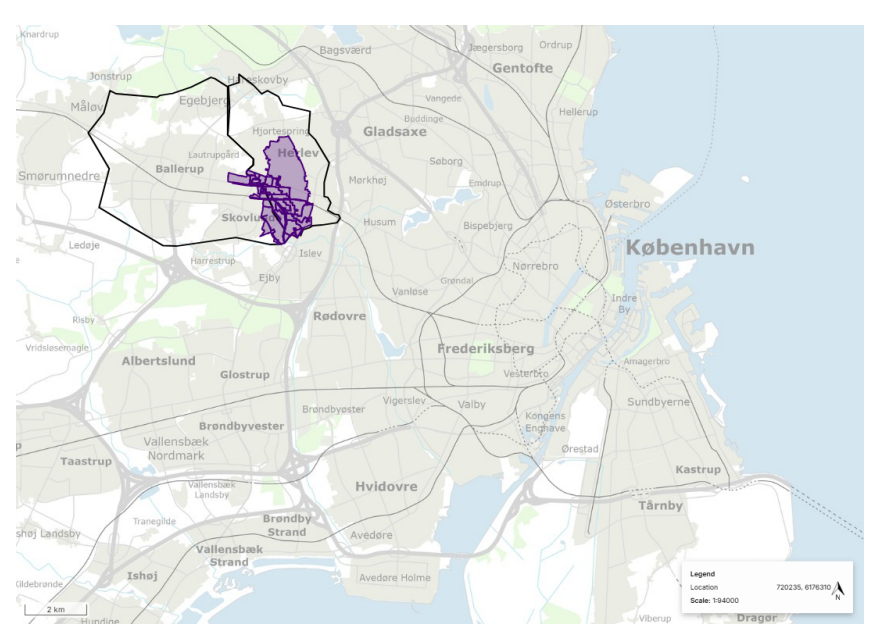


Figure 5.1: Topographic map of the catchment area near Copenhagen, generated using the SCALGO Live software.

Technical files of the catchment area (e.g., shapefiles) provided by Niras were imported into SCALGO and QGIS in order to visualize the catchment—displayed in purple in SCALGO. The boundaries of the two municipalities were manually created, based on visual interpretation and reproduction of their limits from Google Maps.

Ballerup is primarily a residential and industrial area (as indicated in red on the map legend), with a significant presence of vegetation (shown in light and dark green). The total area covers approximately 33.9 km². According to land cover data from 2021 [25], the municipality includes 13.7 km² of buildings and built-up areas, 5.5 km² of roads, railways, and runways, and 3.8 km² of other artificial surfaces. Natural and semi-natural features are also present, including 2.9 km² of forest, 1.7 km² of dry and wet natural habitats, and 1.1 km² of lakes and streams. Additionally, 3.8 km² are used for agricultural crops, while 1.3 km² remain unclassified.

The soil in the area is predominantly composed of fine sand with clay.

The local water supply is provided by the Novafos utility. Part of the wastewater is conveyed to the wastewater treatment plant (WWTP) located in Måløv, a suburb situated just outside Ballerup. The WWTP is operated by Novafos, a major water company serving nine municipalities in eastern Denmark, near Copenhagen. The location of the WWTP can be identified in the northern part of the map shown in

Figure 5.2.To the east of Ballerup lies Sømosen, a natural pond situated on the border with Herlev, which serves as the source of the catchment.

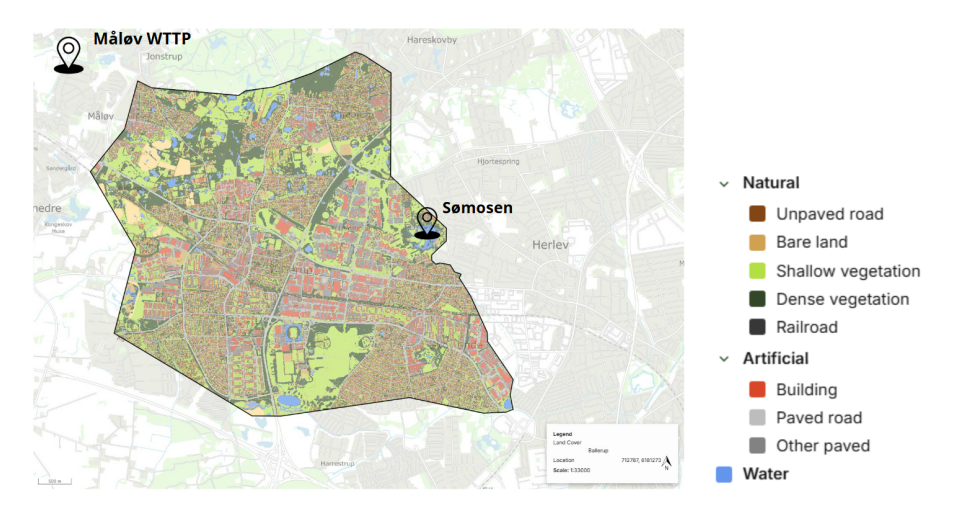


Figure 5.2: Land cover map of Ballerup, generated using the SCALGO Live

Herlev is also mainly a residential area, with the highest population density concentrated in the central part and a large industrial district located in the southern part of the municipality. The total area covers approximately 12.1 km². According to 2021 land cover data [25], Herlev includes 6.4 km² of buildings and built-up areas, 2.4 km² of roads, railways, and runways, and 1.4 km² of other artificial surfaces. The remaining land consists of 0.7 km² of agricultural crops, 0.5 km² of forest, 0.2 km² of dry and wet natural habitats, and 0.3 km² each of lakes and streams, and unclassified areas. The water supply for the municipality is provided primarily by HOFOR, with a smaller contribution from Novafos [26]. As in Herlev, part of the wastewater is conveyed to the WWTP located in Måløv [26]. The spatial distribution and land use patterns of Herlev can be better understood through the map presented in Figure 5.3, where Sømosen is visible to the west, just outside the municipal boundaries of Herlev.

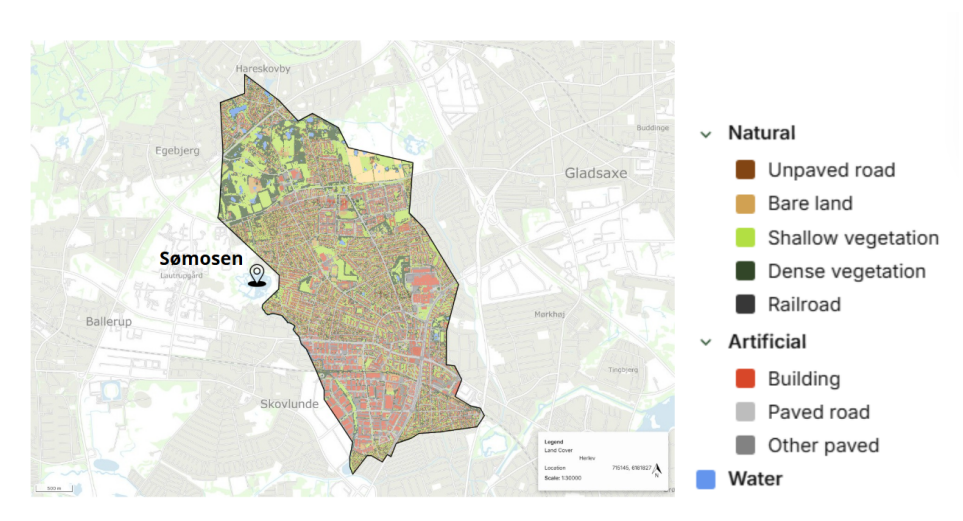


Figure 5.3: Land cover map of Herley, generated using SCALGO Live

Both municipalities aim to expand residential areas, especially Herlev [27]. However, this poses a potential flood risk due to reduced drainage capacity. It is necessary to reassess the urban water management plan and implement solutions to mitigate flood risks. These solutions should be flexible to adapt to future urban changes. Urbanization near the Sømose stream (shown in blue in Figure 5.4, crossing the catch-

ment) could lead to increased flow rates during storm events, as the reduction of pervious surfaces would limit infiltration and promote surface runoff. This, in turn, may elevate the risk of flooding in surrounding areas. Therefore, it is essential to plan urban development using a resilient and adaptive approach to effectively mitigate such risks.

Both municipalities are actively involved in the *Harrestrup Å-Capacity Plan* project, which has been launched in 2015. The primary objective of this project is to handle 100-year flood events effectively [28]. The project involves a total of 10 municipalities: Albertslund, Ballerup, Brøndby, Frederiksberg, Gladsaxe, Glostrup, Herlev, Hvidovre, Copenhagen, and Rødovre [3]. The key utilities participating in the initiative include: HOFOR, Novafos, Frederiksberg Forsyning, and Glostrup Forsyning [3]. This project will be explained more in details in the section 5.2.

Figure 5.4 provides a clearer overview of the development of the catchment area.

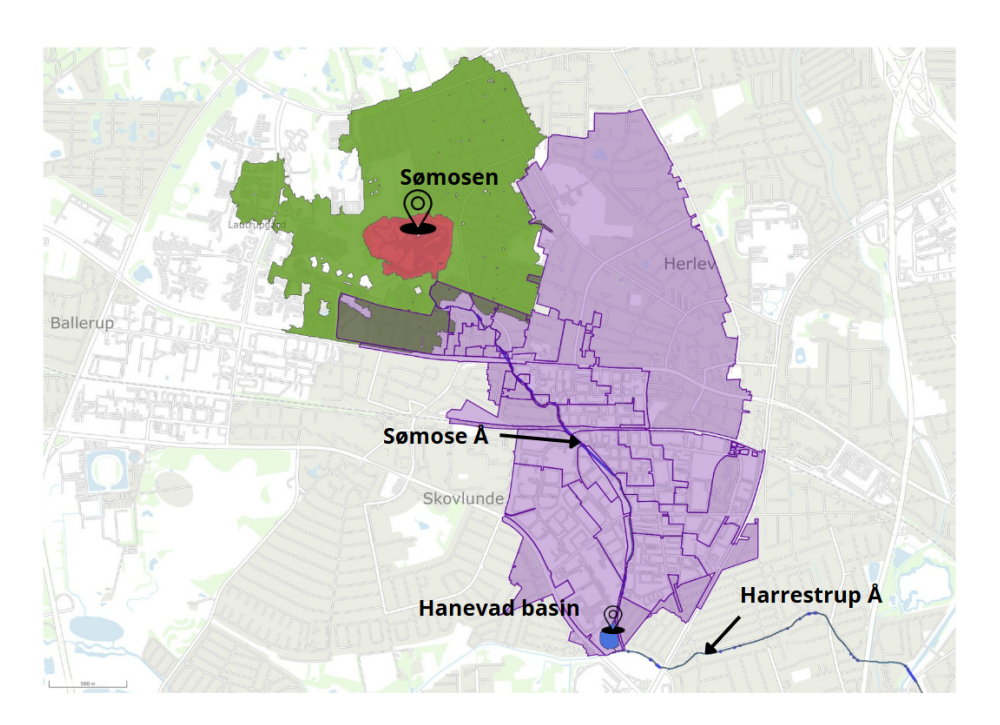


Figure 5.4: Watershed map with related information on the catchment area, generated using SCALGO Live

The region marked in purple represents the catchment boundary. The green area shows the upstream drainage area that contributes runoff to the natural pond Sømosen, which is highlighted in red. This red zone corresponds to a topographic depression—an area of low elevation—as further illustrated in the elevation profile shown in Figure 5.5.

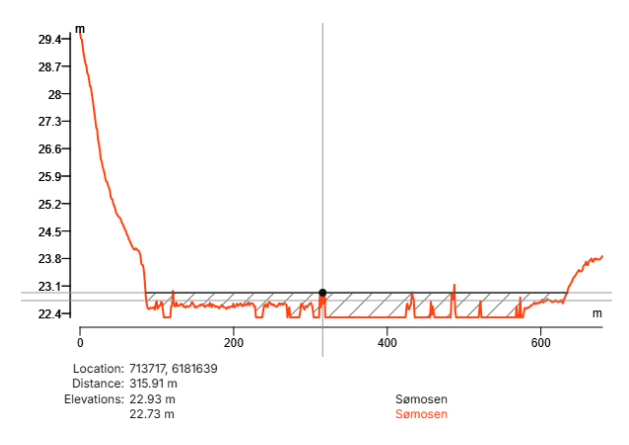


Figure 5.5: Elevation profile across the Sømosen depression generated through SCALGO Live

The profile plot presents a cross-sectional view of the terrain across the Sømosen depression. The transect begins outside the catchment, crosses through its central low-lying area, and ends beyond the depression on the opposite side. The red line indicates ground elevation along the profile. A steep slope appears at the start, followed by a relatively flat section representing the depression's basin floor. Toward the end of the profile, the terrain rises gradually as it exits the depression. The hatch pattern area describes the maximal depressions. This visualization helps convey the geomorphological structure of the depression and its capacity to retain water during rainfall or runoff events. The drainage network continues southward through Sømose Å, shown in blue in Figure 5.4, which extends for approximately 3,215 meters [29]. The outlet is located further downstream in the Hanevad basin. From there, the watercourse connects to Harrestrup Å—the main stream—visible downstream to the right in blue.

Furthermore, Figure 5.6 presents watershed information, offering an overview of the data related to surface runoff.

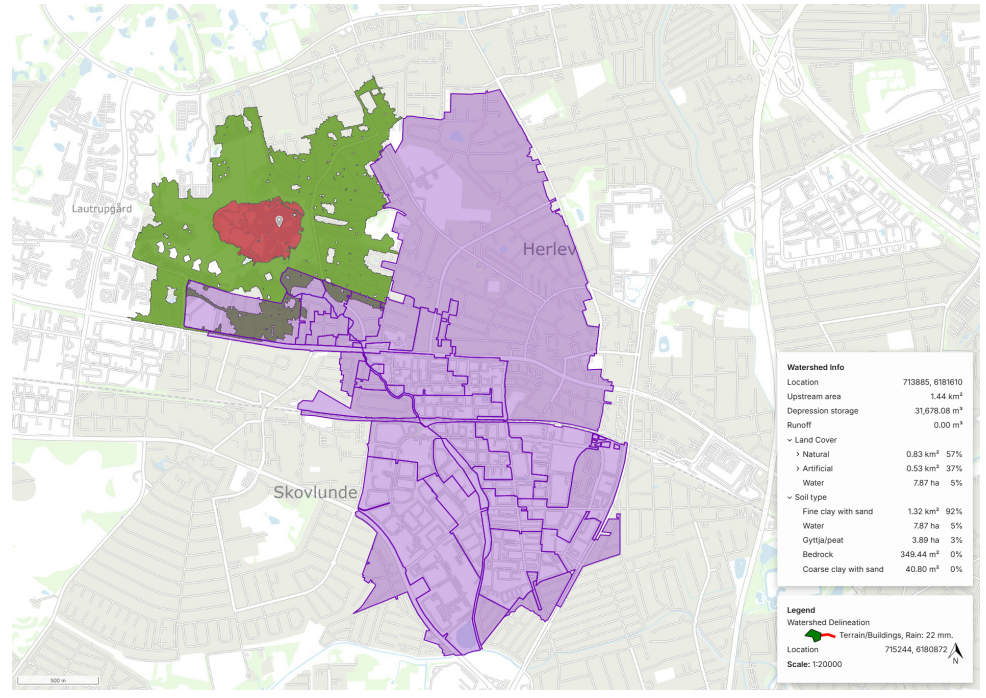


Figure 5.6: Watershed map with related information on the catchment area, generated using SCALGO Live

The analysis is based on an input of 22 mm of rainfall, which corresponds to the expected value in the catchment area for a 5-year return period event lasting 60 minutes, under RCP 2.6. The derivation of this value will be explained in Section 6.1. A 5-year return period is used because, as will be detailed in Section 5.2.1, it reflects the design capacity of the current drainage system.

The upstream drainage area of Sømose Å covers approximately $2.06 \ km^2$, with a depression storage volume of $142,506.07 \ m^3$, and a runoff of $22,298.76 \ mm^3$. Moreover, the land cover data indicate that the area is predominantly natural (56%), including shallow vegetation (29%), dense vegetation (22%), bare land (4%), and unpaved roads (1%). Artificial surfaces make up 40% of the area, with 25% consisting of paved surfaces (9% being roads) and 5% occupied by buildings. The remaining 4% of the watershed is covered by water. Watershed information also provides details about the soil: it is mainly composed of fine clay with sand (87 %), 4% is fine sand with clay, 4% is peat, and the remaining 4% is water.

5.1.1 Land cover

Figure 5.7 provides an overview of the land cover composition in the catchment area, that is outlined in the map. The land cover map uses a color-coded system to distinguish between natural and artificial features.

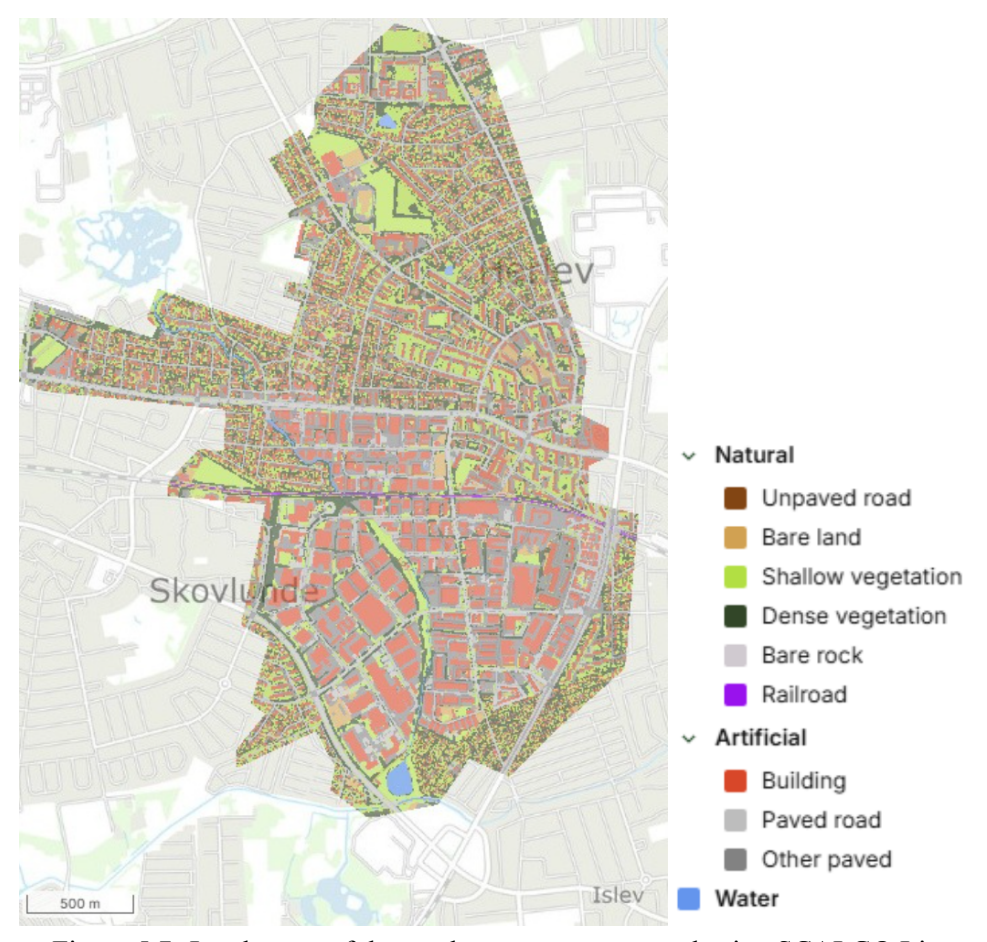


Figure 5.7: Land cover of the catchment area generated using SCALGO Live

The red areas represent buildings, indicating dense urban development concentrated in the central part of the map. Within this highly built-up area, the Sømose Å passes through, posing a significant flooding risk to the nearby population. Surrounding the built-up zones, light green and dark green patches signify

shallow and dense vegetation, respectively, highlighting the presence of parks and forests.

Infrastructure elements are marked with distinct colors: gray for paved roads and dark gray for other paved surfaces, forming a structured network that connects different parts of the area. Brown signifies unpaved roads, while light brown indicates bare land, possibly representing construction sites, undeveloped plots, or agricultural fields.

A presence of blue elements indicates water bodies such as lakes and streams. The purple lines trace the path of railroads.

Using SCALGO in combination with QGIS, it was possible to extract and analyze the land cover characteristics of the study area. Table 5.1 presents a summary of these land cover types, which are visually represented in Figure 5.7. This table represents the land cover distribution within the catchment area, which extends over approximately 467.5 ha. The most prevalent land cover category is *other paved* areas, accounting for 26.9% of the total area. This category includes surfaces such as sidewalks,parking lots and squares. When combined with *buildings and paved roads*, these impervious surfaces (can be defined as *grey area*) make up 64% of the land cover. These areas contribute the most to runoff generation due to their low infiltration rates [30]. Additionally, there is a high concentration of buildings close to the watercourse. This, combined with the low capacity of the soil to infiltrate water, significantly increases the risk of flooding. On the other hand, *green areas*, which generally have higher infiltration rates, help reduce runoff [30]. They cover approximately 35% of the catchment area and include bare land, shallow vegetation, and dense vegetation. Lastly, *blue areas*, which consist of streams, small lakes, and the outlet pond, account for 0.7% of the catchment area.

Land Cover	Area [ha]	Percentage (%)
Bare land	15	3.2
Water	3.5	0.7
Other paved	125.8	26.9
Shallow Veg.	88.9	19
Dense Veg.	57.8	12.4
Paved road	61.4	13.1
Unpaved road	1	0.2
Railroad	0.8	0.2
Building	113.3	24.2

Table 5.1: Land cover in the catchment area

5.1.2 Soil, Groundwater, and Contamination Conditions

The topsoil (upper 1 meter) along the watercourse is classified on the GEUS soil map as postglacial freshwater peat. In the section between the railway (in purple in Figure 5.79 and the Hanevad basin, the upper layers consist of 5 to 15 meters of glacial till clay. Beneath this, there are approximately 5 meters of meltwater sand, which lies directly on top of the Danian limestone [29].

The Danian limestone, together with the overlying meltwater sand, forms the primary aquifer in the area. Groundwater potential decreases from approximately +17.5 meters to +9 meters moving southeast to-

ward the Hanevad basin (see Figure 5.9).

In the stretch between Mileparken and Harrestrup Å (see Figure 5.8), groundwater levels are significantly influenced by remedial pumping and water extraction. Since the riverbed in this section lies at around +9 meters elevation, it is likely that the stream is intermittently fed by groundwater [29].

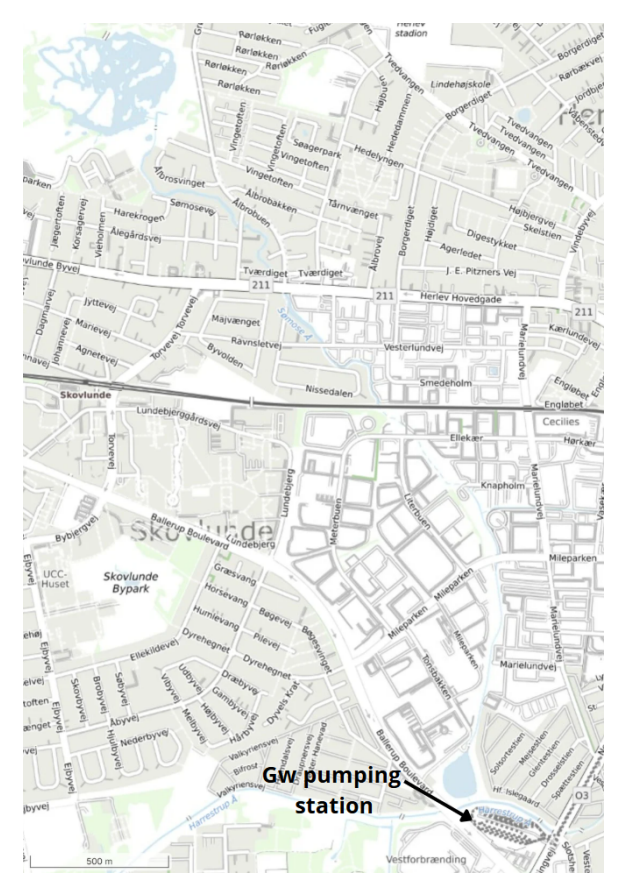


Figure 5.8: Topographic map of the catchment showing the location of groundwater pumping stations, generated using SCALGO Live.

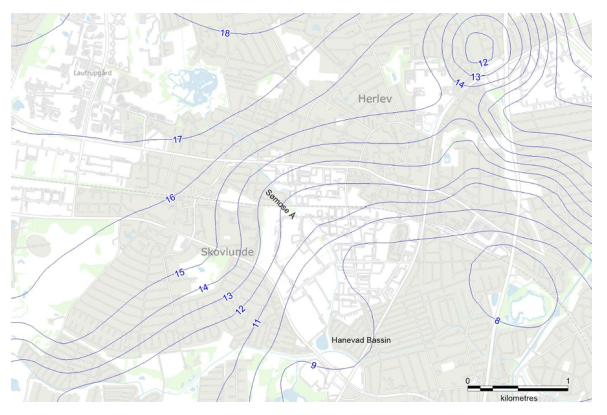


Figure 5.9: Groundwater potential in the limestone aquifer [29].

In the past, industrial activities in the area led to significant groundwater contamination, primarily due to the extensive use of chlorinated solvents. As a consequence, one of HOFOR's groundwater extraction sites, located near the Sømose stream, was shut down, and long-term remediation efforts were initiated to prevent further spread of the pollution [29].

HOFOR extracts groundwater for drinking water purposes at Kildeplads VII, located near the Hanevad basin. The site includes four wells, two of which have been referred to as "remediation wells" in some records. However, according to HOFOR, all four wells are actively used for the drinking water supply [29].

In addition, two other borehole installations have been identified in the area, though their official classification remains unclear. In Figure 5.10, these are labeled "Ukendt 2" and "Ukendt 3" (ukendt meaning "unknown" in Danish), highlighting some uncertainty about their specific status or use [29].



Figure 5.10: Groundwater pumping station with four wells at Kildeplads close to Hanevad basin [29].

5.1.3 Vulnerabilities

Extreme flood map

Figure 5.11 shows the flooded areas within the catchment. Zones without land cover analysis are included to provide a comprehensive overview of the entire catchment, including surrounding areas that may influence its hydrological behavior. The simulation is based on a 50 mm rainfall event, corresponding to a 100-year return period with a duration of 60 minutes. As previously mentioned, the primary objective of the Harrestrup Å Capacity Plan is to manage such extreme events. The rainfall value is based on projections for the period 2026–2070, provided by the Danish Meteorological Institute (DMI) [31]. A water depth threshold of 30 cm was applied to highlight areas affected by significant flooding.

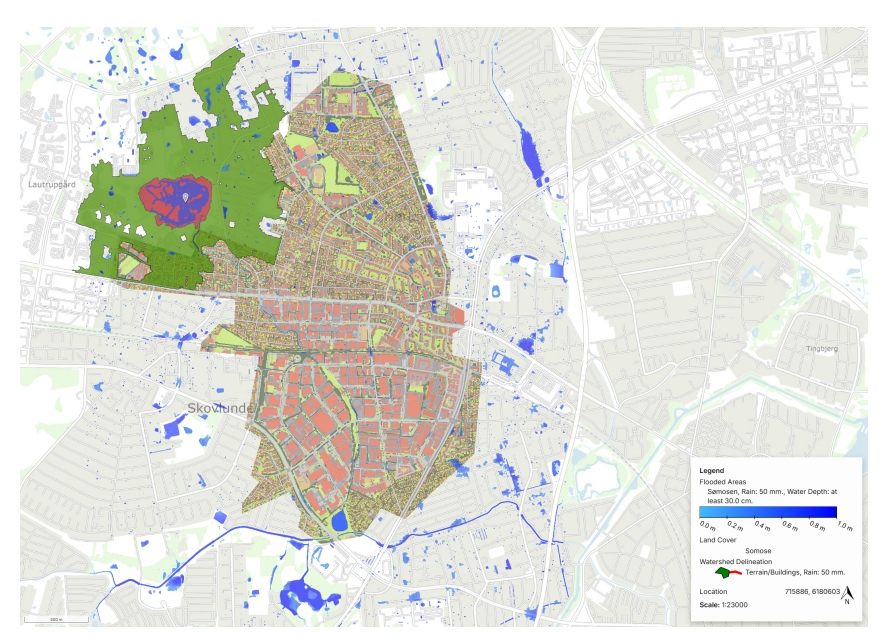


Figure 5.11: Topographic map showing flooded areas within the catchment based on a 100-year rainfall event projected over the next years (2026-2070), generated using SCALGO.

The affected areas, marked in blue, are primarily concentrated near the watercourse, where there is a dense distribution of buildings. The combination of low infiltration capacity and proximity to the stream significantly increases the risk of flooding. Additionally, flooded areas are concentrated in the northern part

of the catchment, near a lake. These information are crucial as they identify the most affected areas, enabling targeted flood mitigation efforts. The concentration of flooded areas near the watercourse suggests that efficient drainage measures should be implemented to reduce flood risks.

According to a report by NIRAS on the first phase of the Capacity Plan [29], the proposed measures for the Harrestrup River include a significant increase in the maximum water level during heavy rain events, particularly in the terminal section of the Sømose River and in the Hanevad Basin. Currently, the water level in the Hanevad basin rarely exceeds 9.00 meters, but according to the plan, it could reach up to 11.73 meters in the future. This expected rise could put pressure on the catchment areas located in the southern part of the Sømose River and the Hanevad Basin, which could compromise their water management capacity [29].

A new drainage system, equipped with pumps (visible in Figure 5.12), has been constructed that conveys water to a discharge point (A) in the Sømose stream and two points (B,C) in the Harrestrup stream (A).



Figure 5.12: Three water diversions into the Sømose and Harrestrup Rivers [29]

However, the construction of a planned dike, that will be illustrated in the section 5.2.1, around the basin will interrupt this natural path, causing the water to accumulate and the resulting risk of flooding the family garden area. The new drainage system is not expected to be sized to cope with the volumes generated by extreme rain events (cloudbursts) [29].

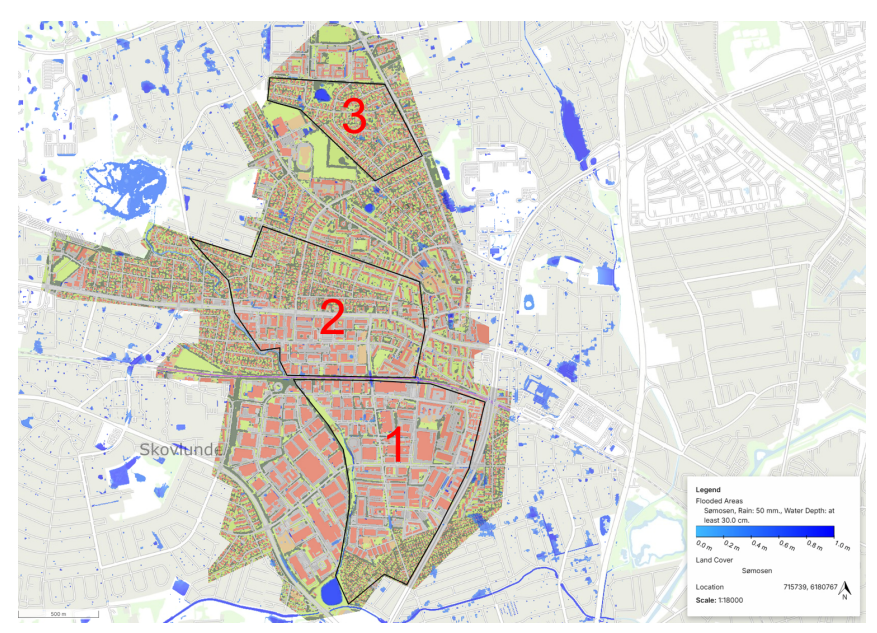


Figure 5.13: Topographic map showing flooded areas within the catchment with outlined 3 areas based on a 100-year rainfall event projected over the next years (2026-2070), generated using SCALGO.

More focus is placed on three distinct zones (outlined in black in Figure 5.13) that exhibit a high concentration of water depths. In particular, Area 1 and Area 2 are more exposed to flooding risk due to their proximity to the watercourse. These zones were selected based on their differing characteristics to explore a range of Nature-Based Solutions (NBS) suitable for each specific context. The selected areas will be examined in detail in Section 6.2.

Elevated groundwater levels

Figure 5.14 shows the most probable groundwater levels near the surface during winter, based on model simulations covering the period 1990–2020. The term most probable refers to the statistically most frequent groundwater level occurring during the winter season across the modeled time span. The data were produced using the national DK-Model HIP (Hydrological Information and Prediction), developed by GEUS (Geological Survey of Denmark and Greenland). This physically based hydrological model simulates groundwater and surface water interactions across Denmark and was run at a spatial resolution of 100 meters. The results were subsequently downscaled to a 10-meter resolution using machine learning techniques, and the visualization was generated using SCALGO Live.

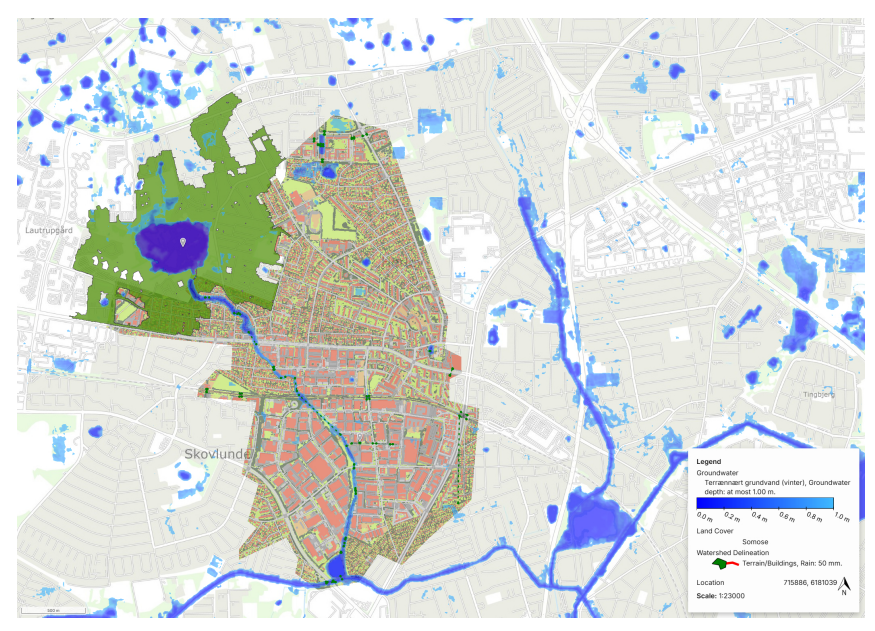


Figure 5.14: Groundwater levels near the surface (1990-2000 model) in winter with a 1 m groundwater depth threshold and 50 mm rainfall input, provided by SCALGO

Focusing on the catchment area, the highest groundwater levels (light blue) are concentrated near the watercourse and towards the northern part of Herlev, ranging between 0.8 meters and 1 meter. These are the same areas affected by flooding, as previously explained. This confirms that these are the most vulnerable areas to flooding. Here is indeed a correlation between flooding and groundwater levels. When an aquifer is already saturated with water, it becomes less able to absorb additional water from rainfall. This is because the ground, having already absorbed as much water as it can hold, cannot accommodate any more, leading to an increase in surface runoff. This runoff can then contribute to flooding, as the excess water flows overland instead of infiltrating the ground.

In areas where the groundwater is at or near the surface, especially during periods of heavy rainfall, the risk of flooding can be heightened. The saturated aquifer prevents effective drainage, which exacerbates the risk of water accumulating on the surface and flooding the surrounding areas[32].

The situation is markedly different in summer, as illustrated in Figure 5.15.

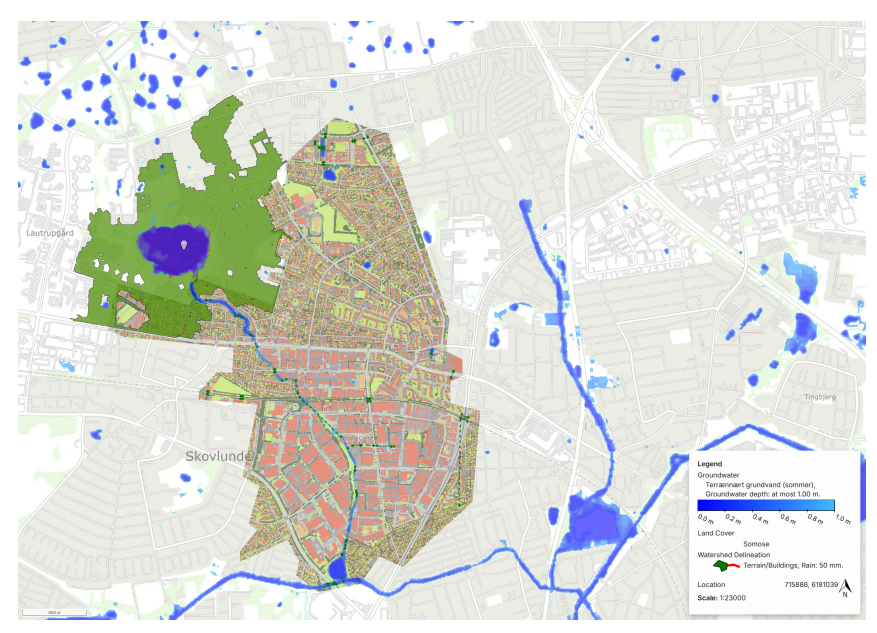


Figure 5.15: Groundwater levels near the surface (1990-2000 model) in summer with a 1 m groundwater depth threshold and 50 mm rainfall input, provided by SCALGO

During this season, only a few areas within the catchment show groundwater levels within 1 meter of the surface, primarily ranging between 0 and 1 meter. These zones are mainly concentrated in the northern part of Herlev. This reduction in shallow groundwater extent is largely due to lower precipitation and higher evapotranspiration rates during the summer months, which limit groundwater recharge compared to winter conditions.

5.1.4 Uncertainties

Numerous uncertainty, both governmental and climate-related, could have an impact on the watershed. Particularly because it has the potential to change rainfall patterns and hence have an immediate effect on the watershed, climate change is a significant source of uncertainty. However, urbanization is fueled by population growth, which frequently prompts towns to replace natural spaces with urban constructions, changing the land use significantly. As a result, this reduces the available space for the application of NBS, which may limit how well they may solve environmental problems.

5.2 Harrestrup Å - Capacity Plan

Ten municipalities within the metropolitan area of Copenhagen (Denmark), together with their utility companies, have collaborated to develop a plan, called *Capacity Plan* for the Harrestrup Å (river) system. The goal of this partnership is to safeguard residents in the catchment area from damage caused by river events occurring up to once every 100 years, projected over the next 30 years, using the most effective methods [28].

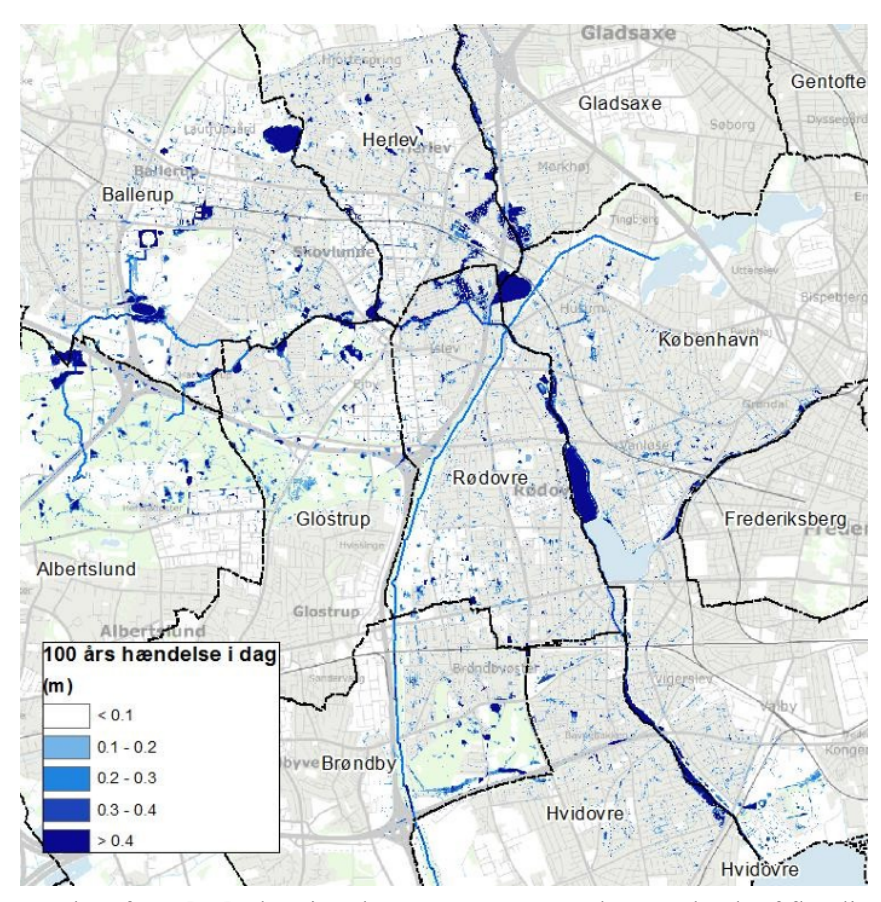


Figure 5.16: Map taken from [28], showing the current extent and water depth of flooding during a 100-year rain event in the catchment area of the Harrestrup river system. Flood-prone areas in the Copenhagen region are identified in the *Capacity Plan*, with colors indicating estimated water depths — from less than 0.1 m (white) to more than 0.4 m (dark blue). The network of the Harrestrup river is highlighted in black [28]

The plan has two primary objectives: first, the municipalities within the catchment area must be equipped to manage cloudbursts by directing rainwater to the river through designated cloudburst pathways. Second, areas adjacent to the Harrestrup River system need protection against flood damage from river events up to the 100-year severity projected into the next 100 years (starting from the year 2018). In the case that this level of protection is not feasible or possible in some areas, the service level may be lowered to a 100 year event projected in 30 years into the future. While the *Capacity Plan* focuses on protecting the Harrestrup river system itself, the responsibility for cloudburst protection lies with the individual municipalities.

Because the river has insufficient capacity to manage the large volumes of water, flooding has occurred along the Harrestrup river system and in the upstream municipalities.

The issues have emerged because the original Harrestrup River valley has been extensively developed and modified over the past 100 years. As a result, the river now runs through the region in a confined channel that is often unable to handle the large volumes of rainfall it receives [28].

Launched in 2015, the Capacity Plan is a collaborative effort between these cities and their wastewater management utilities. The goal of this partnership is to ensure that the river system can handle stormwater and prevent catastrophic flooding.

The participating communities have committed to sharing responsibility for the Harrestrup river system through this cooperative effort, pooling their resources and efforts to deliver the most effective and lasting outcomes.

The plan promotes integrated planning and development to ensure adequate capacity and optimal use of the river.

In addition to flood protection, the *Capacity Plan* seeks multifunctional solutions that provide benefits during drought conditions. This includes the development of recreational floodplains that are usable under everyday conditions and robust enough to withstand sporadic flooding.

Other important information for the delineation of the Capacity Plan—such as an overview of the solutions and the sequence plan—is reported in the Appendix, Section A.1.1 and Section A.1.1.

5.2.1 Subproject-Sømose Å

Delineation of the context

For the development of this thesis, one of the subprojects—Sømose Å—has been selected according to NIRAS, that is involved in this project as the main consulting company.

Sømose Å is a tributary of the Harrestrup Å river, connected via the Hanevad basin. The Harrestrup river system comprises the main watercourses-Damhusåen and Harrestrup Å-as well as several tributaries, including Kags Å, Sømose Å, Rogrøften, Bymoserenden and Grøndalsåen. The Sømose Å project includes sub-projects identified with the numbers 2.07, 1.09 and 1.10, and is part of the northern section of the Harrestrup River Capacity Increase Project, as indicated by the red sign on the map in Figure 5.17 [29].

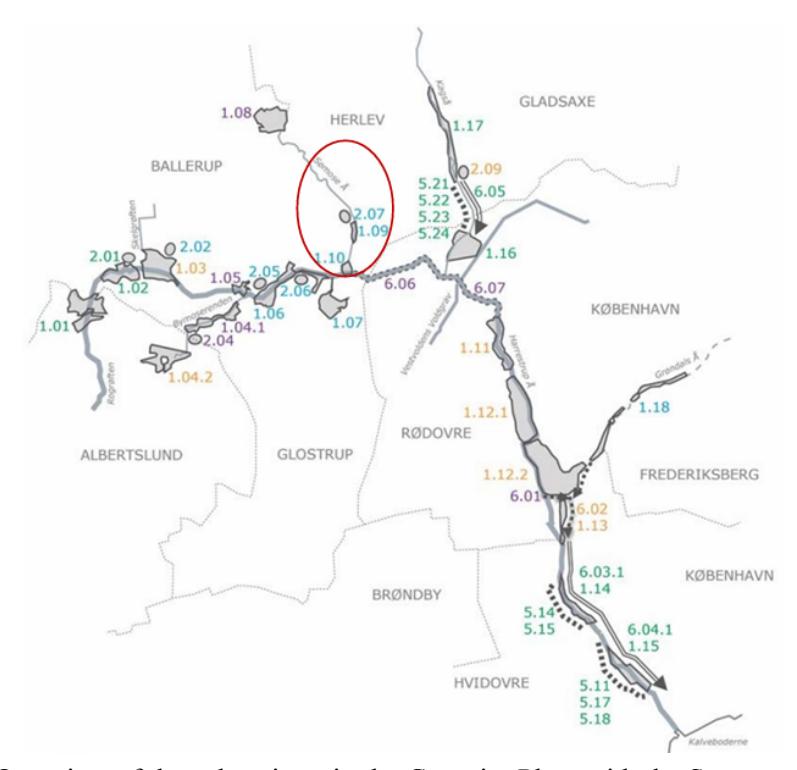


Figure 5.17: Overview of the subprojects in the Capacity Plan, with the Sømose subproject highlighted with a red circle. [29]

The project area is limited to the section delimited by the red outline in Figure 5.18.



Figure 5.18: Overview of the project area. The red boundary indicates zones where construction activities are planned, while the grey boundary marks areas included in the project where no construction work is expected [29].

The project area includes several key elements: the construction of a new pipeline under Herlev Hovedgade (indicated with red circles in Figure 5.18, a tunnel under the railway line, the reopening of a currently piped section downstream of Ellekær, the excavation of reservoirs north and south of Mileparken and the construction of protective embankments [29]. Further details on lowland restoration and ecological connectivity in the Sømose Å area—along with illustrative maps and relevant classifications—are provided in Appendix A.1.2.

Into the project:hydraulic aspects

According to the Capacity Plan for Harrestrup Å and sub-project descriptions 1.09 (Figure 5.19) and 1.10 (see Figure 5.20), the storage capacity of the Hanevad basin must be increased to hold 100,000 m³ of water. In addition, an additional volume of 15,000 m³ must be designed at the same water level of 11.73 meters in an area along the Sømose Å, south of Mileparken. Altogether, a total volume of 115,000 m³ must be managed at this same level [29].

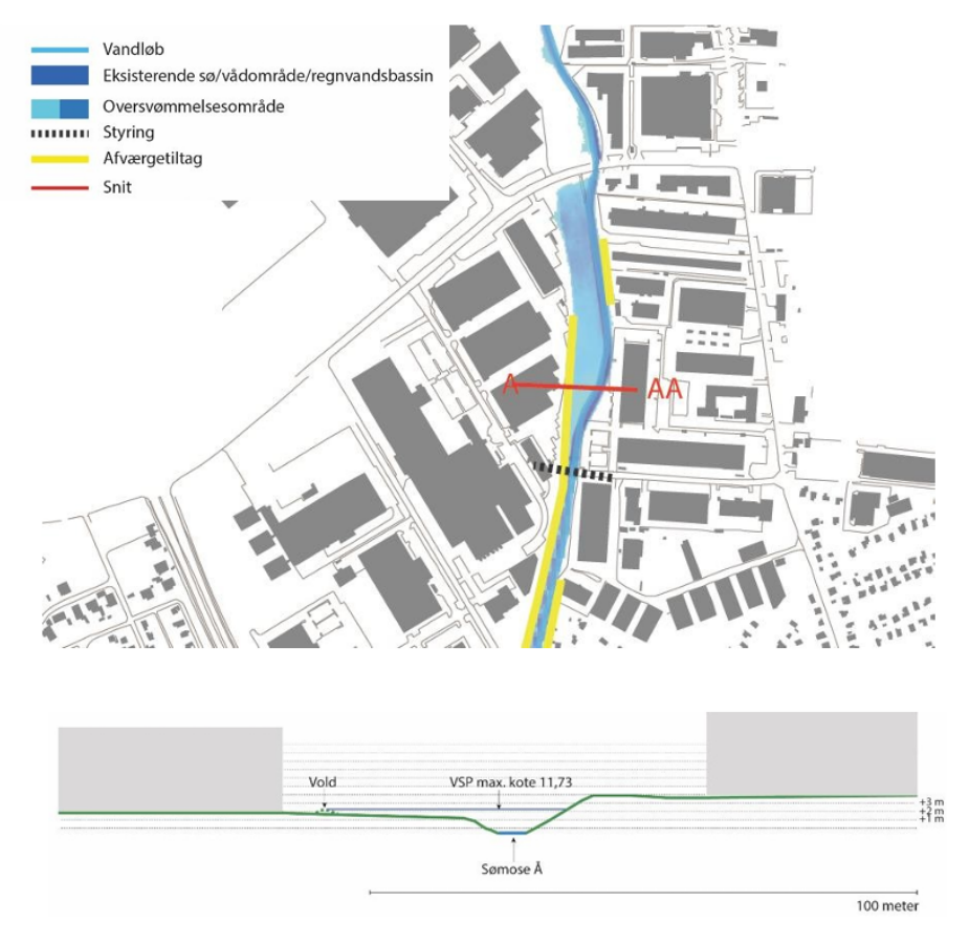


Figure 5.19: Floodplain representation of sub-project 1.09 with corresponding cross-section A–AA [33].

The sketch and cross-section for subproject 1.09 in Figure 5.19 show that the area along the Sømose Å was found to be suitable to temporarily hold water during extreme weather events. The area designated for flooding (Oversvømmelsesområde) can accommodate maximum water levels of VSP ¹ max= 11.73 m DVR90², regulated by hydraulic devices (Styring) such as a sill and choked drain. These elements ensure ordinary flow under normal conditions and controlled backwater during heavy rainfall [33]. Hydraulically, the intervention contributes to reducing and smoothing out discharge, lowering the risk of sudden rises in water level and preserving the base flow during dry periods. Furthermore, the delayed runoff during cloudbursts contributes to improving water quality by reducing erosion pressure [33]. The total maximum volume is 15,000 m³ [33].

In order to protect the surrounding urban areas, particularly to the southwest of Mileparken, a protective embankment (Afværgetiltag) with a top elevation of 11.80 m DVR90 is planned [33]. The existing watercourses (Vandløb) and lamination basins (Eksisterende sø/vådområde/regnvandsbassin) will be maintained, and water quality is expected to improve due to the delayed discharge, which reduces the risk of erosion during flood peaks [33]. As illustrated in the cross-section below (AA), the floodplain on both sides of Sømose Å is framed by embankments (Vold), which provide local flood protection and define the maximum water level elevation at 11.73 m DVR90 [33]. Although the intervention is primar-

¹VSP: maximum water level elevation [33]

²DVR90: Danish Vertical Reference 1990, the official vertical datum used in Denmark to indicate elevation above sea level. It is based on mean sea level measurements from 1990. [34]

ily functional, it does not exclude the possibility of future recreational use, provided that the hydraulic functionality of the area is not compromised [33].

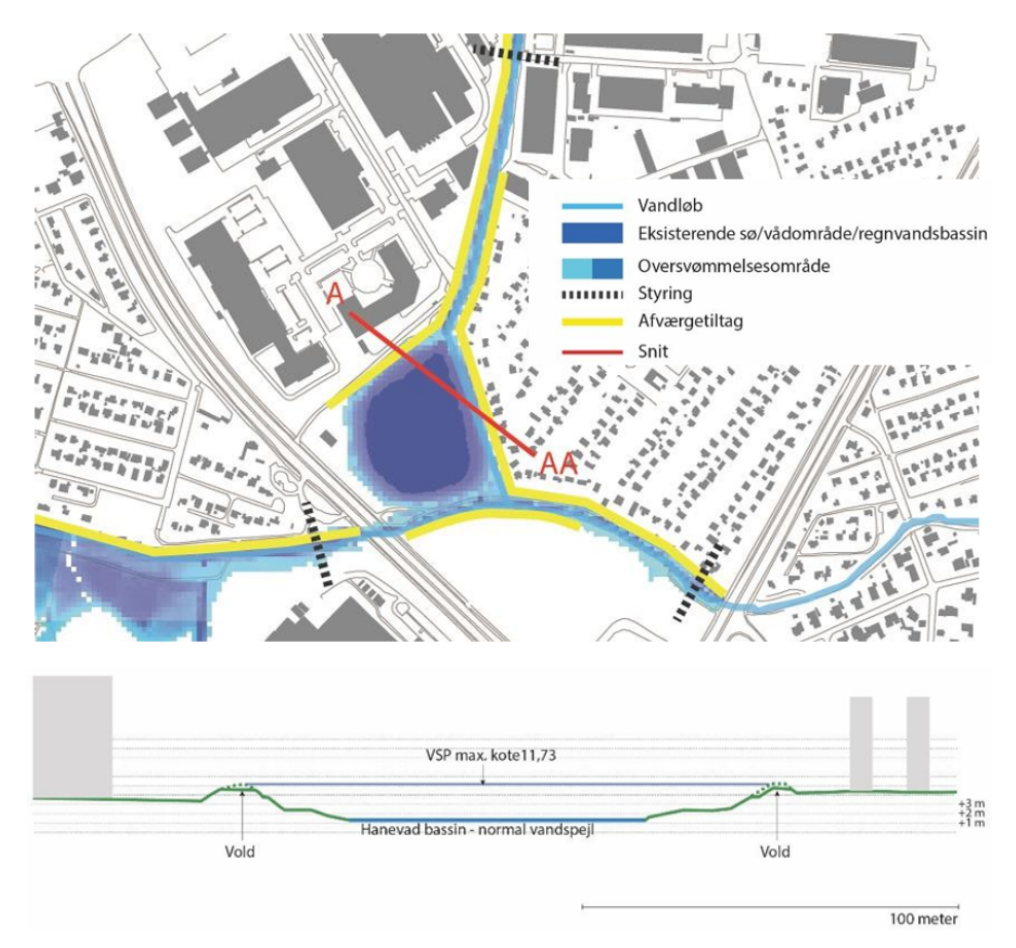


Figure 5.20: Floodplain representation of sub-project 1.10 with corresponding cross-section A–AA[33].

As in sub-project 1.09, the area around the Hanevad basin in sub-project 1.10 (Figure 5.20) was also analysed and identified as suitable for temporary water storage during heavy rain events (cloudburst). The intervention follows the same hydraulic effects: reduction and lamination of runoff flows, maintenance of base flow in dry conditions and improvement of water quality through delayed discharge, which helps to limit erosion. Recreational use of the area remains possible as long as it does not compromise the hydraulic functionality of the intervention [33].

An analysis of the area, confirmed the possibility to estabilish controlled flooding, with a total volume of accumulation estimated at 100,000 m³. Water can safely stagnate up to a critical height of 10.35 m DVR90 without the need for protective measures. Hydraulic control (Styring) will be ensured by means of a sluice gate and choked outlet, which will ensure the normal daily flow and, during extreme events, the controlled return of water to the overflow areas. This will allow the water level of the Sømose Å watercourse to rise to a maximum of 11.73 m DVR90 (VSP max) [33].

As shown in Section AA, the adjacent residential areas will be protected by earthen embankments (Vold) with a top elevation of 11.80 m DVR90, providing adequate protection against flooding while preserving the full rolling capacity of the basin [33].

The project was expected to enter its final phase in 2025, with construction originally scheduled for 2026 [33]. However, according to a consultation with NIRAS in 2025, due to technical issues reported at the

time, the project has been delayed by approximately two years and has not yet reached the tendering phase.

Current Urban Water System

All the drainage areas immediately adjacent to the Sømose River consist of zones with separate sewage systems. The service level for the rainwater drainage pipes has been politically set to manage rainfall events with a return period of 5 years. Consequently, it is assumed that the network can handle events of this magnitude, while more intense storms may lead to surface flooding and sewer overflows [35]. Figure 5.21 provides a schematic representation of the urban water management system.

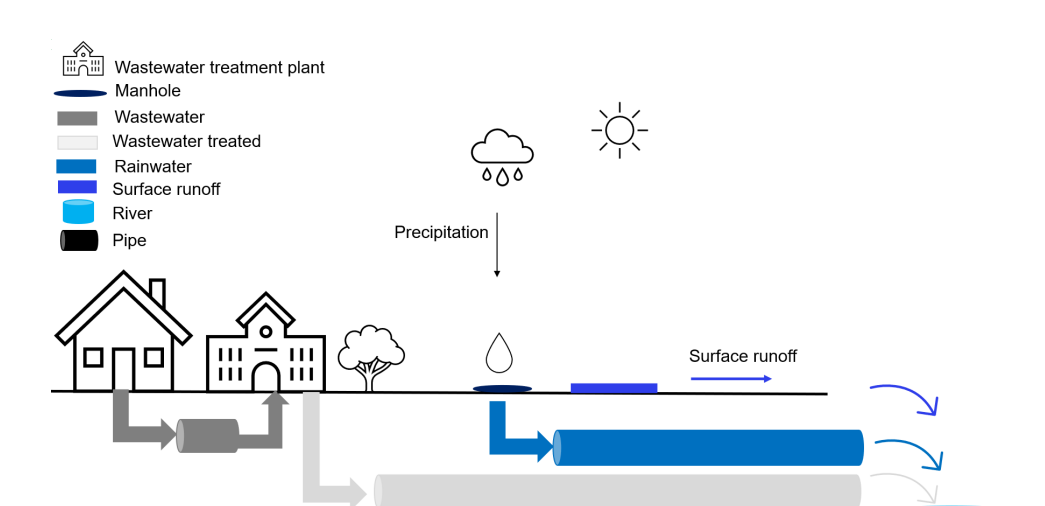


Figure 5.21: Simplified representation of the urban water management system in the Sømose Å Catchment.

As shown, there are three main sources of flow reaching the stream:

- Treated wastewater, which originates from households and is conveyed via underground pipes to the wastewater treatment plant, from where it is discharged into the river.
- Rainwater from the subsurface drainage system, infiltrated through manholes and transported via underground pipes.
- Surface runoff, which flows directly into the stream when rainfall exceeds the infiltration capacity and is not captured by the drainage system.

5.3 Nature Based Solutions (NBS) selected

For the selection of NBS for the catchment studied area, following the guidelines provided by *UNaLab* [36], several parameters were considered, including the space required for implementation, the challenges faced, the benefits and co-benefits, as well as the performance of different NBS sub-types (e.g. infiltration, habitat creation, water storage). NBS must first of all be consistent with the specific characteristics of the context-such as soil type ,local conditions and with the problems to be solved. The main challenge identified is the risk of flooding.

Another key criterion for selection was the availability of useful data on each solution, such as parameters the identify their ability to retain water, essential parameters for proper implementation.

In addition to the identification of flooded areas, it was considered essential to understand where rainwa-

ter comes from, so that it can be retained or slowed down before it reaches critical areas.

Taking into account all the criteria mentioned above, the selected solutions for the catchment area are: permeable pavements, rain gardens, bioswales and green roofs, which will be described below.

5.3.1 Permeable Pavements

Permeable pavements, as shown in Figure 5.22, are surfaces that allow rainwater to infiltrate, while remaining suitable for pedestrian use or light vehicular traffic , such as in car parks or low-traffic roads. Water can infiltrate into the underlying soil or be temporarily retained and released with delay in the drainage system [37].

There are two main types of permeable pavements: porous pavements (such as porous asphalt) and pervious pavements. Porous pavements allow water to pass directly through the material itself. In contrast, pervious pavements are composed of impermeable elements laid with gaps between them or over a permeable subgrade, allowing infiltration through joints or voids [37].

Grassy reinforcement grids, filled with gravel or grass, can only be used in areas with little traffic, such as pavements, schoolyards, private driveways, hotels or company car parks [37].

Permeable pavements provide temporary storage capacity, helping to reduce the flow and peak runoff of rainwater. They also help filter pollutants such as heavy metals, oils, fats and some nutrients [37].

Different studies assess that porous aspalt provides high runoff reduction, but it depends from serveral factors, such as intensity of rainfall events but also the size of the application. For example for stormwater, studies assess that porous asphalt reduces runoff by 70 to 90% [36].

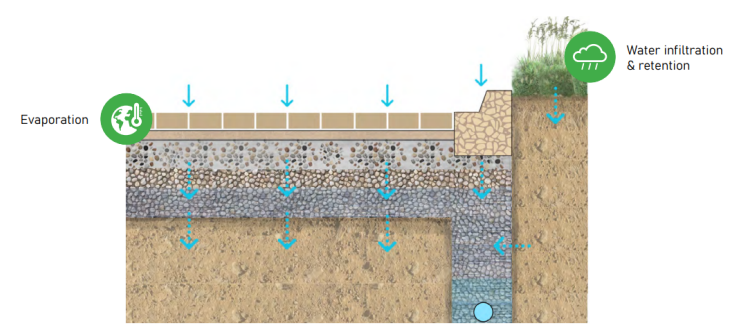


Figure 5.22: An example of a permeable pavement, along with the natural processes it supports and the resulting environmental benefits [38].



Figure 5.23: Example of permeable pavement [36].

Focusing on porous asphalt, there is an ongoing debate about its categorization. Indeed, some consider it as a NBS, because it is inspired by natural soil, as it functions as a porous medium that mimics the permeability and drainage characteristics of soil; while others don't associate it to a NBS because it is

not directly related to nature.

Comparing to the regular asphalt, porous asphalt is composed from larger stones and from different asphalt binders [36]. Its implementation can be challenging, as it often requires the roads to be repaved, which wastes resources and energy. One of the main advantages is that it does not require additional space: it allows stormwater regulation on the same surface used for vehicular traffic, making it an efficient solution in urban settings.

Porous asphalt has been selected for the catchment considering, as explained in Section 6.2, the land cover characteristics of Areas 1 and 2. These zones present a high percentage of grey areas, including paved roads, which are the target surfaces for the implementation of porous asphalt. The aim is to reduce runoff generated from these surfaces, due to their low infiltration capacity.



Figure 5.24: Porous asphalt[36]

5.3.2 Bioswale

Bioswales (or vegetated swales) are generally linear, wide, shallow depressions (or open channels), covered with vegetation. They are planned to manage stormwater runoff, conveying rainwater from impermeable surfaces, such as roads or roofs, allowing it to infiltrate through the permeable soil. They are often placed in urban areas, along or between roadways, with the goal of reducing the risk of flooding during or after intense rainfall events [37].



Figure 5.25: Example of bioswale [36]

In addition to water management, bioswales play an important role in urban biodiversity. Indeed, they introduce vegetation into areas usually lacking in vegetation cover, providing habitats for local fauna. However, a limit is provided by the trees, their excessive presence couldn't allow the water conveyance. Thus, the habitat provision is limited just on the ground level[36].

Another fundamental function of bioswales is the reduction of water pollution. When rainwater flows through vegetation and soil, sediments and pollutants are retained, helping to improve water quality [36]. Figure 5.26 provide a semplified scheme of the the natural process before explained, such as water conveyance, infiltration and evaporation. Additionally, they are able to address water pollution: indeed, biosowale can remove pollutans and sediments, when water flows through the vegetation and the soil layer [36].



Figure 5.26: Bioswale with its related natural processes and benefits [38]

There is a broad choice for the selection of the vegetation, but usually deep-rooted native plants are preferred [36]. In order to have an efficient water infiltration, some swales are equipped with dams or similar constructions [36]. Bioswales are not restricted by national boundaries or climatic conditions [36].

The choice of vegetation is wide, but deep-rooted native plants are generally preferred to ensure stability and functionality. In residential or visually sensitive contexts, herbaceous or ornamental species are often preferred for aesthetic reasons [36].

For their application, bioswales don't have any limitations related to geographical context. However, it is essential that rainwater is properly collected and conveyed to the system. In addition, sufficient space must be available for implementation and, where possible, it is recommended to complement their use

with multifunctional functions, such as recreational spaces [36]. Evaporation plays an important role in the water cycle of the bioswale: some of the retained water evaporates into the atmosphere. In this way, bioswales regulate water balance and improve air quality.

From a technical perspective, the construction of a bioswale requires attention with specific design parameters. The minimum width of the base must be 0.5 meters, while the maximum depth is generally between 400 and 600 mm. The longitudinal slope of the should not exceed 6% [37]. Additionally,the length of the swale should be equal or greater to that of the adjacent road [37].

The performance of a bioswale depends on several factors, including the size of it, the intensity and frequency of rainfall events, and regular and proper maintenance.

Bioswales have different responses in dependence of the rain event. During light rain events, bioswales don't generate runoff. On the other hand, during heavy rainfall events, the swale acts mainly as a conveyance channel, helping to delay peak runoff and reduce the water load in drainage systems. Different studies report that bioswale can reduce runoff volume from the 23 to 48 % [37]. In particular, bioswales have been selected for the catchment with the aim of being applied to the land cover category labeled as "other paved" in SCALGO Live, which typically includes sidewalks and parking lots. As will be described in Section 6.2, this category, part of the grey area, has a high presence across all zones and significantly contributes to runoff. Bioswales are especially suitable for Areas 2 and 3, which have a high concentration of residential land use—contexts where bioswales are commonly implemented.

5.3.3 Rain garden

The rain garden concept is applied in the urban context, inspired by the principle of the "sponge city" (i.e. an urban planning approach that aims to make cities capable of absorbing, retaining and reusing rainwater, reducing surface runoff and promoting groundwater recharge), but with one substantial difference: unlike the latter, the rain garden does not involve the creation of a root porous structure suitable for tree growth, as trees are generally not compatible with this type of application [36].

Rain gardens are classified as bioretention systems, consisting of small areas excavated in urban settings, filled with a specially designed substrate. This substrate layer, usually between 0.7 and 1 meter deep, consists of a mixture of high permeability soil, sand and organic matter, and is generally covered with a mulch layer [37]. Bioretention systems are designed to allow temporary retention of rainwater, with water depths between 15 and 30 centimeters above the substrate [37]. These systems are effective in controlling peak discharge, achieving reductions between 44% and 99% [37]. In addition, they contribute to the reduction of both stormwater volumes and pollutant loads [37].

In urban contexts, rain garden is used for small-scale water management, functioning as a type of urban infiltration basin. Rainwater is usually collected from adjacent streets or roofs and then conveyed into the system [36]. Generally, rain gardens have a compact size [39].

Similar to bioswales, the choice of vegetation is a crucial element. Indeed, it's important to use dense vegetation, preferably native. The selection of plant species should also differ for each zone of the rain garden [36].



Figure 5.27: Rain garden [40]

The operating mechanism of a rain garden (illustrated in Figure 5.28) is similar to that of a bioswale, which is why the two systems are often compared. Rainwater is conveyed into the rain garden, where it is temporarily retained, and then infiltrates the soil or flows into the sewer system. Part of the water is absorbed and transpired by the plants [36].

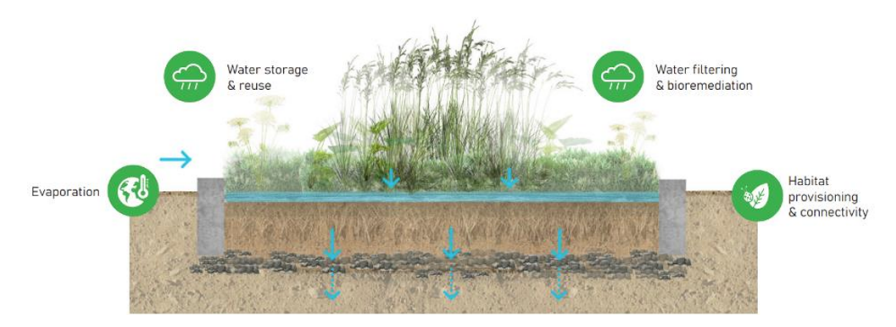


Figure 5.28: Raingarden with its related natural processes and benefits [38]

Rain gardens are not constrained to specific climatic conditions. As with bioswales, regular maintenance is required to ensure proper functioning. A moderate slope favours infiltration, and adequate space availability is a necessary condition for their construction [36].

As with bioswales, the choice of aesthetically pleasing plant species is important, especially in residential areas or public spaces where landscape integration is important. In addition, rain gardens help to counteract the loss of biodiversity by introducing vegetation in urban areas that often lack green spaces [36]. The selection of rain gardens for the catchment area follows the same considerations made for bioswales. The difference that led the choose between them depends on the available space, as will be explained later in 6.2.

5.3.4 Green roofs

When a city is predominantly made up of buildings, a strategic solution for rainwater management is green roofs. A green roof consists of several layers installed roof structure of the building, with a vegetated upper surface [37].

There are two main types of green roofs: extensive and intensive.

Extensive green roofs have a thin substrate layer, less than 150 mm, and are characterized by plants that require low maintenance, such as grasses and herbs [37]. Their vegetation is often installed on rooftops that are not intended for public access or recreational purposes [36].

On the other hand, intensive green roofs have a deeper substrate, above 150 mm, with higher variety

of vegetation, but also requires more maintenance [37]. Their vegetation is often estabilished on rooftops that are intended for public access or recreational purposes. Indeed, they always provide space for human activities: gardening, relaxing and socializing [36]. A visual comparison of both types is shown below. Green roofs help address several urban challenges. They are able to manage stormwater by temporarily



(a) Extensive green roof [41]

(b) Intensive green roof [42]

retaining rainwater, reduce the urban heat island effect, cool buildings through evapotranspiration, improve air and water quality,improve biodiversity and increase the aesthetic value of buildings [37]. The two figures below illustrate the structural layering of both extensive and intensive green roofs, highlighting the properties discussed above.

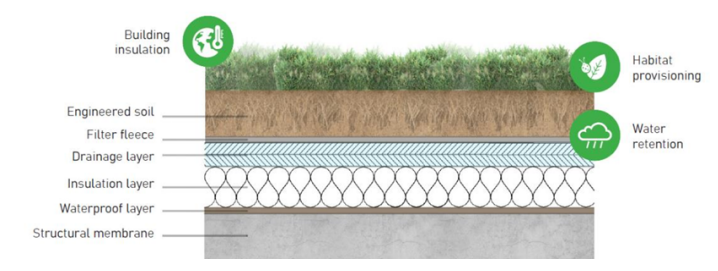


Figure 5.30: Conventional layer of extensive green roof [38]



Figure 5.31: Conventional layer of intensive green roof [38]

The ability of a green roof to retain rainwater depends on several factors, such as the thickness of the substrate layer, the type of vegetation and the slope of the roof [37].

As also observed in other NBS previously mentioned, the effectiveness of green roofs in mitigating flood risk is influenced by several variables. One of the main factors is rainfall intensity, that influences how much water is absorbed by the substrate and then returned to the atmosphere through evapotranspiration [37].

Another important factor is the runoff generated after the attenuation time of the flood peak, which depends on both the intensity of precipitation and the degree of substrate saturation. When the rainfall is light and the substrate is dry, no runoff is generated and the water retention capacity is 100%. On the other hand, when the rainfall is heavy and the substrate is already saturated, runoff is generated almost immediately and the retention capacity is significantly low[37].

Green roofs are among the most studied NBS, and from numerous studies emerges that they can reduce average runoff volumes by approximately 56% to 71% [36]. The implementation of green roofs requires certain conditions, including solid and stable concrete buildings, flat concrete roofs or underground concrete structures, and artificial irrigation systems or, at least, a rainwater-based irrigation system. However, there are some limitations, such as limited undisturbed habitat development due to human activities or public use, a reduced spread of flora and fauna due to regular maintenance and management, and limited space for root development[36].

Green roofs are selected for the catchment area because, as mentioned in Section 5.1.3, the three zones—particularly Areas 1 and 2—show a high percentage of grey areas, with a significant presence of buildings. These buildings represent the surfaces where green roofs will be implemented.

In particular, Area 3, being predominantly a residential zone, is more suitable for the application of intensive green roofs. In contrast, Areas 1 and 2, which include both residential and industrial zones, are suitable for the implementation of both intensive and extensive green roofs.

5.3.5 Summary of the NBS selected

Table 5.2 gives an overview of the selected NBS, pointing out their limitations, the conditions under which they can be used, and the costs involved. To evaluate their effectiveness in addressing flooding, the table also includes runoff reduction values, expressed as percentages, for each NBS. The reported values represent a reference value assumed valid in this thesis for rain events with a return period of 5 years. This parameter is relevant, because, as it will be explained in the section 6.3, is a key point in process of the application of NBS through SCALGO Live.

Since the runoff reduction values reported in Section 5.3 come from various sources and use different metrics (e.g., some refer to peak flow reduction), a consistent and comparable reference was needed. Therefore, the values used are derived from the table in Figure 4.7, calculated as the average between the median and the 75th percentile of the reported range. An exception is made for porous asphalt: in Figure 4.7, the values are associated with the broader category of permeable pavements, and porous asphalt is not always explicitly included in this group. To ensure consistency with the range previously provided in the Figure 4.7(70–90%), a value of 75% has been adopted, corresponding to the 75th percentile of the range reported. Rain garden is associated with the runoff reduction values reported for bioretention systems in Table in Figure 4.7. since, as explained in Section 5.3.3, it is often categorized as a form of bioretention. For bioswales, the values corresponding to dry swales are adopted, as they are more appropriate when compared to wet swales. The main difference between the two lies in their infiltration capacity, which is the key feature relevant to this application. Dry swales promote infiltration and are

therefore more effective in reducing runoff volume, whereas wet swales primarily function as biofiltration systems designed to improve water quality [43]. Extensive and intensive green roofs are assigned the same runoff reduction value in Table 5.2, since no distinction between them is made in the data presented in Figure 4.7. For this reason, when green roofs are applied in the three selected areas, it is not possible to differentiate their performance in terms of runoff reduction. As can be seen from the Table 5.2, porous asphalt has the highest runoff reduction, followed by rain gardens, bioswales and green roofs. Due to the lack of standardized and information of the costs for some NBS (such as porous asphalt in the Table [19], the reported values are derived from an integration of different sources ([19],[44],[45]). All costs take into account both installation and maintenance.

NBS		Challenges addressed				Runoff reduction (%)	Cost (€/m²)	Conditions for implementation	Limitations		
	Flooding	Water/Air pollution	Biodiversity loss	Heat stress	Rapid urban growth	Health issues (climate)	Habitat loss				
Porous asphalt	X							75	100	Road has to be repaved	_
Rain garden	X		X					60	1.38	Space	_
Bioswale	X	X	X					50	72.73	Stormwater from roofs/roads need to be collected to direct them into the bioswale; Space	Habitat provision limited on ground level due to low presence of trees
Extensive green roof	X	Х	X	X		X		52	109	Suitable for existing buildings with structural limitations	Does not address rapid urban growth and habitat loss
Intensive green roof	X	X	X	X	X	X	X	52	273	Requires strong structural support; suitable for new or retrofitted buildings	High cost; higher maintenance; limited applicability to existing lightweight roofs

Table 5.2: Comparison between the selected NBS

6 Methodology

6.1 Catchment Climate Scenarios

In this thesis, particular attention is given to precipitation scenarios within the studied catchment area, with a focus on the Representative Concentration Pathways (RCP) 2.6, 4.5, and 8.5.

5 year event

The starting point for these scenarios is a 5-year return period event—defined as a rainfall event that has a statistical probability of occurring once every five years on average. As explained in Section 5.2.1, the current drainage system in the catchment is designed to manage events of this magnitude, making it a critical reference point for assessing potential flooding risks.

The Danish Meteorological Institute (DMI) provides predicted precipitation values for events with a return period of 5 years and a duration of 60 minutes (see Figure 6.1). Indeed, through their online platform *Climate Atlas* [46], it is possible to obtain these data by selecting a point within the catchment area. These values are associated with the different RCP scenarios previously mentioned (2.6, 4.5, and 8.5) [31].

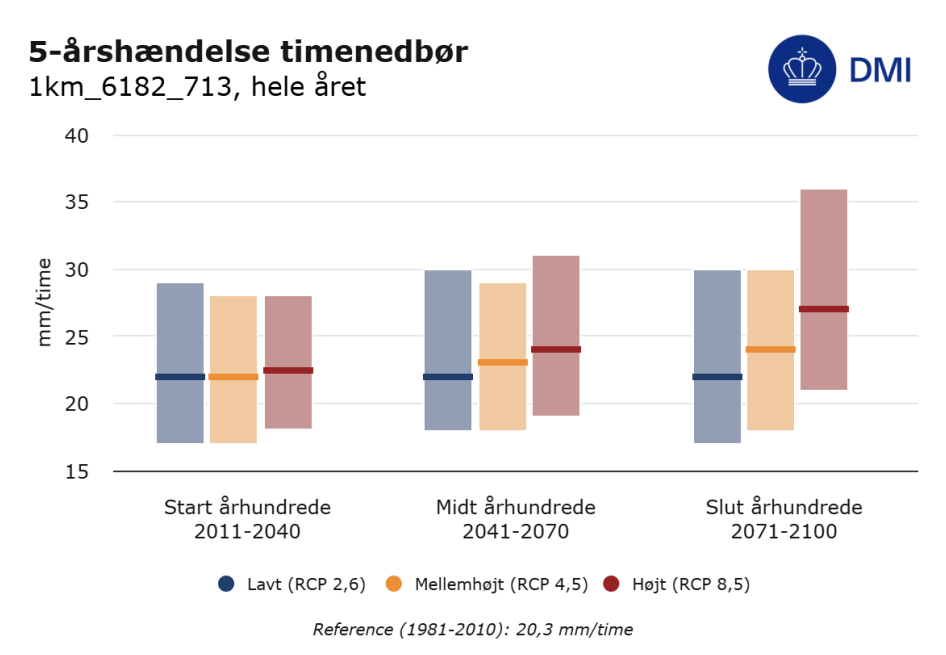


Figure 6.1: Projected 5-year return period hourly precipitation for the catchment area under three climate scenarios (RCP 2.6, RCP 4.5, RCP 8.5) for the periods 2011–2040, 2041–2070, and 2071–2100. The bars represent the range of model outputs, while the horizontal lines indicate the median values. The reference value from 1981–2010 is 20.3 mm/h [31].

Taking into account the median precipitation values reported in the Figure 6.1, the Climate Factor (CF) was calculated for each precipitation value and each RCP scenario using the following formula [47]:

$$CF = \frac{i_{t_0 + \Delta t, T, dur, location}}{i_{t_0, T, dur, location}}$$
(6.1)

where:

- $i_{t_0+\Delta t,T,dur,location}$ is the intensity of the climatic event at a future time $(t_0 + \Delta t)$, for a given return period T, event duration dur, and geographical location;
- $i_{t_0,T,dur,location}$ is the reference (historical) intensity of the same event at time t_0 , using the same T, dur, and location;
- CF is the Climate Factor, which quantifies the projected change in event intensity due to climate change.

The Climate Factor is a parameter used to quantify the impact of future climate conditions relative to historical baselines. In this analysis, it is defined as the ratio between the projected future precipitation intensity and the historical reference intensity, as derived from the DMI dataset shown in Figure 6.1. The following graphs illustrate the Climate Factor computed for each RCP scenario and time period, along with the corresponding future precipitation values.

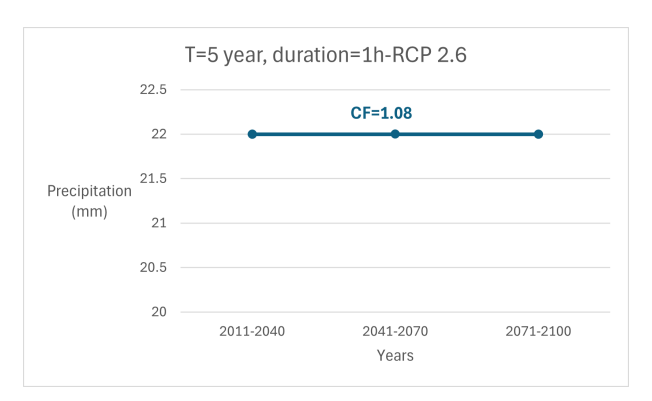


Figure 6.2: Projected 5-year return period hourly precipitation for the catchment area under climate scenario RCP 2.6 for the periods 2011–2040, 2041–2070, and 2071–2100.

As can be seen from the graph in Figure 6.2, under RCP 2.6, the precipitation value remains constant across all three future periods. In this case, the Climate Factor is 1.08. This scenario, often referred to as the "sustainable future", assumes effective climate action and significant reduction of greenhouse gas emissions. The constancy of the CF across the periods reflects a stabilized climate with minimal variation in extreme precipitation events.

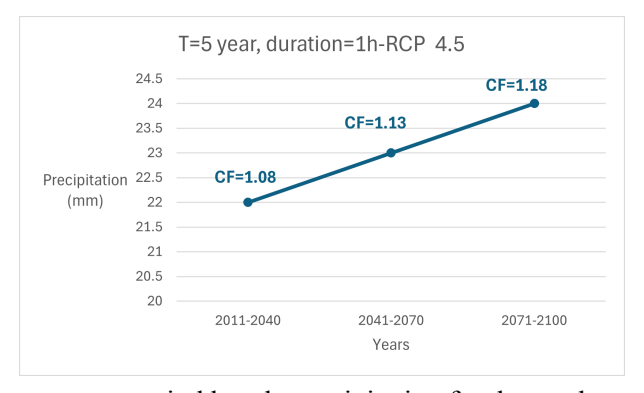


Figure 6.3: Projected 5-year return period hourly precipitation for the catchment area under climate scenario RCP 4.5 for the periods 2011–2040, 2041–2070, and 2071–2100.

The situation differs for RCP 4.5 (the "moderate" pathway), as shown in Figure 6.3, where a linear

increase of approximately 1 mm of precipitation is observed across the three time periods. The climate factor starts at 1.08 (as in RCP 2.6), increases to CF = 1.13 with a precipitation of 23 mm in the period 2041–2070, and reaches CF = 1.18 (24 mm) in the last period. This represents a gradual intensification of extreme precipitation, consistent with moderate mitigation measures.

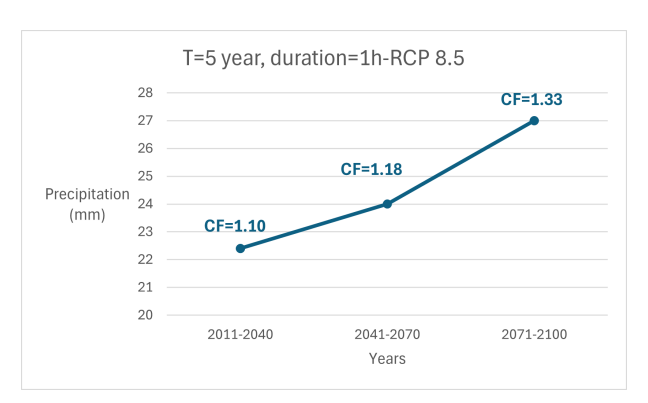


Figure 6.4: Projected 5-year return period hourly precipitation for the catchment area under climate scenario RCP 8.5 for the periods 2011–2040, 2041–2070, and 2071–2100.

For the RCP 8.5 scenario, the increase in precipitation is even more pronounced. As shown in Figure 6.4, a significant change in slope occurs during the second period (2041–2070), indicating a sharper rise. In the first period, the CF reaches 1.10 with a precipitation value of 22.4 mm. This increases to CF = 1.18 (24 mm) in the second period, and finally reaches CF = 1.33 with 27 mm in the last period. While the difference in precipitation between the first two periods is 1.6 mm, the increase between the second and third periods is larger—3 mm. It is important to note that the CF of 1.18, which is only reached in the final period under RCP 4.5, is already reached one period earlier in RCP 8.5. This reflects the more critical nature of the RCP 8.5 scenario, characterized by high greenhouse gas emissions, limited climate policies that increase global warming.

In this study, a duration of 1 hour was initially chosen because the DMI only provides Intensity-Duration-Frequency (IDF) data, which describe the statistical relationship between rainfall intensity, duration, and return period, for just two durations: 1 hour and 24 hours. Among these, the 1-hour duration is more relevant in terms of rainfall intensity, and is therefore used to compute the climate factor. However, a 1-hour duration alone is not sufficient for urban drainage design, as it does not adequately capture the temporal distribution of a critical rainfall event. For this reason, the Chicago Design Storm (CDS) is applied. A Chicago Design Storm (CDS) is a synthetic rainfall event used in hydrological modeling, constructed so that the total accumulated rainfall over a given duration matches the corresponding value from the Intensity-Duration-Frequency (IDF) curve. The rainfall is distributed asymmetrically in time, with the peak intensity typically located near the center of the storm, allowing the event to reflect realistic temporal dynamics of intense rainfall [48].

In this study, a duration of 4 hours was selected for the CDS, as it represents a critical timescale for the catchment area under analysis. This duration is long enough to capture significant runoff generation processes, while still being short enough to represent high-intensity events that are relevant for urban drainage design. Using a 4-hour CDS allows for consistent and representative testing of the system's response across different climate scenarios.

The choice of a 4-hour duration was further supported by a technical consultation conducted in 2025 with experts from NIRAS, who confirmed that this timescale is commonly adopted in Danish practice for the

design and assessment of urban drainage systems.

Therefore, using the SVK spreadsheet [49], the values derived from the 1-hour IDF data were converted to a 4-hour duration. The climate factor originally calculated for the 1-hour event was retained, and the final CDS was constructed with a total duration of 4 hours, which represents a commonly adopted standard in urban hydrological design practice. Due to the lack of available IDF projections for the 4-hour duration, it was not possible to compute a new climate factor specific to that timescale. As a result, the climate factor determined for the 1-hour event was assumed to remain valid for the 4-hour CDS construction. The recalibrated precipitation values are shown in Figure 6.5. RCP 2.6 has a constant value of 34 mm across the three periods; RCP 4.5 has values of 34 mm for 2011–2040, 36 mm for 2041–2070, and 37 mm for 2071–2100; RCP 8.5 shows values of 35 mm, 37 mm, and 42 mm for the respective periods.

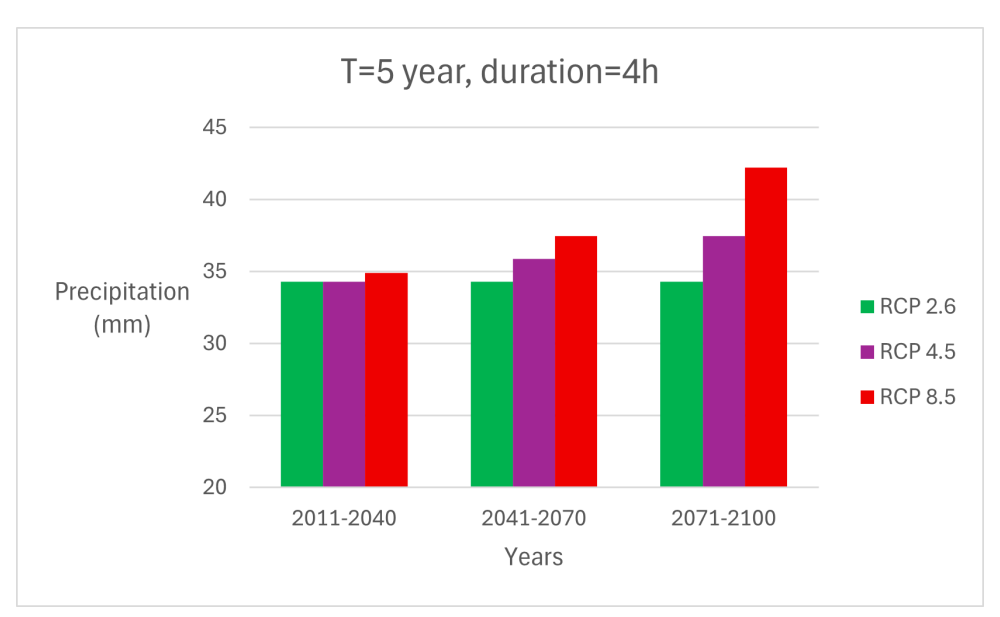


Figure 6.5: Projected 5-year return period precipitation with a 4-hour duration for the catchment area under three climate scenarios (RCP 2.6, RCP 4.5, RCP 8.5) during the periods 2011–2040, 2041–2070, and 2071–2100.

From these new derived precipitation values, a linear interpolation was performed. As a result, the graph in Figure 6.6 was developed, showing the estimated precipitation with a duration of 4 hours and a return period of 5 years, for each year in the period 2025–2100.

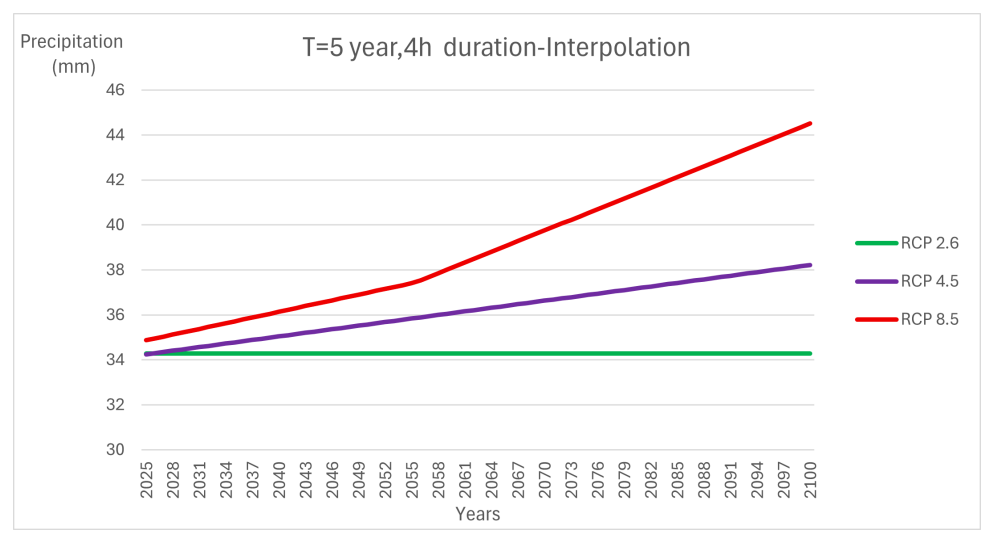


Figure 6.6: Precipitation values for a 5-year return period event with 4 hour duration in the catchment, during the period 2025–2100, under RCPs scenarios.

6.1.1 Tipping point

In order to evaluate flood risk across the entire catchment area based on water depth, a threshold of 0.5 meters has been selected. This value was chosen based on findings from the Water Research Laboratory of the University of New South Wales (UNSW), as reported in their publication Smith [50], which analyzes the impacts of flooding on people, buildings, and vehicles. According to the report, small cars can become buoyant and be washed off roads at water depths as shallow as 0.3 meters. At a depth of 0.5 meters, however, primary-age children and elderly individuals can lose their footing and become unstable. Using the precipitation values previously calculated, the analysis was carried out in QGIS. The Raster Calculator tool was applied to the flood depth raster files exported from SCALGO Live to compute the areas (in hectares) within the catchment exceeding 0.3 m and 0.5 m in water depth.

The 0.5-meter threshold was selected for further analysis in order to account for risks to pedestrians, including the potential loss of stability among vulnerable individuals such as children and the elderly.

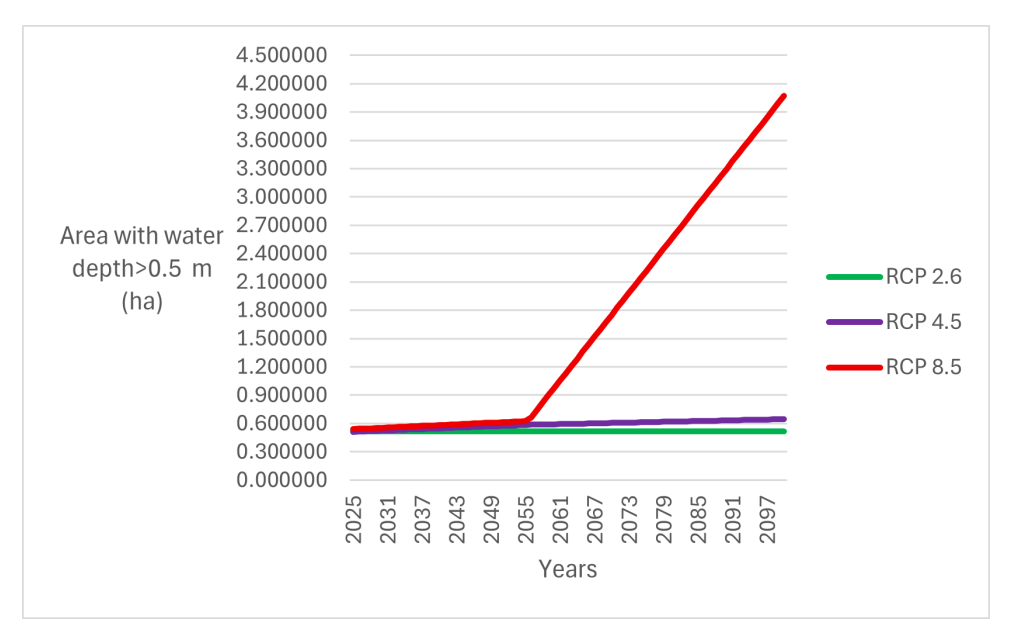


Figure 6.7: Area with water depth above 0.5 m across the entire catchment from 2025 to 2100 under RCP 2.6, RCP 4.5, and RCP 8.5 scenarios. This output is derived from the application of precipitation values corresponding to a return period (T) of 5 years and a duration of 4 hours.

Because a fundamental aspect of the DAPP approach is the identification of the tipping point—as explained in Phase 2 of the DAPP methodology (Section 4.1)—the tipping point has been defined as the actual area with water depth above 0.5 meters recorded in 2025 under the RCP 8.5 scenario, which is equal to 0.541 hectares.

The value for 2025 was selected because, as shown in Figure 6.7, the lines representing the different RCPs begin to diverge after this year, indicating that action should be taken before the gap between scenarios becomes significantly different. A single threshold value was adopted to compare the performance of Nature-Based Solutions (NBS) across all RCPs, in order to highlight the differences in criticality.

The value achieved from RCP 8.5 was chosen for several reasons: to provide consistency with the further future analysis. Indeed, this value is also valid for RCP 4.5, which reaches it in 2036, as will be shown in Section 7 starting from 2025. Instead, it is not reached by RCP 2.6, which maintains a constant value of 0.515 hectares throughout the years. Furthermore, the actual value of RCP 4.5 in 2025 is not reached by RCP 8.5 in future years because it is already exceeded before 2025; likewise, RCP 2.6 does not reach

it either. Additionally, RCP 8.5 represents the most critical scenario that requires the greatest attention and should be avoided with all possible efforts.

RCP	Area with water depth > 0.5 m (ha)		
2.6	0.515		
4.5	0.514		
8.5	0.541		

Table 6.1: Area with water depth > 0.5 m in 2025 for different RCP scenarios

6.2 Application areas

The analysis focuses on the three areas of the catchment introduced in Section 5.1.3, which are shown in greater detail below. Area 1 is the largest, covering 93.2 hectares out of the total 467.5 hectares of the catchment, followed by Area 2 with 86 hectares, and Area 3 with 31.4 hectares. Together, these three areas account for approximately 45% of the entire catchment.

The focus is just on a portion of the catchment to limit the scope of the analysis and avoid dispersing the focus over the entire catchment, which would have increased complexity and data requirements substantially. Selecting these three areas allows a manageable and detailed assessment while still capturing diverse land uses and varying exposure to flooding risks.

These areas were selected because they represent distinct land use types and varying exposure to flooding risks, making them suitable for evaluating and applying different Nature-Based Solutions (NBS). Their contrasting characteristics allow for an analysis of how NBS can be tailored effectively to diverse urban and natural environments within the catchment.

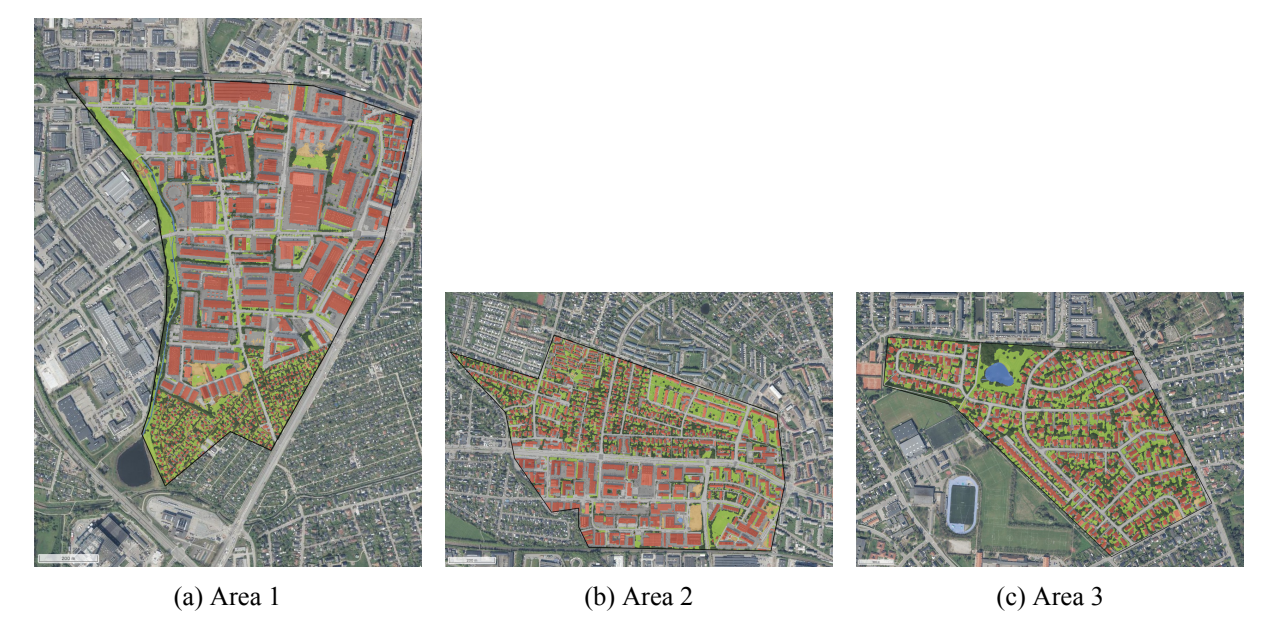


Figure 6.8: Land cover maps of the three selected areas within the catchment, used for the application of Nature-Based Solutions (NBS). Data obtained from SCALGO Live.

Area 1 is primarily an industrial district, showing a significant imbalance between grey and green areas. Table 6.2 provides an overview of the land cover in this area, which spans approximately 93.2 hectares. Grey areas account for 74%, confirming the industrial nature of the area, while green areas make up only 24%.

Land Cover	Area [ha]	Percentage (%)
Bare land	1.8	2
Water	0.4	0.4
Other paved	31	33.2
Shallow Veg.	10.9	11.7
Dense Veg.	10	10.7
Paved road	11.1	11.9
Unpaved road	0.7	0.7
Bare rock	0.01	0
Building	27.3	29.3

Table 6.2: Land cover in Area 1

Area 2 covers about 86 hectares and exhibits a smaller gap between green and grey areas, as shown in Table 6.3. Green areas account for 31%, while grey areas represent 69%. This shift is due to an increase in residential land use, often accompanied by public parks and private gardens.

Land Cover	Area [ha]	Percentage (%)	
Bare land	1.6	1.9	
Water	0	0	
Other paved	24.3	28.3	
Shallow Veg.	13.5	15.7	
Dense Veg.	11.5	13.4	
Paved road	13.3	15.5	
Unpaved road	0.1	0.1	
Bare rock	0.01	0	
Building	21.7	25.2	

Table 6.3: Land cover in Area 2

Area 3 is mainly residential and extends over 31.4 hectares. In this zone, green areas increase significantly to 47%, due to the high presence of parks and private gardens, while grey areas drop to 28%, as detailed in Table 6.4.

Land Cover	Area [ha]	Percentage (%)
Bare land	0.3	0.9
Water	0.4	1.2
Other paved	6.1	19.3
Shallow Veg.	7.5	24
Dense Veg.	6.9	21.9
Paved road	2.8	8.9
Unpaved road	0	0
Building	7.42	23.7

Table 6.4: Land cover in Area 3

For each area, a percentage of application of the artificial surface has been selected for each NBS, as shown in the table below.

NBS	Application surface (artificial) in SCALGO Live	Area 1	Area 2	Area 3
NDS	Application surface (artificial) in SCALGO Live	Percentage of application		
Porous asphalt	Paved road	50	30	0
Rain garden	Other paved	30	0	30
Bioswale	Other paved	30	30	0
Green roof	Buildings	30	30	30

Table 6.5: Percentage of application of the selected NBS on artificial surfaces across the three selected areas, according to SCALGO Live classification.

As can be seen from the table above, the percentages applied across all artificial surfaces where NBS are implemented range between 30% and 50%. These values are assumptions made to provide a scenario that is as realistic as possible. Indeed, as explained in Section 4.3.2, there are several barriers to implementing NBS, including financial constraints and difficulties in ensuring the active participation of all relevant stakeholders.

The differences in the percentage of application across the three areas for porous asphalt were defined by considering the traffic volume of each area, in order to reduce the risk of water contamination from vehicle-related pollutants.

The highest percentage (50%) was applied in Area, which—based on Figure 6.8a—is largely composed of industrial areas extending from Area 2, with generally low traffic volumes. Only a small portion in the far south of Area 3 presents a high concentration of buildings.

In contrast, Figure 6.8b shows that Area 2 consists of a highly built-up northern section and a southern part with less construction, where an industrial district is developing. Consequently, considering the presence of both high and low traffic zones, porous asphalt was applied to 30% of the paved roads in Area 2.

Area 3, as described before and shown in Figure 6.8c, is a residential zone with a high concentration of buildings. This implies a high traffic volume, which—as explained in Section 5.3.1—makes porous asphalt unsuitable due to the increased risk of contaminating infiltrated water.

In Table 6.6, the exact surface of paved roads covered with porous asphalt is shown for each area.

Area	Paved road (ha)	Porous asphalt applied (ha)
1	11.1	5.55
2	13.3	3.99
3	2.8	0.84

Table 6.6: Total paved road area and portion covered with porous asphalt in each area (in hectares).

A 30% application rate has been chosen for both bioswales and rain gardens. This decision is based on an analysis of the three areas shown in Figure 6.8, where "other paved areas" (e.g., sidewalks, parking lots) often fall within private properties—such as private parking spaces—rather than public domains where municipalities could intervene directly.

As mentioned in sections 5.3.3 and 5.3.2, bioswales are suitable for extended, longitudinal spaces, whereas rain gardens require a more compact area. During the initial screening with SCALGO Live, when appropriate space was not available in large portions of the area, the choice between the two NBS types was made accordingly. Suitable space for bioswales is present in Area 1 and Area 2, while in Area 3, where such elongated space is lacking, rain gardens were applied in the "other paved" category. In contrast, rain gardens were not applied in Area 2, where most "other paved" surfaces are more compatible with the linear geometry required by bioswales.

Area 1 presents a unique case: the available space within the "other paved" category is sufficiently compatible with both bioswales and rain gardens. Consequently, both solutions were considered. However, to streamline the evaluation process in SCALGO Live, only one nature-based solution is applied at a time to enable individual performance assessment.

Tables 6.7 and 6.8 present the estimated surface coverage of rain gardens and bioswales, based on the application percentages previously discussed.

Area	Other paved (ha)	Rain garden (ha)
1	31.0	9.30
2	24.3	0.00
3	6.1	1.83

Table 6.7: Other paved surfaces and corresponding rain garden implementation per area (in hectares).

Area	Other paved (ha)	Bioswale (ha)
1	31.0	9.30
2	24.3	7.29
3	6.1	0.00

Table 6.8: Other paved surfaces and corresponding bioswale implementation per area (in hectares).

For the application of green roofs, the situation is more complex and context-specific. In fact, the vast

majority of building rooftops are part of private properties—such as private apartments and company facilities—where municipalities cannot intervene directly. In real-world scenarios, implementing green roofs on such properties would require the support of legislative and incentive-based frameworks, including public subsidies or tax deductions to encourage private owners to replace conventional roofs with vegetated ones.

Nevertheless, for the purpose of this analysis, it was decided to proceed with a hypothetical scenario in which such enabling conditions exist. Under this assumption, green roofs are considered applicable across all three study areas, using a uniform application rate of 30%. This percentage was chosen as a conservative estimate, acknowledging the practical and regulatory challenges described above. It is important to note that building surfaces were used as a reference for calculating green roof coverage, since SCALGO Live does not provide a specific land cover class for rooftops. As a result, the green roof area was derived as a percentage of the total building area in each zone.

Table 6.9 below presents the estimated green roof coverage (in hectares), calculated as a portion of the total building area in each study area.

Area	Building area (ha)	Green roof (ha)
1	27.3	8.19
2	21.7	6.51
3	7.42	2.23

Table 6.9: Estimated green roof coverage per area, based on 30% of total building surface (in hectares).

Even though, as explained in Section 5.3.5, it is not possible to accurately distinguish the performance between extensive and intensive green roofs due to a lack of detailed information, some general assumptions have been made.

Area 1, being primarily composed of an industrial district, is considered more suitable for extensive green roofs, which—as discussed in Section 5.3.4—are typically not accessible to the public. Based on this, it is assumed that 80% of the green roofs applied in Area 1 (8.19 ha) are extensive, and the remaining 20% are intensive; these intensive roofs are usually accessible to the public.

Area 2, which presents a hybrid character between residential and industrial zones, is assumed to have an even distribution: 50% extensive and 50% intensive green roofs, out of a total of 6.51 ha.

Finally, Area 3 is entirely residential, and therefore all the green roofs applied (2.23 ha) are assumed to be intensive.

Table 6.10 below presents the resulting distribution (in hectares) between extensive and intensive green roofs, based on these assumptions.

Area	Green roof (ha)			
	Extensive	Intensive	Total	
1	6.552	1.638	8.19	
2	3.255	3.255	6.51	
3	0	2.226	2.226	

Table 6.10: Distribution of extensive and intensive green roofs by area (in hectares).

6.3 Curve Number Method for NBS

As briefly introduced in Section 4.4, there are currently no standard Curve Numbers (CN) specifically defined for Nature-Based Solutions (NBS). However, in order to implement NBS on a large scale through SCALGO, it is necessary to establish them. To address this, an iterative method has been developed to estimate the CN for each NBS.

The starting point for this estimation is the CN value that SCALGO Live assigns to artificial surfaces that are sewered, which is 73. A proportionality factor of 0.1 is used, as illustrated in Figure 6.13. This starting value was chosen because the NBS are applied to surface types that SCALGO Live classifies as artificial surfaces, including the categories "other paved," "buildings," and "paved roads." For these categories, SCALGO assigns the CN associated with artificial surfaces.

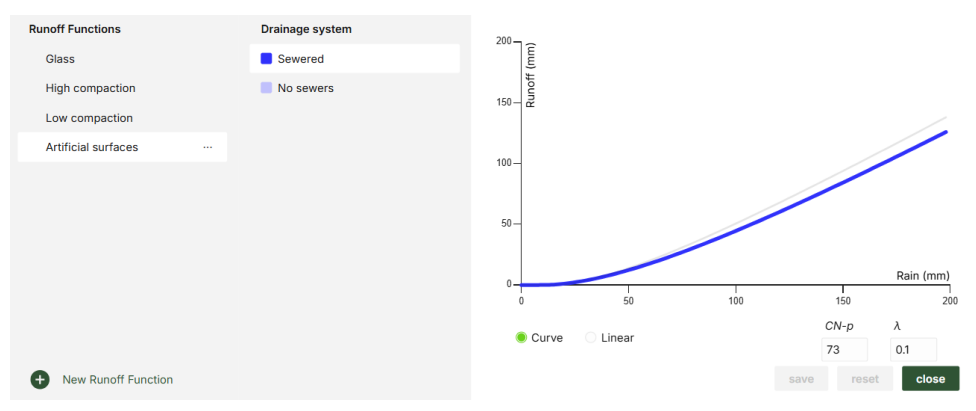


Figure 6.9: Behavior of artificial surfaces (sewered) in relation to precipitation and runoff generation. The graph illustrates the runoff response of artificial surfaces (sewered) to varying precipitation levels, ranging from 0 to 200 mm. A Curve Number (CN) of 73 is used, along with a proportionality factor of 0.1. This data is provided by SCALGO Live.

It's worth noting that this CN value is slightly different from the standard values provided in the traditional CN table shown in Figure 4.10. For example, paved roads in hydrologic soil group A typically have CN values ranging from 72 to 74. This difference arises because SCALGO, in their documentation on the rainfall-runoff model used to generate flash flood maps in SCALGO Live [22], explain that the original CN method had to be adapted to fit their modeling approach. Indeed, the original CN method was developed to estimate total runoff from catchments (measured in hectares or acres), incorporating both surface and subsurface flow contributions. In contrast, SCALGO Live models local surface runoff at the scale of individual terrain model cells and considers only true surface runoff [22]. To address this mismatch, SCALGO recalibrates CN values using alternative methods that account for the differences in scale and the definition of runoff. The results of these methods are then approximated using Curve

Numbers, as these offer similar hydrological behavior. Consequently, the final CN values applied in SCALGO Live are generally well correlated with those derived from the traditional CN method [22]. The iterative method developed aims to calculate the CN for each NBS considered. It is based on precipitation values corresponding to a 5-year return period and a 4-hour duration, as previously described in Section 6.1. To ensure statistical robustness, 30 precipitation values were selected, ranging from 0 to 44 mm (with 42 mm being the maximum value under the RCP 8.5 scenario). For each precipitation value, runoff was calculated using the formula provided in Equation 4.1. Accordingly, the graph shown earlier in Figure 6.13 has been updated to reflect the new precipitation range, while maintaining the same CN (73) and proportionality factor (0.1) for simplicity. The updated graph is presented below.

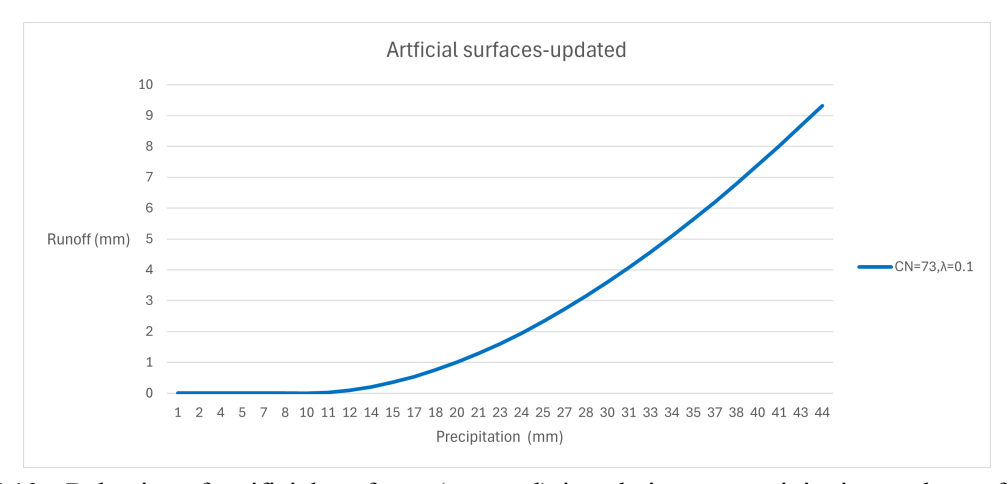


Figure 6.10: Behavior of artificial surfaces (sewered) in relation to precipitation and runoff generation. The graph illustrates the runoff response of artificial surfaces (sewered) to varying precipitation levels, ranging from 0 to 44 mm, based on a rainfall event with a return period (T) of 5 years and a duration of 4 hours. A Curve Number (CN) of 73 is applied, using a proportionality factor (λ) of 0.1 to represent the relationship between precipitation and generated runoff.

Following this, the water retention capacity—representing the amount of water retained by the soil or drainage system—was calculated for each of the 30 data points using Equation 6.2. From the resulting distribution, the median retention value (expressed as a percentage) was derived.

W.R. (%) =
$$\left(1 - \frac{R}{P}\right) \cdot 100$$
 (6.2)

W.R.
$$(\%)$$
 = Water retention capacity (percentage)
$$R = \text{Runoff (m)}$$

$$P = \text{Precipitation (m)}$$

This median value was then used to compute the corresponding median runoff using Equation 6.3.

$$R.G. (\%) = 1 - W.R. (\%)$$
 (6.3)

R.G. (%) = Runoff generated (median), without NBS

W.R. (%) = Water retention capacity (median), expressed in percentage

The median was chosen because the objective is to analyze the runoff generated from the NBS, and the runoff reduction values in Table 4.7 are provided for the median (Level 1) and 75th percentile (Level 2), making this choice the most consistent. Finally, the runoff generated from the NBS was calculated using Equation 6.4, applying the median runoff and the reference value of runoff reduction provided for each NBS selected in Table 5.2.

$$R.G._{NBS}$$
 (%) = $R.G.$ (%) · (1 – $R.R.$ (%)) (6.4)

 $R.G._{NBS}$ (%) = Runoff generated (median) from NBS, expressed in percentage

R.G. (%) = Runoff generated (median), without NBS, expressed in percentage

R.R. (%) = Runoff reduction, midpoint between median and 75th percentile values, expressed in percentage

Since all runoff values are derived from Equation 4.1—the final step of the Curve Number (CN) method—and this method begins with Equation 4.3, where the CN is introduced, and continues with Equation 4.2, which incorporates the proportionality factor λ , it is therefore possible to compute the runoff for any given combination of CN and λ values.

In particular, for artificial surfaces (with CN = 73 and $\lambda = 0.1$), the median runoff generated, expressed as a percentage of precipitation, is approximately 7%, while the corresponding median water retention capacity is about 93%. In absolute terms (mm), this means that for a median precipitation of 22.5 mm, the runoff generated is 1.60 mm. Once the new runoff is computed by applying the runoff reduction to the runoff generated by artificial surfaces (e.g., assuming a runoff reduction of 40%, and applying Equation 6.4), the resulting runoff generated from the NBS is 4.3%, which corresponds to 0.96 mm.

The figure below summarizes this workflow, illustrating the main steps of the calculation from artificial surfaces to the application of the NBS, with all quantities expressed in absolute terms.

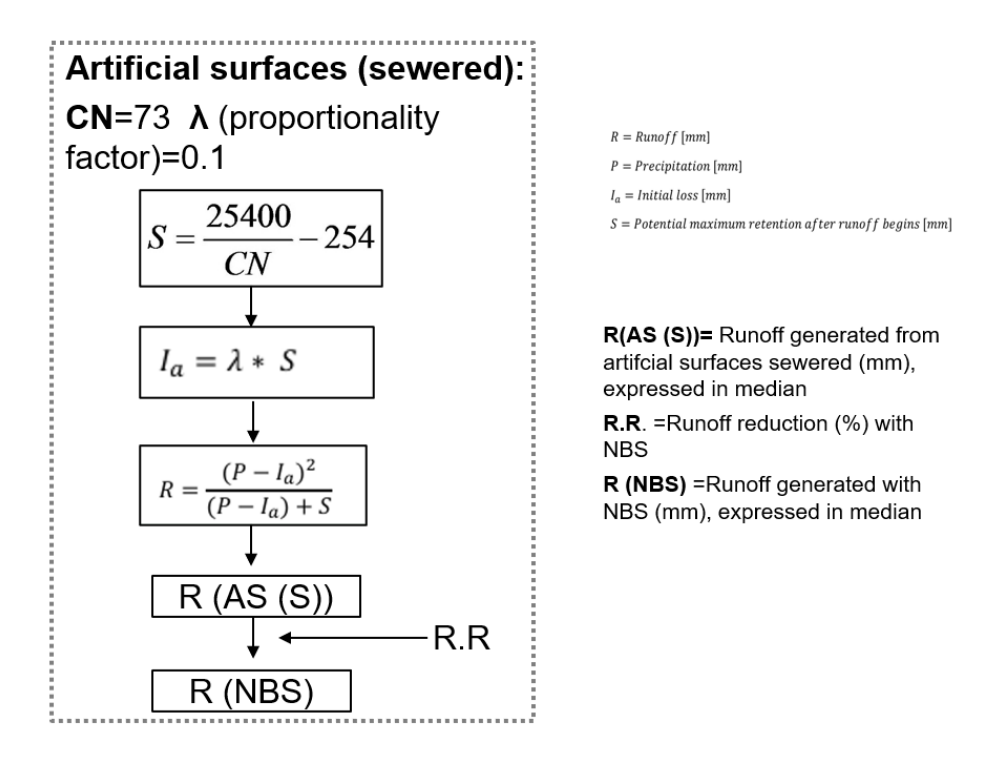


Figure 6.11: Schematic representation of the runoff calculation process, from artificial surfaces to NBS application

The objective is to iteratively adjust the CN and λ values until the runoff generated (via Equation 4.1) matches the expected runoff for the selected NBS.

The scheme below illustrates the iterative method used to define the Curve Number (CN) and the proportionality factor (λ) for each Nature-Based Solution (NBS).

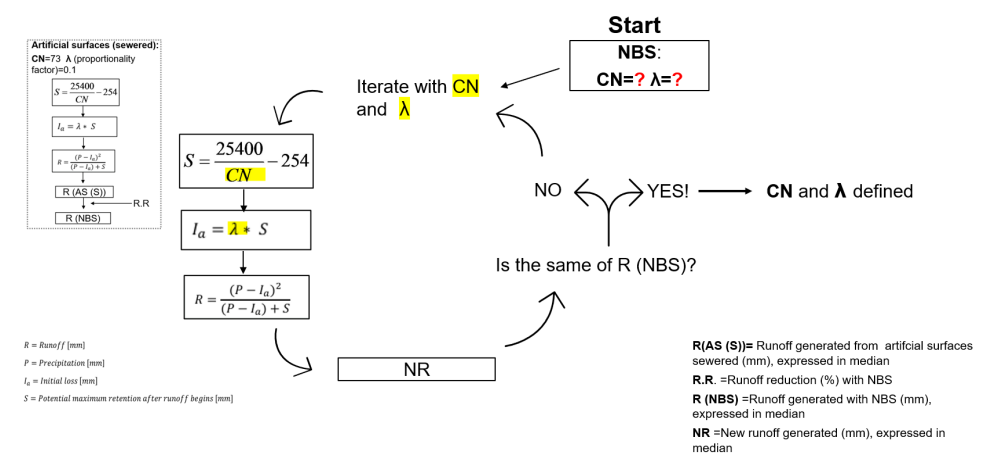


Figure 6.12: Schematic representation of the iterative method. The step outlined in dotted grey corresponds to the calculation of the runoff generated with NBS (R (NBS)), as shown previously.

This figure also includes the preceding step—shown in Figure 6.11—which clarifies the overall workflow. It begins with the calculation of the runoff generated by the NBS (highlighted in dotted grey), and proceeds through the iterative method where different combinations of CN and λ are tested. The process continues until the new calculated runoff (NR) matches the previously obtained (R (NBS)). At that point, the corresponding CN and λ values are considered as defined.

The graph below illustrates the runoff–precipitation behavior of artificial surfaces (sewered) and the selected NBS, using their corresponding CN and proportionality factor values, computed through the iterative method.

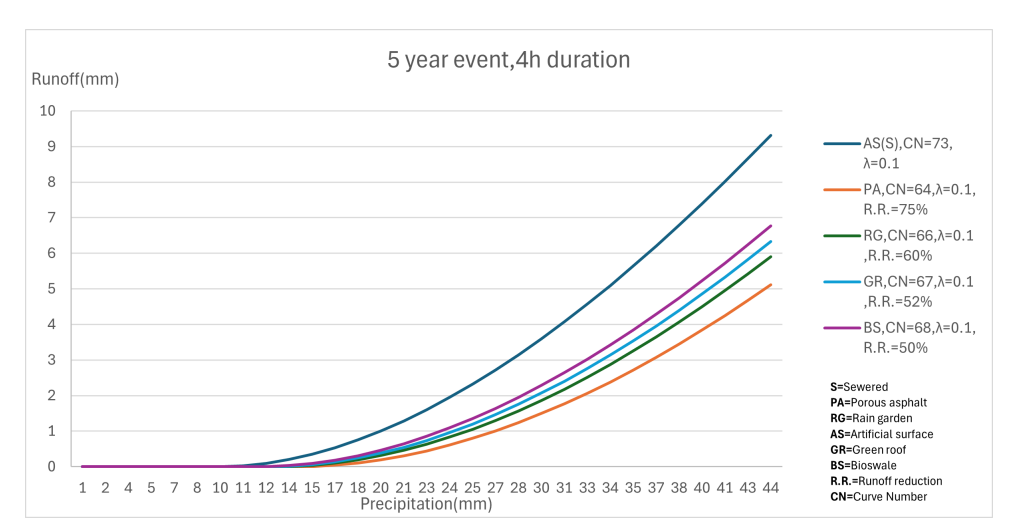


Figure 6.13: Behavior of artificial surfaces (sewered) and NBS in relation to precipitation and runoff generation. The graph illustrates the runoff response of artificial surfaces (sewered) and the selected NBS to varying precipitation levels, ranging from 0 to 44 mm, based on a rainfall event with a return period (T) of 5 years and a duration of 4 hours. For artificial surfaces, the original Curve Number (CN = 73) and proportionality factor (λ = 0.1) provided by SCALGO are used. For the NBS, the CN and proportionality factor were obtained through the iterative method.

Because, as has been explained in section 6.2, the NBS are applied only to a portion of the artificial surface area (including other paved areas, buildings, and paved roads), the computed Curve Numbers have been recalibrated accordingly. This recalibration follows the scheme illustrated below, taking porous asphalt as an example.

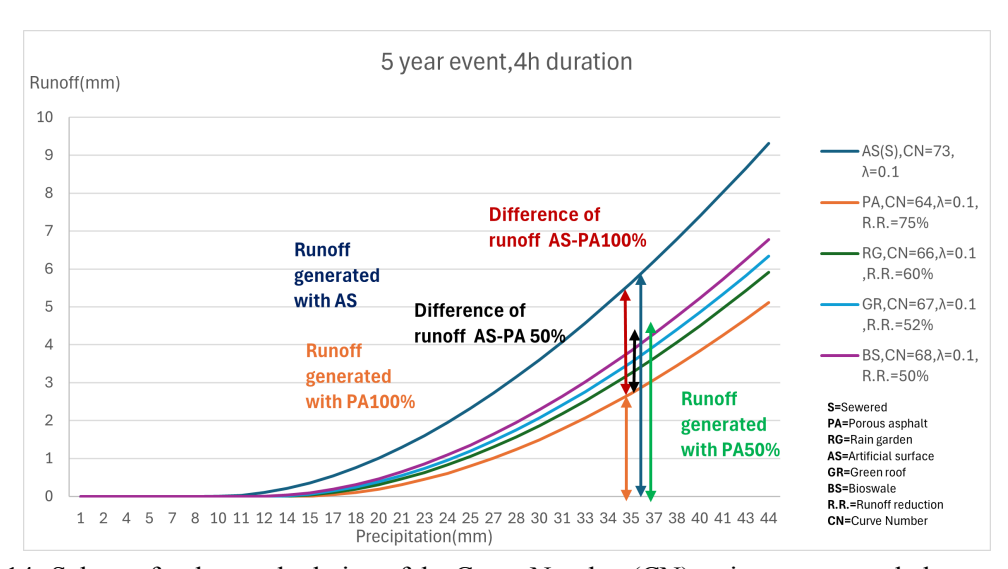


Figure 6.14: Scheme for the recalculation of the Curve Number (CN), using porous asphalt as an example. Assuming the NBS (porous asphalt) is applied to only 50% of the artificial surface—in this case, a paved road—the CN is recalculated based on the modified runoff generated from this partial application.

The new normalized CN values, adjusted for the percentage of application area, are based on the new

runoff generated by adding the runoff corresponding to 100% application of porous asphalt (indicated by the orange arrow) to half of the difference between the runoff generated by artificial surfaces (indicated by blue arrow) and that generated by 100% porous asphalt application. The formula below summarizes this approach:

$$N.R. = Runoff_{NBS(100\%)} + \left(Runoff_{AS(S)} - Runoff_{NBS(100\%)}\right) \times \left(1 - Percentage \ of \ Application\right) \ \ (6.5)$$

N.R. = New runoff generated (mm)

 $Runoff_{AS(S)} = Runoff$ generated from artificial surfaces (sewered) (mm)

 $Runoff_{NBS(100\%)} = Runoff$ generated with 100% NBS applied on artificial surfaces (mm)

Percentage of Application = Fraction of total area where NBS are applied (e.g., 0.4 for 40%)

After that, the CN and the proportionality factor for the NBS are recalculated using the same iterative method described earlier. The graphs below illustrate the updated runoff behavior of the NBS for two different application scenarios: 50% and 30% coverage of the artificial surfaces.

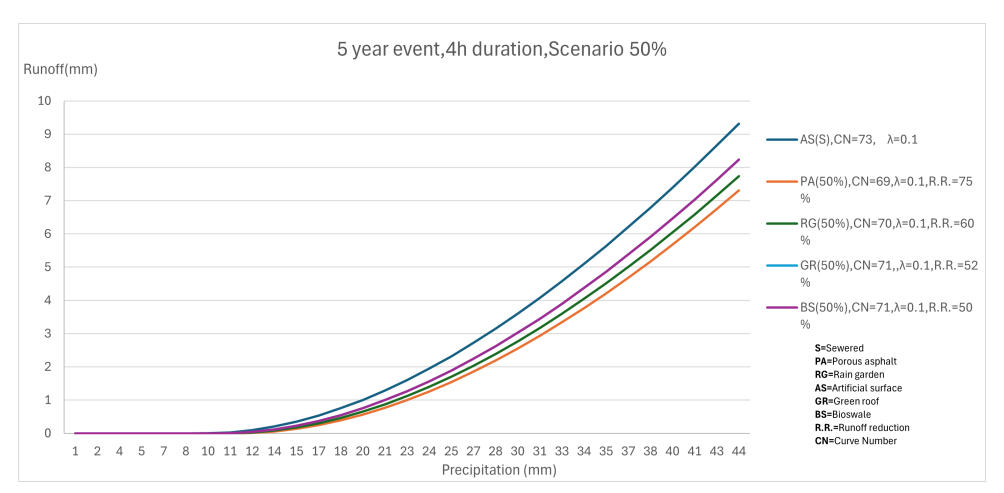


Figure 6.15: Behavior of artificial surfaces (sewered) and NBS (applied to 50% of the application area) in relation to precipitation and runoff generation. The graph illustrates the runoff response of artificial surfaces (sewered) and the selected NBS across varying precipitation levels, ranging from 0 to 44 mm, for a rainfall event with a return period (T) of 5 years and a duration of 4 hours. For artificial surfaces, the original Curve Number (CN = 73) and proportionality factor (λ = 0.1) provided by SCALGO are used. For the NBS, the CN and proportionality factor were recalculated using the iterative method, considering the partial (50%) application scenario.



Figure 6.16: Behavior of artificial surfaces (sewered) and NBS (applied to 30% of the application area) in relation to precipitation and runoff generation. The graph illustrates the runoff response of artificial surfaces (sewered) and the selected NBS across varying precipitation levels, ranging from 0 to 44 mm, for a rainfall event with a return period (T) of 5 years and a duration of 4 hours. For artificial surfaces, the original Curve Number (CN = 73) and proportionality factor (λ = 0.1) provided by SCALGO are used. For the NBS, the CN and proportionality factor were recalculated using the iterative method, considering the partial (30%) application scenario.

6.4 Investigated outcome

Once the selected Nature-Based Solutions (NBS) are applied in the three identified areas, the objective is to evaluate how the overall catchment responds in terms of surface area exceeding 0.5 m of water depth under different RCP scenarios. This assessment is based on the precipitation calculated in Section 6.1 for a 5-year return period event, which corresponds to the service level of the current drainage network, as explained in Section 5.2.1. Therefore, it represents a critical criterion for assessing potential future flooding risks.

Specifically, for RCP 4.5 and RCP 8.5, the analysis focuses on how much the implementation of NBS—assumed to begin in 2025—can delay the occurrence of the tipping point in the identified year, and to what extent NBS can provide flexibility in this regard.

In addition to the impact of individual solutions, the combined effect of certain NBS implemented simultaneously—such as rain gardens and porous asphalt, as well as the combination of rain gardens, porous asphalt, and green roofs—was also investigated. On the other hand, for RCP 2.6—since the tipping point is never reached during the simulation period, as explained in Section 6.1.1—the analysis is limited to assessing how each NBS influences the constant value observed over the years, compared to the projected baseline scenario.

7 Results

7.1 RCP 2.6

As explained in the previous section, for RCP 2.6 the analysis focuses solely on assessing how each Nature-Based Solution (NBS) influences the constant value reached during the projected years, as shown in the figure below.

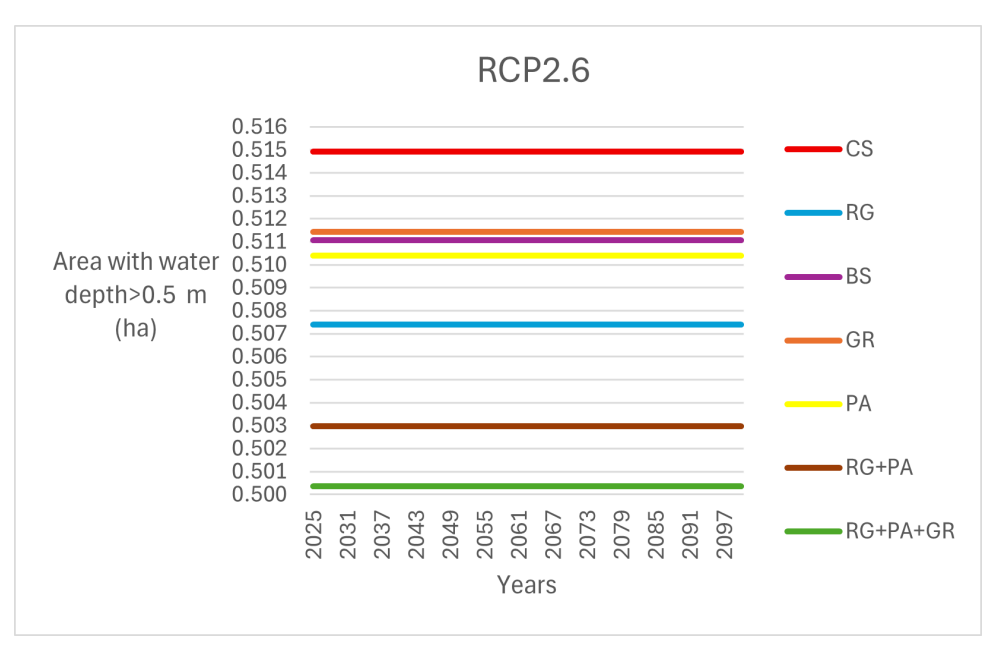


Figure 7.1: Values of surface area (expressed in hectares) in the entire catchment with water depth above 0.5 m during the period 2025–2100 under RCP 2.6, after applying different Nature-Based Solutions. CS = Current Scenario; PA = Porous Asphalt; RG = Rain Garden; BS = Bioswale; GR = Green Roof.

As shown in Figure 7.1, when considering individual Nature-Based Solutions, the rain garden has the greatest impact in reducing the area with water depth exceeding 0.5 m. Interestingly, even though the rain garden does not achieve the highest runoff reduction (60%, as reported in Table 5.2), it is applied to "other paved" surfaces, which represent the highest percentage across the selected areas. In contrast, porous asphalt, which has the highest runoff reduction (75%), is applied mainly to paved roads that occupy a smaller portion of the total surface. The difference in surface coverage between these two types is especially significant in Areas 2 and 3, where it ranges between 10% and 20%.

Green roofs show the lowest impact, both due to their lower runoff reduction (52%) and smaller applicable surface area compared to where rain gardens are applied. However, they still slightly outperform bioswales (which have a 50% runoff reduction) by a difference of 0.001 hectares. This is consistent with the fact that the respective application surfaces—buildings for green roofs and "other paved" for bioswales—have a similar percentage distribution across the three areas (with a slightly higher percentage of "other paved" in Areas 1 and 2, and the opposite in Area 3).

The most interesting results come from the combined application of NBS. When rain gardens and porous asphalt are applied together on their respective surfaces, the total area with water depth above 0.5 m

decreases from 0.515 hectares (current scenario) to approximately 0.503 hectares, a reduction of 0.012 hectares. When green roofs are also included, the value decreases further to around 0.500 hectares. This aligns with the earlier observations: green roofs contribute the least among the three, while porous asphalt has a moderate influence, and rain gardens have the most significant impact.

7.2 RCP 4.5

For RCP 4.5, each individual Nature-Based Solution (NBS) and their combinations exhibit a significant influence on the catchment in terms of flood reduction when compared to the current scenario, as illustrated in the graph below.

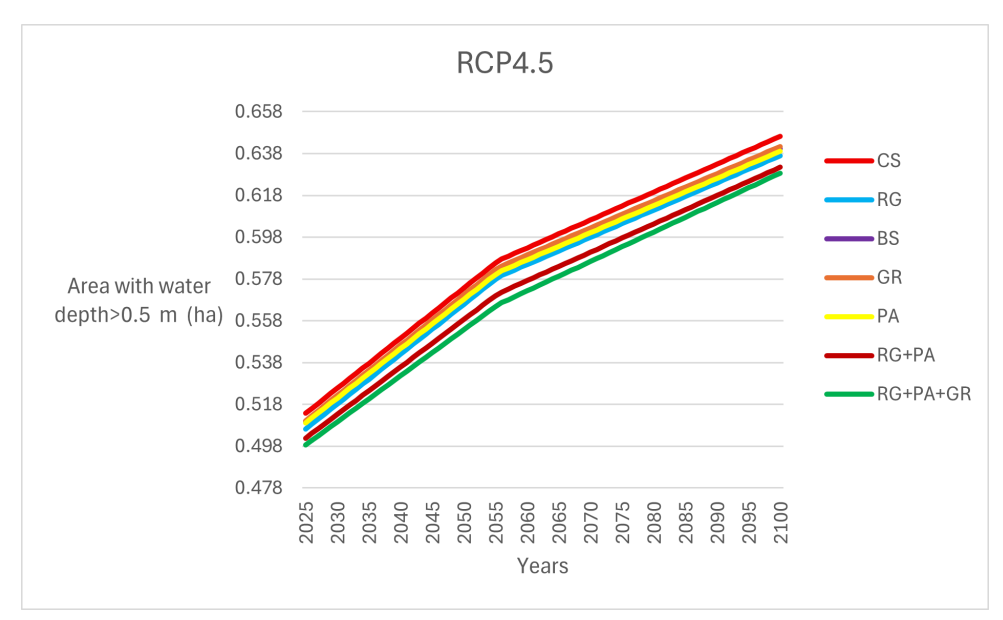


Figure 7.2: Values of surface area (expressed in hectares) in the entire catchment with water depth above 0.5 m during the period 2025–2100 under RCP 4.5, after applying different Nature-Based Solutions, including the combination between rain garden, porous asphalt, and green roof. CS = Current Scenario; PA = Porous Asphalt; RG = Rain Garden; BS = Bioswale; GR = Green Roof.

As explained in Section 6.1.1, the tipping point threshold (0.541 ha) under RCP 4.5 is reached in 2036 in the current scenario. The scheme below summarizes the results shown in Figure 7.2, indicating the year in which the tipping point is reached when applying each individual NBS and when applying two combinations:a double combination (rain garden and porous asphalt) and a triple combination (rain garden, porous asphalt, and green roofs).

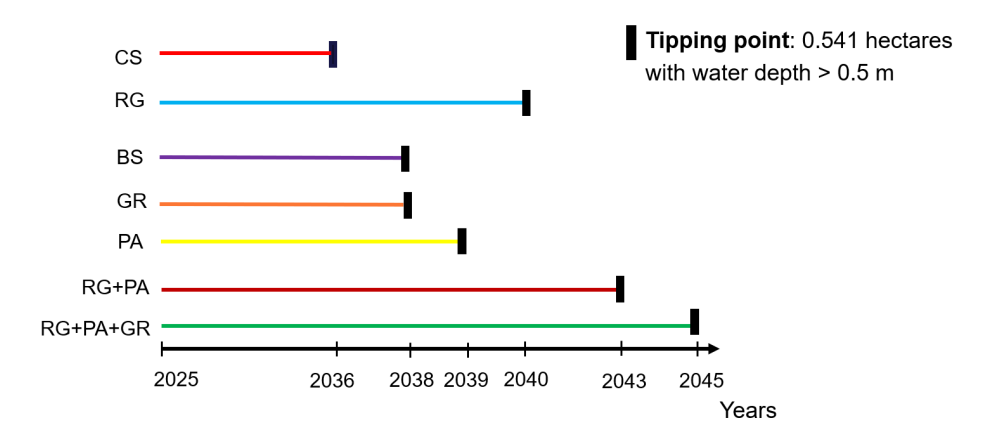


Figure 7.3: Year in which the tipping point is reached under the current scenario and after applying individual Nature-Based Solutions and their combination (rain garden, porous asphalt, and green roof) under RCP 4.5. CS = Current Scenario; PA = Porous Asphalt; RG = Rain Garden; BS = Bioswale; GR = Green Roof.

As shown in Figure 7.3, the tipping point is reached in 2036 under the current scenario. When applying the rain garden, the tipping point is delayed by 4 years, being reached in 2040. This represents the longest delay observed among the individual NBS. Bioswale and green roof both delay the tipping point by 2 years (reached in 2038), while porous asphalt results in a 3-year delay (reached in 2039).

The effect becomes more significant when NBS are applied in combination. The application of both rain garden and porous asphalt delays the tipping point by 7 years (reached in 2043). When green roofs are also included in the combination, the tipping point is reached in 2045—corresponding to a total delay of 9 years compared to the baseline scenario.

7.2.1 Adaptation Pathway

Following the DAPP (Dynamic Adaptive Policy Pathways) approach, the Adaptation Pathway map has been developed for RCP 4.5, as shown in the figure below.

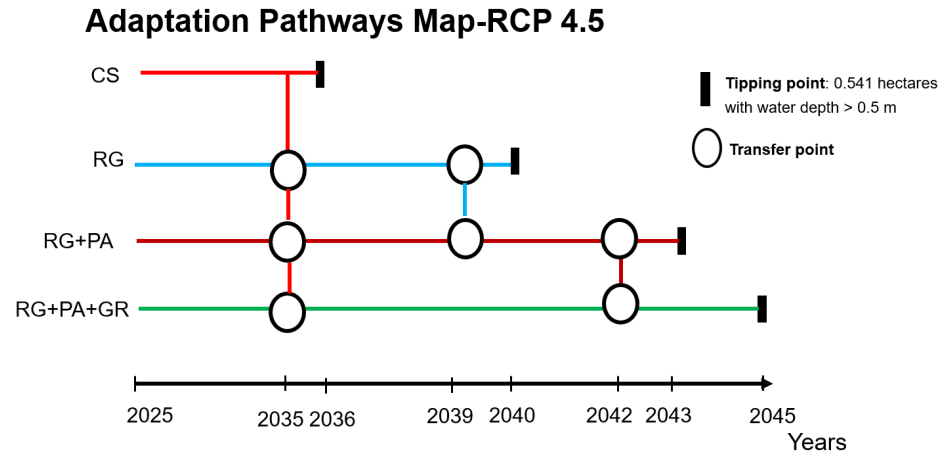


Figure 7.4: Adaptation Pathways Map under RCP 4.5 focusing on Rain Garden, Porous Asphalt, and Green Roof.

Starting from the current scenario, the tipping point is reached in 2036. In order to avoid exceeding this threshold, a transition to an alternative solution must occur no later than the year before—that is, by 2035. This year represents the transfer point.

From the current scenario, several adaptation options are available:

- Rain Garden (RG) alone, which delays the tipping point until 2040;
- Rain Garden + Porous Asphalt (RG + PA), delaying it until 2043;
- Rain Garden + Porous Asphalt + Green Roof (RG + PA + GR), pushing the tipping point further to 2045.

The last option ensures the longest-lasting effect from the beginning. However, to pursue a more flexible and cost-effective strategy, a dynamic solution may be adopted—prioritizing the implementation of the most cost-efficient measures first (i.e., rain gardens), followed by porous asphalt and finally green roofs, as discussed in Section 5.3.5.

In this sense, the adaptive pathway may proceed as follows:

- Start with Rain Garden (blue path), active until 2039;
- Before reaching the tipping point in 2040, Porous Asphalt is added in 2039, transitioning to the red path (RG + PA);
- This combination is viable until 2042. To prevent reaching the tipping point in 2043, Green Roofs must be added in 2042, transitioning to the green path (RG + PA + GR), which remains effective until 2044 (as the tipping point is reached in 2045).

This final pathway demonstrates the longest delay achievable through a sequential and adaptive strategy. However, it still represents a medium-term solution, as it remains effective only until 2045. Further considerations regarding long-term resilience are discussed in Section 8.1. The figure below illustrates how the surface area affected by water depth above 0.5 m evolves over time under these different strategies.

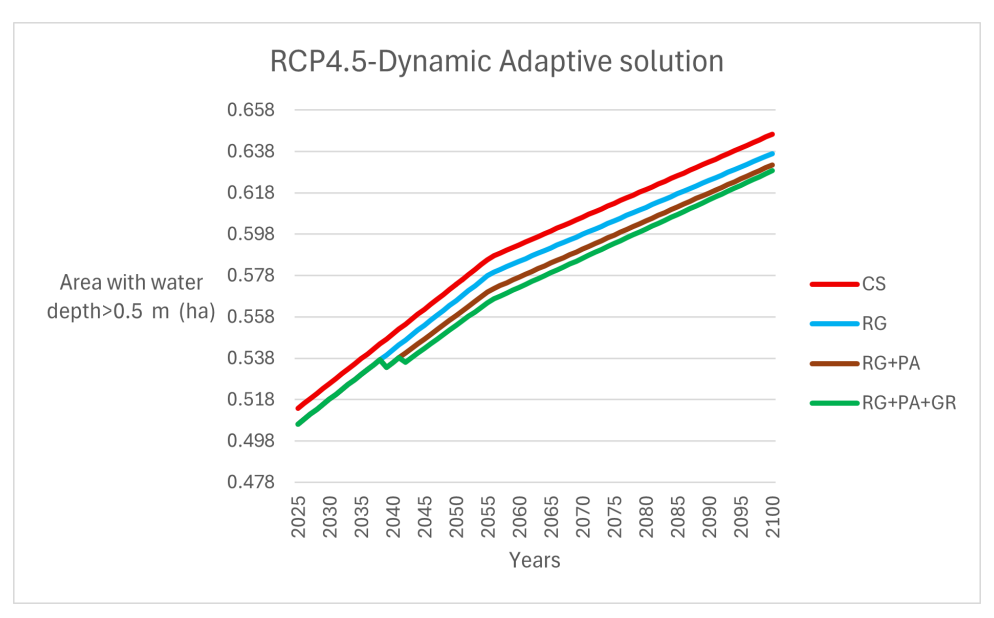


Figure 7.5: Values of surface area (expressed in hectares) in the entire catchment with water depth above 0.5 m during the period 2025–2100 under RCP 4.5, after applying single and dynamic adaptive solutions. CS = Current Scenario; PA = Porous Asphalt; RG = Rain Garden; GR = Green Roof.

As shown in the graph above, the catchment's response in terms of surface area with water depth above 0.5 m differs under various strategies. The green line (RG + PA + GR) overlaps the blue line (RG only) until 2039, because until that point just rain garden is included in the triple combination. At this point, a clear drop is observed as porous asphalt is added. The line then continues overlapping the dark red line (RG + PA) until 2042. When the green roof is added, another drop occurs, and the green line diverges again from the dark red one.

This stepped behavior reflects the sequential implementation of measures within a dynamic and adaptive management framework.

7.3 RCP 8.5

For RCP 8.5, the impact of individual nature-based solutions (NBS) and their combinations is less pronounced compared to RCP 4.5, but it is still observable, as shown in the Figure 7.6.

To improve visual clarity—given the wide range of values under RCP 8.5—and considering that differences across scenarios (including the current one) are small and mostly within decimal ranges, the time axis has been limited to the year 2050, also taking into account that the tipping point is reached in all scenarios before that year.

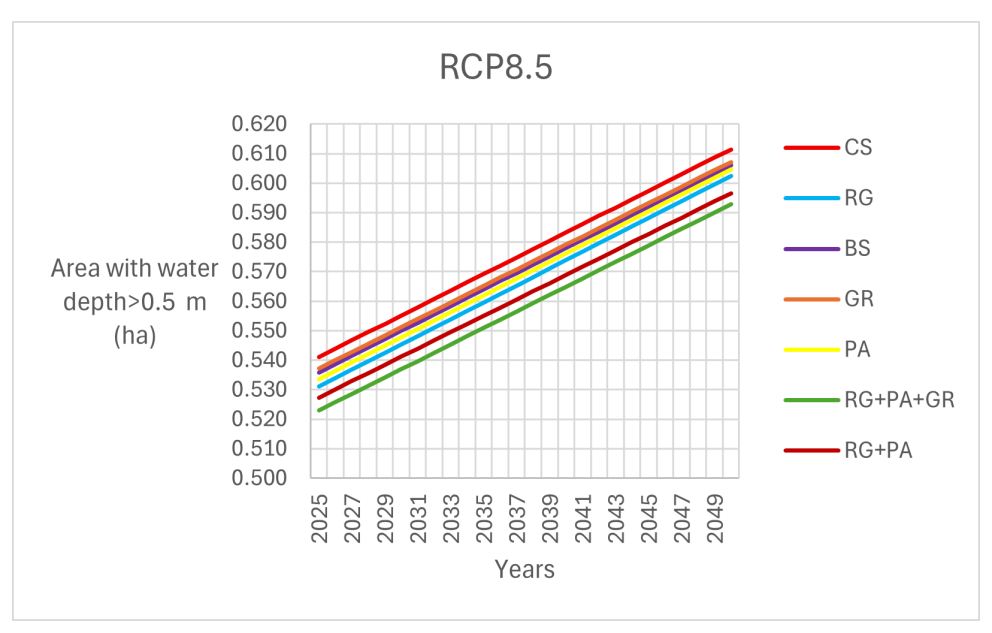


Figure 7.6: Values of surface area (expressed in hectares) in the entire catchment with water depth above 0.5 m during the period 2025–2050 under RCP 8.5, after applying different nature-based solutions, including the combination of rain garden, porous asphalt, and green roof. CS = Current Scenario; PA = Porous Asphalt; RG = Rain Garden; BS = Bioswale; GR = Green Roof.

From the perspective of tipping points, the situation differs from RCP 4.5, as the tipping point (as explained in Section 6.1.1) is already reached in 2025.

The following figure shows how much each individual and combined NBS delays the tipping point under RCP 8.5:

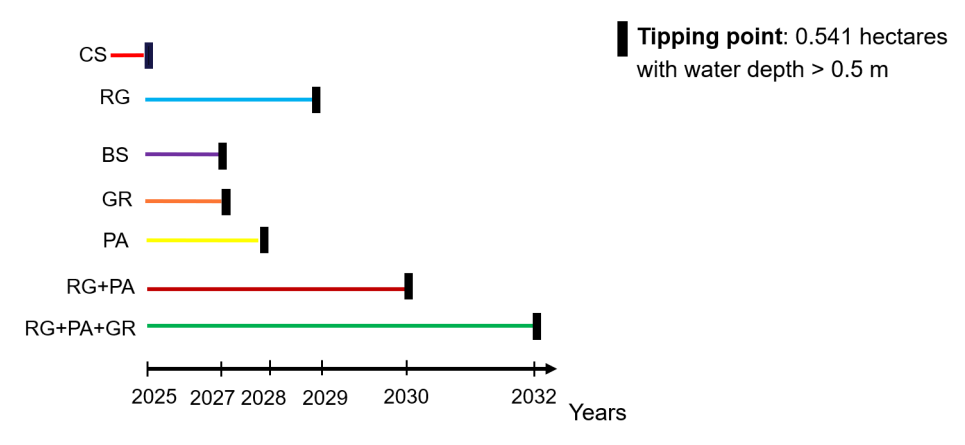


Figure 7.7: Year in which the tipping point is reached under the current scenario and after applying individual nature-based solutions and their combinations (rain garden, porous asphalt, and green roof) under RCP 8.5. CS = Current Scenario; PA = Porous Asphalt; RG = Rain Garden; BS = Bioswale; GR = Green Roof.

As shown in Figure 7.7, the rain garden delays the tipping point by four years (to 2029), while both the bioswale and the green roof provide only a two-year delay (to 2027). When rain garden and porous asphalt are combined, the tipping point is delayed by five years (to 2030). Adding the green roof to this combination further delays the tipping point by seven years in total (to 2032).

7.3.1 Adaptation Pathway

As was done for RCP 4.5, an adaptation pathways map has been developed for RCP 8.5, as shown below.

Adaptation Pathways Map-RCP 8.5 CS Tipping point: 0.541 hectares with water depth > 0.5 m Transfer point Transfer point Transfer point 2025 2026 2028 2029 2030 2032 Years

Figure 7.8: Adaptation pathways map under RCP 8.5 focusing on rain garden, porous asphalt, and green roof.

Starting from the current scenario, the tipping point is already reached in 2025. This means immediate intervention is required. Therefore, the first transfer point is assumed to be in 2026. From the current scenario, several adaptation options are available:

- Rain garden (RG) alone, which delays the tipping point until 2029;
- Rain garden and porous asphalt (RG + PA), delaying it until 2030;
- Rain garden, porous asphalt, and green roof (RG + PA + GR), pushing the tipping point further to 2032.

The last option ensures the longest-lasting effect from the beginning. However, as in the case of RCP 4.5, the implementation order is determined based on cost-effectiveness—starting with rain gardens, followed by porous asphalt, and finally green roofs, as discussed in Section 5.3.5.

In this sense, the adaptive pathway may proceed as follows:

- Start with rain garden (blue path), active until 2028;
- Before reaching the tipping point in 2029, porous asphalt is added in 2028, transitioning to the red path (RG + PA);
- This combination is viable until 2029. To prevent reaching the tipping point in 2030, green roofs must be added in 2029, transitioning to the green path (RG + PA + GR), which is viable until 2031 (the tipping point is reached in 2032).

This final path demonstrates that this is not a long-term solution (up to 2100), which will be further discussed in Section 8.1.

The figure below illustrates how the surface area affected by water depth above 0.5 m evolves over time under these different strategies.

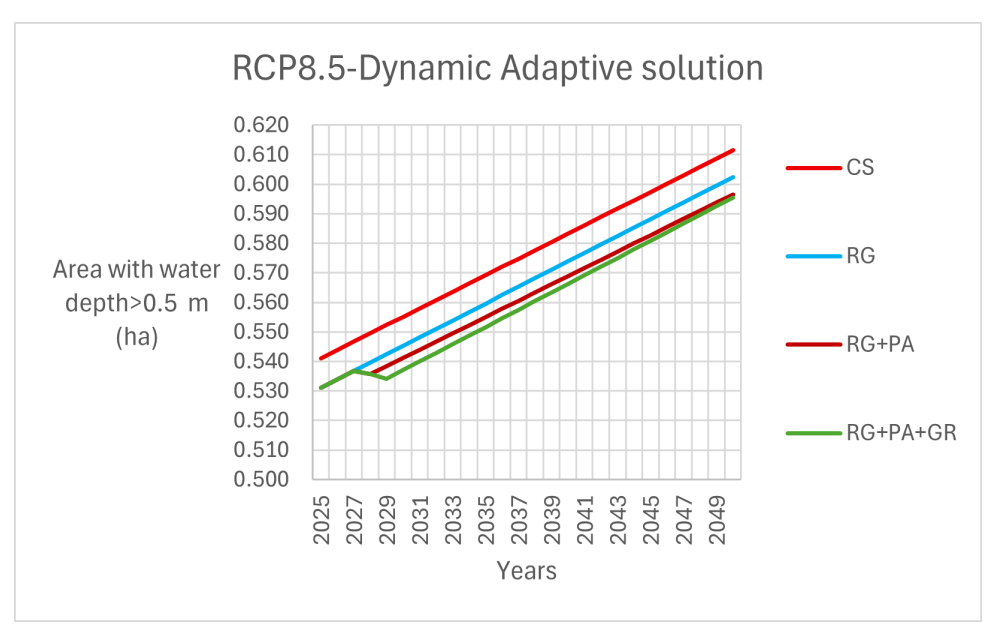


Figure 7.9: Values of surface area (expressed in hectares) in the entire catchment with water depth above 0.5 m during the period 2025–2050 under RCP 8.5, after applying single and dynamic adaptive solutions. CS = Current Scenario; PA = Porous Asphalt; RG = Rain Garden; GR = Green Roof.

As shown in the graph above, the catchment's response in terms of surface area with water depth above 0.5 m differs under the various strategies. The green line (RG + PA + GR) overlaps with the blue line (RG only) until 2028, as only the rain garden is active. At that point, a clear drop is observed as porous asphalt is added. The line then follows the dark red line (RG + PA) until 2029. When the green roof is added, another drop is visible, and the green line diverges again from the dark red one.

7.4 Water balance

In order to evaluate the impact of Nature-Based Solutions (NBS) in terms of water balance, the precipitation value of 34 mm was selected as a representative example, as it corresponds to one of the values shown in the graph in Figure 6.14, representing a 5-year return period event with a duration of 4 hours. This enables the assessment of NBS effectiveness under realistic and impactful rainfall conditions. In this case, rain garden has been chosen as a representative example among the selected NBS.

The water balance is calculated using the following formula, taken directly from [51]:

$$\Delta S = P - ET - R \tag{7.1}$$

where:

 ΔS = Water storage change,

P = Precipitation,

ET = Evapotranspiration

R = Runoff.

7.4.1 Before NBS

Below is a schematic representation of the water cycle showing the water balance calculated before the implementation of NBS.

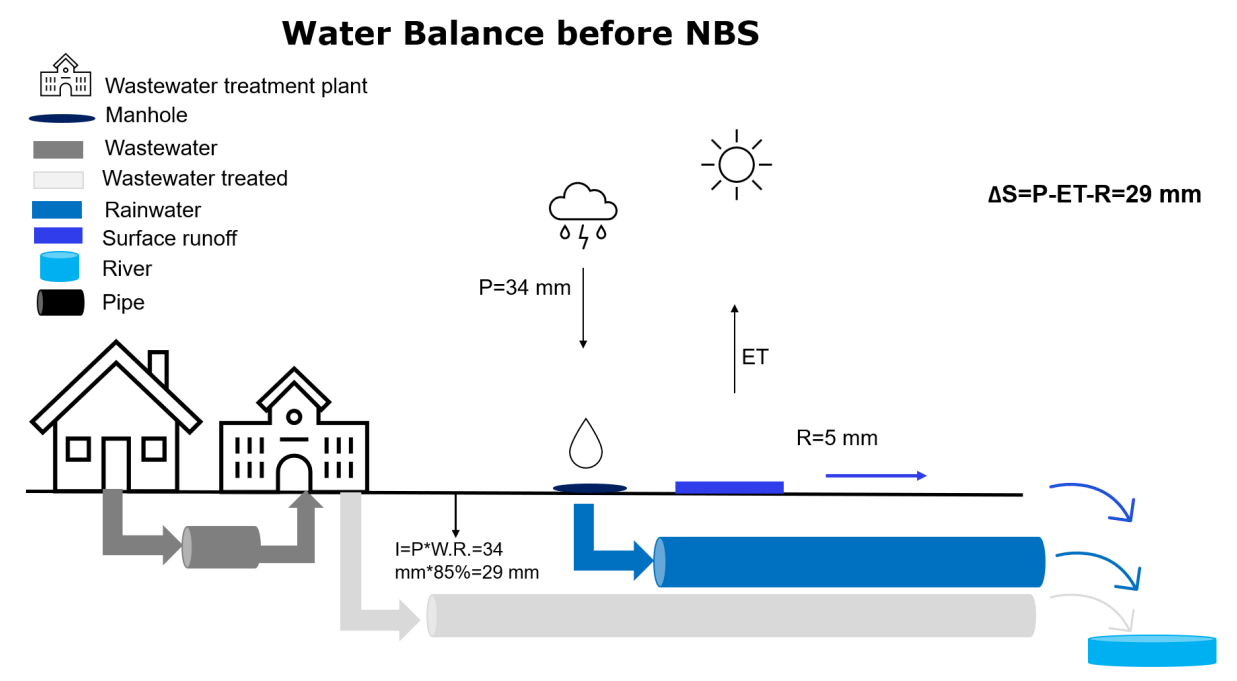


Figure 7.10: Water balance before implementing NBS. P = precipitation; ET = evapotranspiration; R = runoff; ΔS = change in water storage; I = infiltration.

As illustrated in the scheme above, a precipitation event of 34 mm over a 4-hour period results in rainwater flowing into the sewer system, identifiable as the manhole. Given the system's water retention capacity of 85%—a value derived using the method described in Section 6.3 based on a 34 mm rainfall—only 29 mm enters the sewer system, which is subsequently discharged into the Somose River.

It is important to note that rainfall is not the only source contributing to the streamflow; treated wastewater also adds to the total volume. Ultimately, this precipitation event generates a runoff of 5 mm from the initial 34 mm.

Evapotranspiration is negligible during these intense rainfall events due to its longer timescale, and is therefore omitted from the calculation. Therefore, using Equation (7.1), the change of water storage results in 29 mm, which, since evapotranspiration is neglected, is equal to the infiltration.

7.4.2 After NBS

After implementing Nature-Based Solutions (NBS)—in this case, a rain garden—the situation changes significantly. The illustration below shows how the key elements of the water balance behave when the rain garden is added, considering its runoff reduction of 60%.

Water Balance after NBS

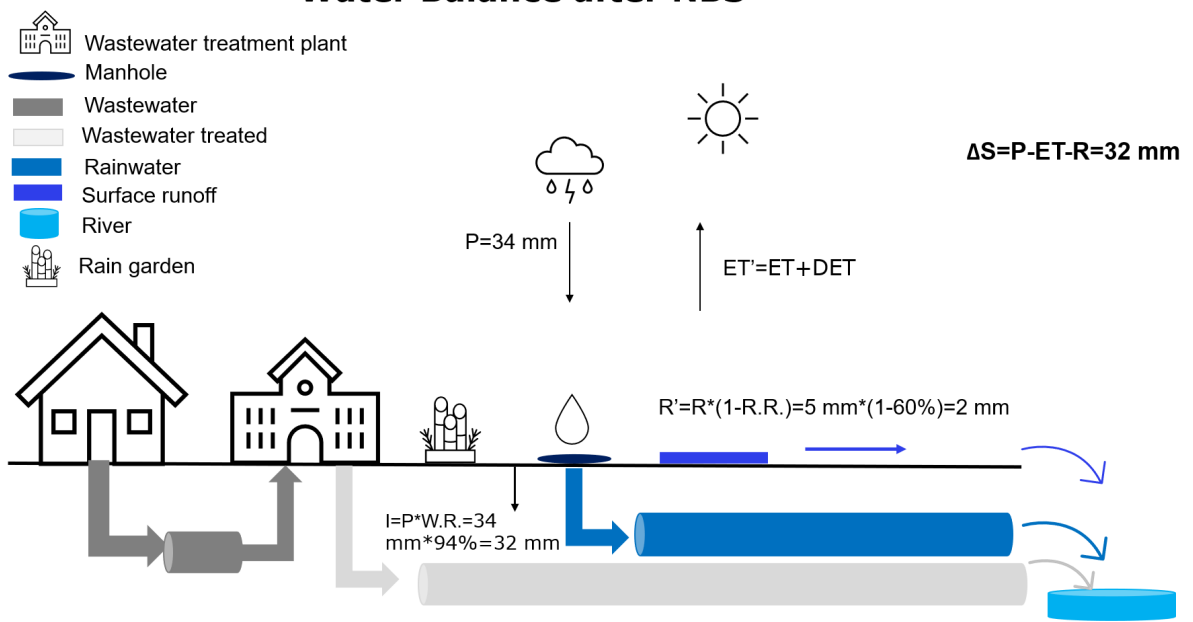


Figure 7.11: Water balance after implementing NBS (rain garden). P = precipitation; ET = evapotranspiration without rain garden; ET' = evapotranspiration with rain garden; DET = difference in evapotranspiration (ET' - ET); R = runoff; ΔS = water storage change; W.R. = water retention capacity (%); R.R. = runoff reduction (%); I = infiltration.

As shown in Figure 7.11, the addition of a rain garden on artificial surfaces leads to an increase in infiltration, which now reaches 32 mm. The rain garden has a water retention capacity of approximately 94%, resulting in a significantly reduced runoff of just 2 mm—a reduction of 3 mm compared to the condition before the rain garden was introduced.

Consequently, the water storage (ΔS) increases to 32 mm, calculated using Equation 7.1, compared to 29 mm in the scenario without NBS. Additionally, evapotranspiration increases by a small amount—denoted here as DET, which represents the difference in evapotranspiration before and after the rain garden implementation. However, as in the previous case, this increase is considered negligible for the purposes of this analysis.

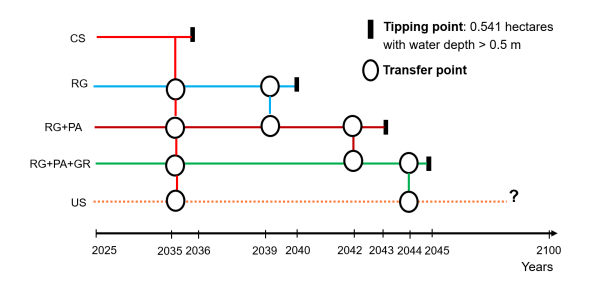
8 Discussion

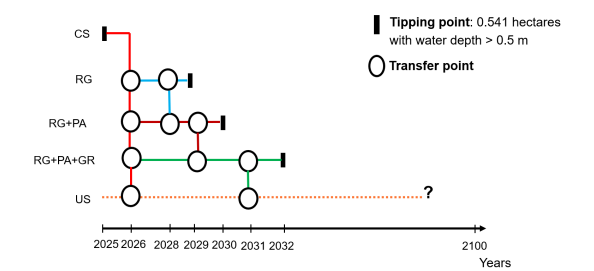
8.1 Unknown Scenario

As mentioned in Sections 7.2.1 and 7.3.1, the adoption of the most extended "safe" solution—rain garden (RG), porous asphalt (PA), and green roof (GR)—does not appear to provide long-term effectiveness (i.e., until 2100). For both RCP 4.5 and RCP 8.5, these Nature-Based Solutions (NBS) can be classified as short-term measures, as their maximum benefit is the delay of the tipping point only until 2045 in the case of RCP 8.5.

Therefore, even after adopting the green pathway, a new policy intervention—referred to as the "Unknown Scenario" (US)—must be implemented shortly before the tipping point. This is illustrated in the following figure.

As can be seen in the diagrams above, the transition to a new policy must occur before reaching the





(a) Adaptation Pathways Map for RCP 4.5 until 2100 including US (Unknown Scenario). RG = rain garden; PA = porous asphalt; GR = green roof.

(b) Adaptation Pathways Map for RCP 8.5 until 2100 including US (Unknown Scenario). RG = rain garden; PA = porous asphalt; GR = green roof.

Figure 8.1: Comparison of Adaptation Pathways Maps under RCP 4.5 and 8.5 scenarios including the need for the Unknown Scenario (US).

tipping point—set in 2044 for RCP 4.5 and 2031 for RCP 8.5. This new policy, currently labelled as *Unknown Scenario*, has not been thoroughly investigated due to time constraints in the computational phase. However, some hypothetical strategies can be proposed.

For instance, the Unknown Scenario could involve the addition of bioswales—which are not considered in the adaptive pathways due to time constraints—in Area 2 that is not occupied by rain gardens. If this proves insufficient, the coverage percentage of each existing NBS could be increased as much as physically and spatially feasible, also taking into account the municipality's willingness and capacity to invest. Other unexplored NBS types could also be included—such as vegetated grid pavers (classified as permeable pavement)—which offer high runoff reduction and could be installed on sidewalks or other surfaces currently categorized as "other paved."

Furthermore, it is important to note that these results are based on the application of NBS to only around 45% of the total catchment area, as mentioned in Section 6.2. Thus, the Unknown Scenario could also involve the extension of the NBS implementation to additional sub-areas of the catchment.

8.2 Cost

According to the land covered by each NBS applied in the three areas (as described in Section 6.2) and the cost values reported in Table 5.2, the total cost for each implemented NBS has been calculated and is reported below.

NBS	Land covered (ha)	Cost (million EUR)
Porous asphalt	10.38	10.43
Rain garden	11.13	0.15
Bioswale	16.59	12.12
Extensive green roof	9.81	10.75
Intensive green roof	7.12	19.52

Table 8.1: Land coverage and cost of each NBS option (in million EUR)

From the table above, rain gardens clearly emerge as the cheapest solution, followed by porous asphalt, bioswales, and green roofs. The combined cost of both extensive and intensive green roofs reaches approximately 30.27 million EUR. This confirms how the dynamic solution follows a cost-effectiveness approach: starting with the most economical option—rain gardens—and concluding with the most expensive—green roofs.

Considering the cost and performance together, green roofs demonstrate low cost-effectiveness: despite their high price, they only delay the tipping point by two years (as shown in Figures 7.3 and 7.7). On the other hand, rain gardens not only represent the most affordable intervention but also provide a delay of up to four years, highlighting their strong cost-effectiveness.

8.3 Trigger point

As mentioned in Section 4.1, the trigger point represents a crucial moment at which a policy—here identified with the implementation of Nature-Based Solutions (NBS)—should be activated. If missed, it may be too late to act effectively, especially considering the required time for planning, permitting, and constructing the interventions, commonly referred to as "lead time".

Typically, the trigger point can be interpreted as the last warning signal prompting the need to switch to a new policy due to the declining performance of the current one. However, in this context, defining the trigger point based on a specific threshold—such as the number of hectares exceeding 0.5 meters of water depth—is too complex, as the flood-related damages cannot be accurately identified or quantified. Consequently, the performance of the implemented solutions cannot be reliably assessed on this basis. Therefore, the trigger point is identified solely based on construction time. For the same reason, the adaptation signal—generally considered the first early warning of decreasing performance—is not taken into account in this analysis.

The figure below illustrates the conceptual relationship between lead time, transfer point, trigger point, and tipping point.

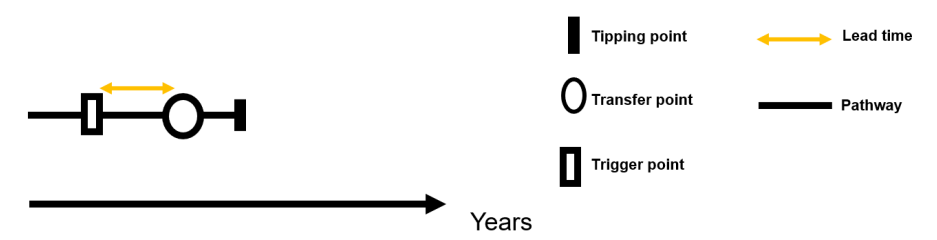


Figure 8.2: Conceptual scheme showing the relationship between lead time, transfer point, trigger point, and tipping point.

With regard to construction time, estimations based on internal data and expert experience from NIRAS (consultation 2025) suggest an average duration of 3 years for the implementation of rain gardens, and 2 years for porous asphalt.

The case of green roofs is considerably different: as discussed in Section 6.2, since green roofs are installed on private buildings, their implementation requires a broader municipal strategy. This may involve active citizen engagement and potentially economic incentives to encourage participation, making both planning and execution significantly more complex and time-consuming. Additionally, some intervention on the roof structure is usually required before installation. After these considerations, a construction time of 15 years is suggested, based on estimates provided by NIRAS (2025). These values are reported in the table below.

NBS	Construction Time (years)
Rain Garden	3
Porous Asphalt	2
Green Roof	15

Table 8.2: Estimated construction time for the implementation of different NBS.

Taking into account the construction time for each RCP scenario and focusing on the developed adaptation pathways, the trigger points for each path and RCP have been identified, as shown in the scheme below.

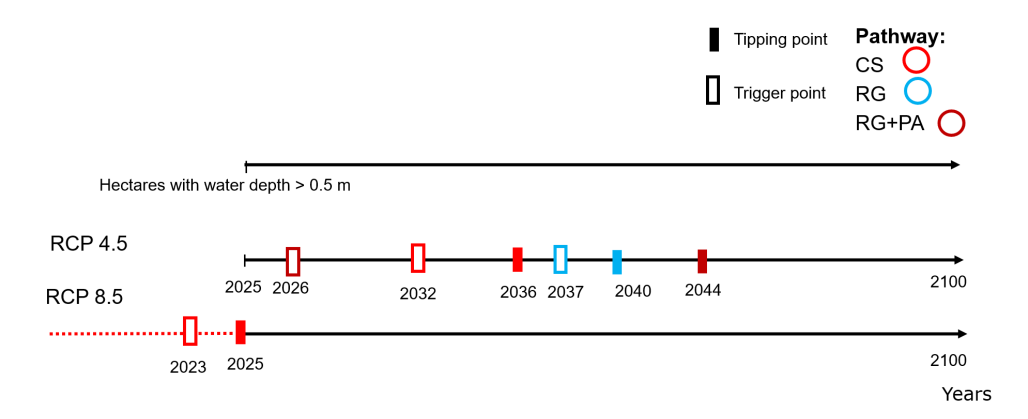


Figure 8.3: Timing of the trigger point associated with the increase in surface area within the catchment exceeding 0.5 m of water depth for each pathway under RCP 4.5 and RCP 8.5. Both the trigger point and the tipping point refer to surface thresholds within the catchment: the tipping point is defined as 0.541 hectares with water depth above 0.5 m. The analysis focuses on dynamic solutions applied starting from the current scenario, with the implementation year set one year before reaching the tipping point. RG = rain garden, PA = porous asphalt, GR = green roof, CS = current scenario.

As shown in the Figure above, focusing on RCP 4.5 and the dynamic adaptive strategy discussed in Section 7.2.1, the sequence of implementation (i.e., rain garden \rightarrow porous asphalt \rightarrow green roof) starts from the current scenario (represented in red). In order to adopt the first policy—rain gardens—in 2035, one year before the expected tipping point, a lead time of 3 years is required. Consequently, the trigger point for the current scenario is set in 2032. Once the rain garden strategy (blue pathway) is implemented, the adoption of the second measure—porous asphalt—in 2039 (one year before its tipping point in 2040) requires a two-year lead time, placing its corresponding trigger point in 2037.

These trigger points are linked to an increase in the area with water depth exceeding 0.5 m within the catchment. Notably, the trigger point identified for the current scenario, which enables the implementation of rain gardens, corresponds to a smaller flooded area compared to the trigger point that allows the adoption of the second policy (adding porous asphalt). The assessment for green roofs differs significantly. Given the long lead time of 15 years, this solution cannot be implemented dynamically because the required trigger point would have been in 2026. Since the tipping point for the current scenario is expected in 2036, the green roof strategy would only be viable if selected as the initial policy—making it incompatible with a dynamic response sequence. Moreover, considering its high cost and low cost-effectiveness, as explained later in Section 8.2, it does not align with the criterion of starting with the NBS options that offers the best cost-effectiveness. Therefore, it is not advisable to begin with green roofs.

The figure below presents the revised dynamic adaptive pathway, developed by integrating the identified trigger points for RCP 4.5 and excluding the pathways that include green roofs.

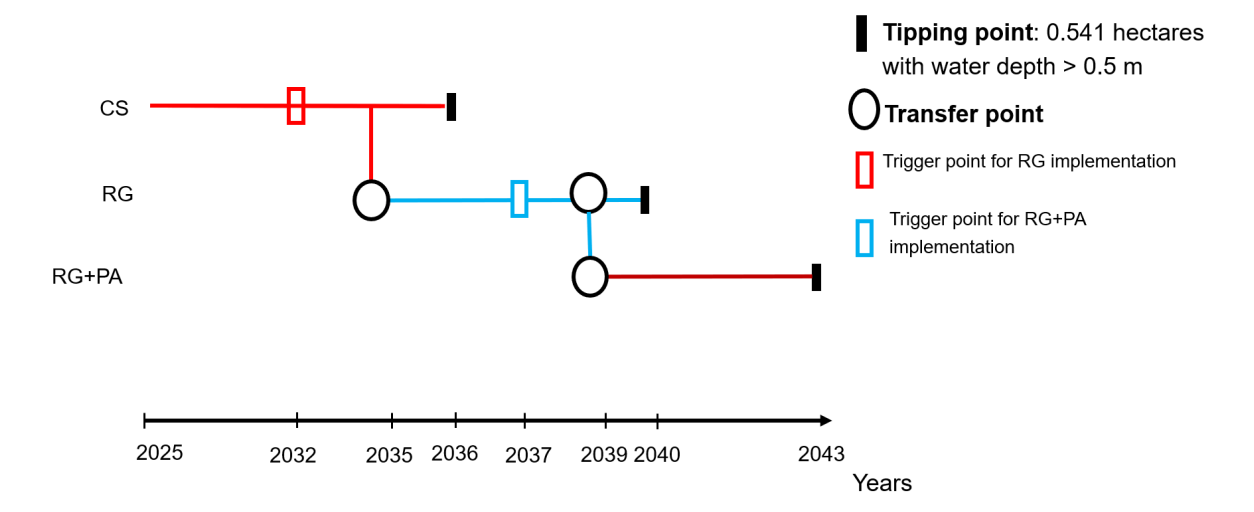


Figure 8.4: Revised dynamic adaptive solution for RCP 4.5, based on identified trigger points. RG = rain garden, PA = porous asphalt, CS = current situation.

In contrast, the assessment for RCP 8.5 is notably different. As shown in Figure 8.3, starting from the current situation, the first policy is scheduled to be implemented in 2026—one year after the tipping point, which is reached in 2025. Therefore, the corresponding trigger point for the implementation of rain garden should have occurred in 2023 (considering, making it already too late).

This implies that if the 3-year lead time for the implementation of rain garden is to be respected and the trigger point is established now (in 2025), the first policy could not be implemented before 2028. Given that the tipping point is reached in 2029, this solution becomes entirely unfeasible, as the second policy (porous asphalt) would need to be adopted in 2028—precisely when the rain garden (the first policy) is under implementation. Also, the implementation of porous asphalt alone as first policy is not applicable. Considering its 2-year lead time, it would be completed by 2027; however, a new policy would already need to be adopted in that same year, since—as shown in Figure 7.7—the tipping point is expected to be reached in 2028.

Until now, trigger points have only been identified for the dynamic solution that includes the first policy option—namely, the rain garden. However, combined strategies such as the rain garden with porous asphalt (RG + PA), or the full triple solution including green roofs (RG + PA + GR), can also be considered as initial policies. These combined options may provide longer-term effectiveness, as discussed in Section 7.2.1. The following scheme illustrates the trigger points associated with these combined solutions, assuming implementation is fixed in 2035 and the starting point is the current scenario.

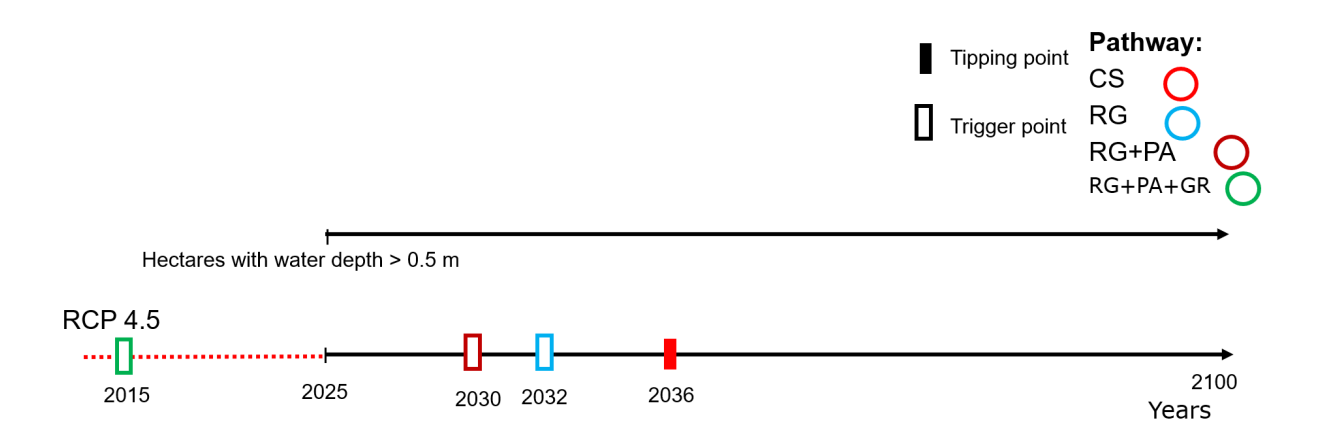


Figure 8.5: Timing of the trigger point associated with the increase in surface area within the catchment exceeding 0.5 m of water depth for each pathway under RCP 4.5. Both the trigger point and the tipping point refer to surface thresholds within the catchment: the tipping point is defined as 0.541 hectares with water depth above 0.5 m. Trigger points for the rain garden and combined solutions are identified under RCP 4.5, with implementation year set to 2035, starting from the current scenario. RG = rain garden, PA = porous asphalt, GR = green roof, CS = current scenario.

To prevent the tipping point expected under RCP 4.5—reached in 2036 if no action is taken—rain gardens can be implemented as the first policy. As explained earlier, the corresponding trigger point is set in 2032, considering a 3-year lead time, with implementation scheduled for 2035.

When considering the adoption of a combined policy of rain garden and porous asphalt, the lead time becomes 5 years in total (3 years for rain garden and 2 years for porous asphalt). Therefore, the trigger point (indicated in dark red) is identified as 2030, in order to meet the 2035 implementation target.

On the other hand, the triple solution (rain garden + porous asphalt + green roof) is not applicable as a first policy. Given the required lead times—3 years for rain garden, 2 years for porous asphalt, and 15 years for green roof—the total lead time would be 20 years, pushing the trigger point back to 2015, which is clearly no longer feasible.

The following figure presents the new Adaptation Pathways Map for RCP 4.5, based on the updated trigger points as explained above.

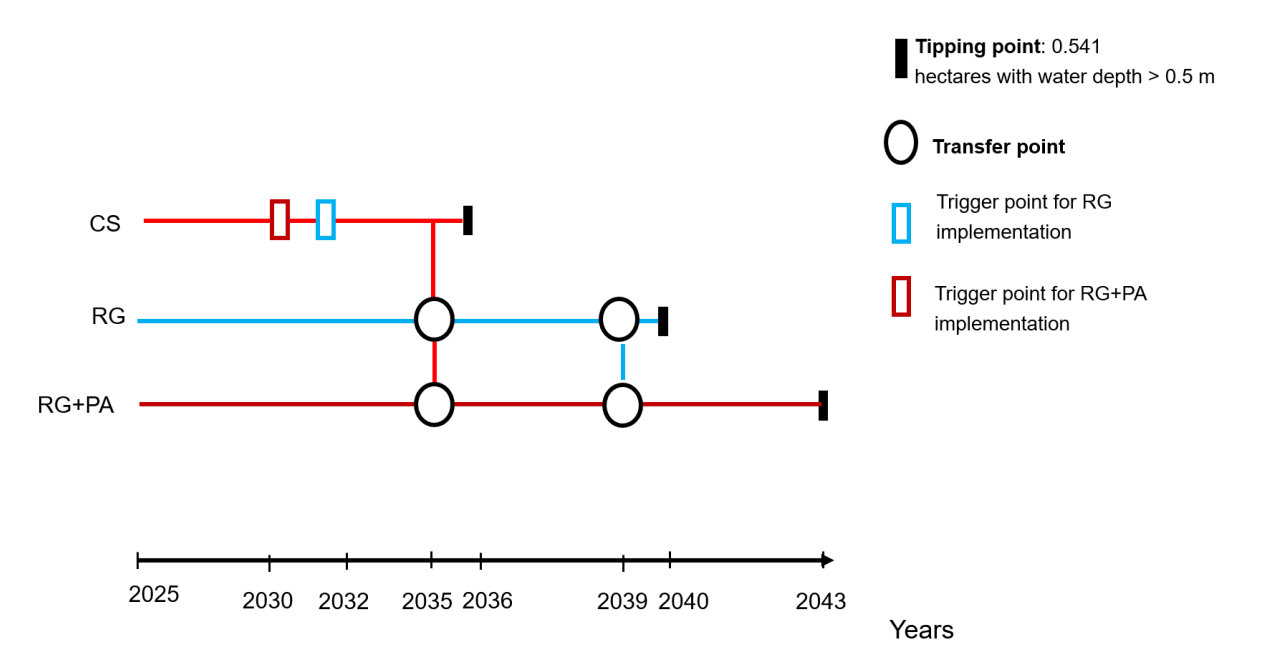


Figure 8.6: Updated Adaptation Pathways Map for RCP 4.5 including trigger points for rain garden and its combination with porous asphalt. RG = rain garden; PA = porous asphalt; CS = current scenario.

The figure below presents the refined Adaptation Pathways Map for RCP 4.5, which integrates all identified trigger points. It includes the trigger point related to the rain garden (RG) pathway shown in Figure 8.3, which enables the subsequent adoption of porous asphalt (PA), as well as the two distinct trigger points associated with the current scenario (CS), shown in Figure 8.6. The first CS-related trigger point (RG+PA) allows for the implementation of both measures, considering their respective lead times, while the second—occurring two years later, in 2032—permits a transition only to the blue pathway (RG).

Adaptation Pathways Map-RCP 4.5

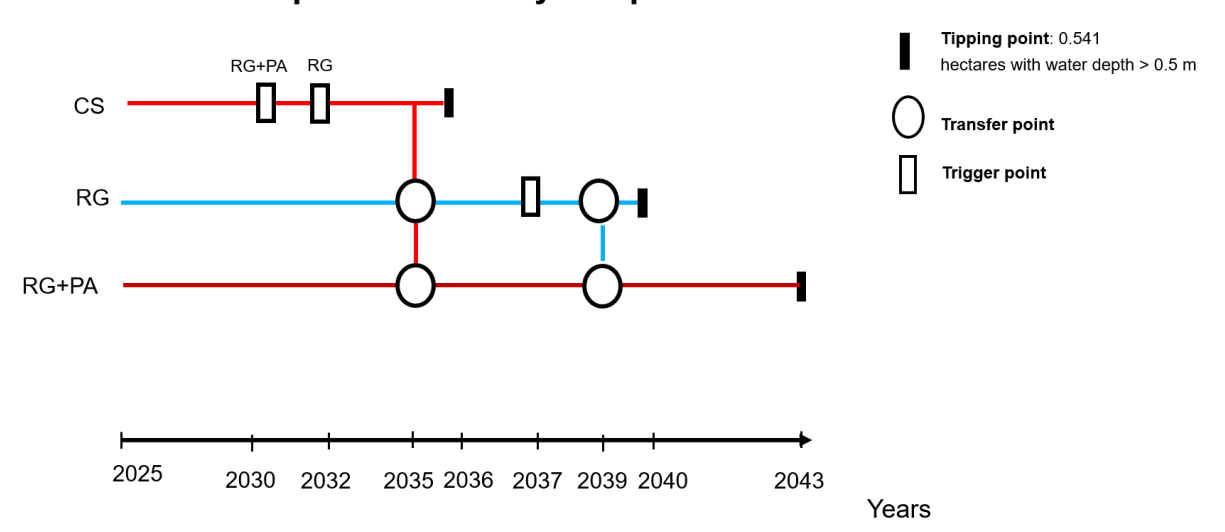


Figure 8.7: Refined Adaptation Pathways Map for RCP 4.5, including all trigger points for rain garden and its combination with porous asphalt. RG = rain garden; PA = porous asphalt; CS = current scenario. The current scenario encounters a first trigger point that allows the adoption of both the red and blue pathways, and a second trigger point that allows only the blue pathway.

8.4 Flooding Contribution Analysis

8.4.1 SCALGO Live Artificial Categories

Due to time constraints, it was not possible to conduct a detailed analysis of the specific SCALGO Live artificial surface categories—namely *paved road*, *other paved*, and *buildings*—to which the Nature-Based Solutions (NBS) were applied. However, based on the results obtained from their implementation, some general considerations can be made.

As discussed in Section 6.2, and considering both the spatial distribution of these categories across the three application areas and their respective impact on total catchment flooding, it is possible to assess that other paved surfaces (e.g., sidewalks, parking lots) contribute the most to flooding.

This conclusion is supported by the fact that other paved is by far the most extensive artificial surface in all three areas (with the exception of Area 3, where buildings slightly exceed it). Buildings generally represent a smaller portion (the difference ranges between 3% and 5%), while paved roads are the least present among the artificial surfaces, typically showing a 10%–20% difference compared to other paved. Moreover, although rain gardens—applied to other paved surfaces—have a lower runoff reduction efficiency (60%) compared to porous asphalt (75%), they demonstrate a higher influence in reducing flooding at the catchment scale. Furthermore, bioswales—also applied to other paved—have the lowest runoff reduction capacity among the NBS considered (50%), even lower than green roofs (52%) applied to buildings.

It is important to highlight that the flooding was evaluated in terms of total area with water depth greater than 0.5 meters. Therefore, combining the high spatial extent of other paved areas with the relatively modest efficiency of the NBS applied to them, it can be concluded that other paved surfaces are the main contributors to critical flooding conditions within the catchment.

8.4.2 Influence of the areas selected on the Tipping point

The tipping point, defined as a total flooded area of 0.541 hectares with water depth above 0.5 m, was analyzed considering the three application areas, which together represent only 45% of the entire catchment area. The flooded areas in each of these areas are detailed in Table 8.3, showing 0.066 ha for Area 1, 0.014 ha for Area 2, and 0.018 ha for Area 3. These values sum to 0.098 ha, which corresponds to approximately 18.1% of the total flooded area at the tipping point.

Area	Area with water depth above 0.5 m (ha)	% of Tipping Point
1	0.066	12.2%
2	0.014	2.6%
3	0.018	3.3%
Total	0.098	18.1%

Table 8.3: Flooded areas with water depth above 0.5 m for each application area compared to the total flooded area at the tipping point.

These results highlight the importance of extending the analysis to the entire catchment for a more comprehensive flood risk assessment, and suggest that intervention strategies, such as the implementation of Nature-Based Solutions (NBS), should also target the currently excluded areas to maximize flood mitigation effectiveness.

8.5 Limitations

8.5.1 Monitoring Phase

The DAPP approach, as mentioned in Section 4.1, includes a monitoring phase in which attention should be paid to the performance of each pathway during the time by identifying key signals. This ensures that the strategy can be periodically reviewed and revised in light of new data. However, since this thesis is developed from a preliminary project-phase perspective, and due to the complexity of identifying such signals—such as the adaptation signal discussed in Section 8.3, which gives an early indication of how the strategy is performing—this monitoring phase has not been investigated.

8.5.2 Uncertainties and Vulnerabilities

As mentioned in Section 5.1.4, in addition to climate change, other relevant sources of uncertainty include land use changes and legislative developments in the catchment area that may arise during the project implementation phase.

Due to time constraints, these factors were not addressed in this thesis. However, it would be valuable to investigate how NBS might perform under such evolving conditions. For instance, the municipality could decide to build on areas where NBS have been implemented, reducing the green space available for these solutions. This could both increase flood risk and limit the area in which NBS can be applied, potentially reducing their effectiveness.

Incorporating these additional dimensions of uncertainty into future analyses would provide a more comprehensive understanding of the resilience and adaptability of NBS in real-world planning scenarios.

Additionally, in Section 5.1.3, elevated groundwater levels are considered vulnerabilities for the catchment. It would be interesting to analyze the correlation between flooding and groundwater levels in this thesis; however, due to time constraints, this was not possible.

8.5.3 SCALGO Live

Adopting SCALGO Live for flood analysis entails several limitations that should be acknowledged. First of all, SCALGO Live does not account for the temporal dynamics of flooding, as it does not include any reference to time or duration of the rainfall events. Consequently, it only provides a static representation of water accumulation and flow paths, limiting its ability to simulate the full hydrological response of the catchment over time.

Furthermore, for the sake of computational speed and simplicity, the tool does not consider the specific size, placement, or design details of the implemented Nature-Based Solutions (NBS); it only reflects their overall effect on surface runoff reduction based on the area and type of intervention applied. To simulate the impact of NBS within SCALGO Live, the Curve Number (CN) method was used, adjusting the land surface classification to reduce runoff generation accordingly. While this method provides a quick estimation of NBS effectiveness, it does not capture the full complexity of hydraulic and hydrological interactions, especially in urban contexts.

Additionally, when the "Flooded Area" analysis option is activated in SCALGO Live, all water bodies present in the terrain model—such as rivers, lakes, and ponds—are included in the calculation of total flooded area. This may lead to an overestimation of the effective flooding caused by rainfall events, as permanent water bodies are counted together with temporary flood zones.

8.5.4 Curve Number for NBS

In this thesis, the Curve Number (CN) method was applied iteratively to estimate the CN values for each NBS, as explained in Section 6.3. However, this approach presents important limitations that affect the accuracy and applicability of the results. As a baseline for estimating the CN values associated with the implemented NBS, the reference CN for artificial sewered surfaces provided by SCALGO Live was adopted. This reference value is based on standard scenarios involving rainfall events of up to 200 mm. By contrast, the precipitation scenarios considered in this study have a maximum precipitation of only 42 mm. This discrepancy may introduce inaccuracies, as CN values are sensitive to rainfall depth and may not adequately capture runoff behavior under lower-intensity events, thus reducing the representativeness of CN-based assumptions.

8.5.5 Spatial extent of NBS application

A key limitation of this thesis is that Nature-Based Solutions (NBS) were applied only to three selected areas, covering less than half of the catchment. As a result, the effectiveness of NBS across the entire catchment could not be fully assessed. Nevertheless, despite this restricted spatial implementation, the results demonstrate a significant positive impact on flood mitigation. This underscores the strong potential of NBS to reduce flooding even when applied on a limited scale. Therefore, a broader application across the entire catchment would not only enhance flood mitigation outcomes but also allow for a more comprehensive and accurate evaluation of the long-term adaptation potential.

8.5.6 Data on NBS

One important limitation concerns the availability and consistency of data on Nature-Based Solutions (NBS). A critical issue was the difficulty in finding a single, comprehensive source that includes all necessary information, such as runoff reduction rates, since some studies provide parameters for certain NBS but omit others. Moreover, the data provided for NBS, including runoff reduction rates, often do not specify details about the type or configuration of the NBS (e.g., size, design) or the specific rainfall event characteristics on which they are based. Additionally, the terminology used is often broad and inconsistent; for example, some sources categorize porous asphalt as a type of permeable pavement, while others do not.

Another crucial point relates to the Curve Number (CN) values needed for modeling the implementation of NBS. Since there are currently no established CN values specifically for NBS, an iterative method was developed in this thesis to estimate them.

These gaps highlight the need for further research on NBS and the adoption of standardized terminology to improve clarity and comparability across studies.

9 Conclusion

As stated in Section 1.3, the aim of this thesis was to assess whether Nature-Based Solutions (NBS) can offer flexible responses to climate-related water challenges—specifically flooding—and how the DAPP approach can support their implementation by addressing the uncertainties associated with climate change. The results show that NBS, when integrated within a DAPP framework, can provide flexibility under the RCP 4.5 scenario, which foresees an increase in precipitation over the period 2025–2100.

Under this scenario, NBS demonstrate the capacity to dynamically adapt to increasing precipitation and delay the tipping point until 2045. This result highlights how, due to their flexibility, NBS may also form part of the so-called "Unknown Scenario" introduced in Section 8.1, by either increasing their coverage or combining them with new, yet-to-be-identified policy measures.

However, in a dynamic implementation perspective, green roofs fall outside the feasible adaptation options, due to their long construction time. Given their relatively low effectiveness and high implementation cost, they should be further improved if they are to be considered for addressing extreme rainfall events.

On the other hand, results show that NBS—despite the flexibility offered by the DAPP approach—cannot effectively address the challenges posed by the RCP 8.5 scenario. The rapid progression toward the tipping point in this scenario does not allow sufficient time for implementation, especially considering the construction lead times of each NBS. This confirms that RCP 8.5 is a scenario that should be avoided through all possible mitigation efforts; otherwise, as demonstrated, it will be too late to effectively adapt. It would be valuable to extend this analysis to a broader spatial scale, such as the entire catchment area. As discussed in Section 8.4.2, the current implementation of NBS covered only a limited portion of the catchment—representing approximately 18% of the total influence on the tipping point—yet still managed to delay it by up to 9 years under RCP 4.5 (7 years if green roofs are excluded). Therefore, a more extensive application across the remaining areas of the catchment could be expected to produce even greater benefits.

Additionally, as highlighted in Section 4.3.2, NBS address multiple urban and environmental challenges beyond flooding, including water scarcity, biodiversity loss, and the urban heat island effect. Future research should further investigate the co-benefits of NBS in these areas, which would strengthen the evidence for their effectiveness—not only in terms of versatility, but also as a means to enhance the resilience of urban systems. By integrating natural processes into city infrastructure, NBS help build urban environments that are more adaptive, robust, and capable of withstanding future climate extremes.

In this context, the Dynamic Adaptive Policy Pathways (DAPP) approach emerges as a fundamental planning framework. Its integration into future urban and environmental planning is essential, and municipalities should consider adopting it to enhance adaptability and flexibility in addressing the challenges posed by climate change. By incorporating DAPP into city planning, decision-makers can develop strategies that are flexible, forward-looking, and responsive to deep uncertainty. This approach helps prepare for unpredictable future conditions in the best possible way—avoiding the need to restart planning from scratch and reducing implementation time by having prior knowledge of the various lead times required for new solutions. By considering these lead times alongside identified trigger points, planners can act promptly and effectively. The DAPP framework thus enables continuous adaptation rather than reactive

crisis management, ensuring that measures such as Nature-Based Solutions (NBS) can evolve dynamically over time, maintaining their effectiveness as climate and urban conditions change.

In conclusion, this thesis confirms that Nature-Based Solutions (NBS) offer resilient and effective responses for cities facing climate change, while also delivering valuable co-benefits. NBS represent one of the most promising pathways for tackling climate change, both in terms of mitigation and adaptation. By offering a multifunctional, integrated approach—rather than separate, resource-intensive solutions for each issue—NBS can reduce implementation time and resource use, while generating synergistic benefits across a wide range of climate-related challenges. Coupled with the Dynamic Adaptive Policy Pathways (DAPP) framework, they become not only practical solutions but integral components of an adaptive planning mindset necessary for building resilient and future-proof cities.

A Background and Analysis

A.1 Harrestrup Å - Capacity Plan

A.1.1 Solutions

A variety of solution types are planned for implementation within the project to effectively achieve the previously outlined objectives.

Green floodplains

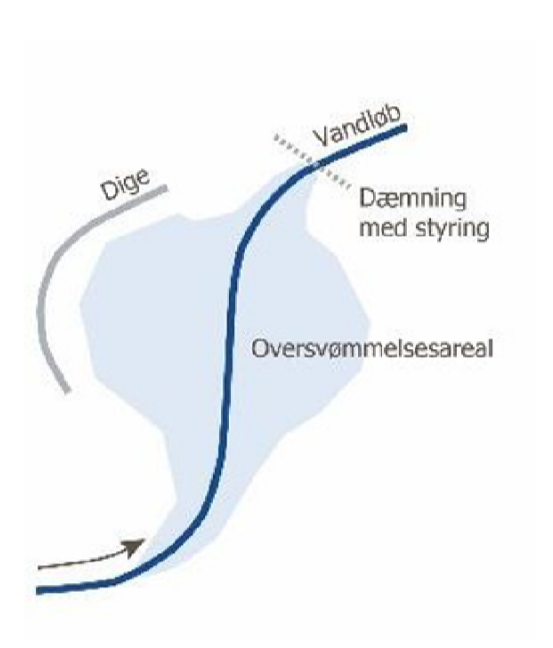


Figure A.1: Schematic representation of an online floodplain solution [28]

The creation of floodplains, which serve to temporarily store excess water during periods of heavy rainfall, is one such solution. By exploiting the natural topography of the river valley, it is possible to create a considerable storage volume, delaying water runoff until the downstream system once again has sufficient capacity. These basins are integrated directly into the watercourse-known as online basins-allowing optimal use of space and flow dynamics [28].

However, the development of floodplains results in raising the critical water level in adjacent areas, with the risk of causing flooding upstream. For this reason, their development should generally follow a top-down approach, starting upstream and proceeding downstream [28].

The proper functioning of these systems depends on centralized, risk-based management that can control when to retain or release water[28].

As shown in the Figure A.1, the floodplains (Oversvømmelsesareal) are located adjacent to the main course of the river (Vandløb) and are regulated by a dam with a control system (Dæmning med styring). A dike (Dige) helps contain and direct the water, ensuring that it returns to the river once levels drop[28].

Cloudburst pools

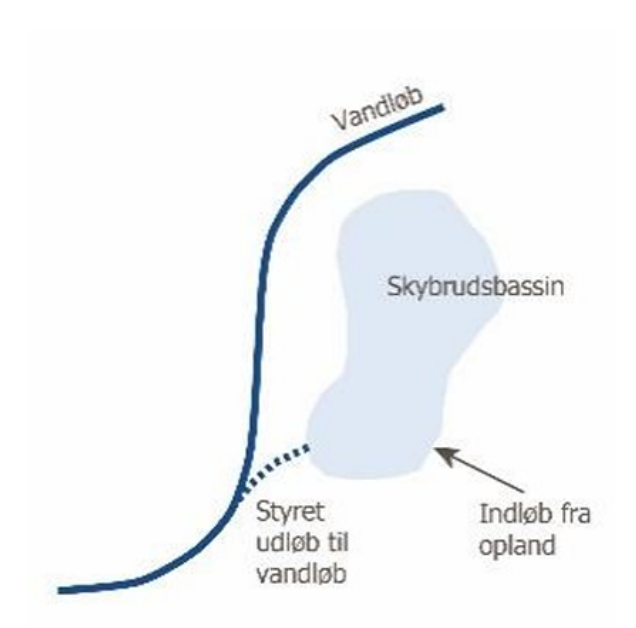


Figure A.2: Schematic representation of clouburst pools [28]

Another fundamental solution is represented by the intensive storm basins (cloudburst basins), which are preferably constructed in areas where the morphology of the terrain allows for maximum volume with minimal excavation. Unlike flood plains, these basins are located far from the main river course and do not raise the critical water level, making it possible to build them independently of other sub-projects[28]. Their function is to temporarily retain rainwater from the catchment area and gradually release it into the river through a controlled discharge. Here again, the adoption of a centralized risk management system is essential to effectively regulate the inflows and outflows [28].

As illustrated in the image above, the catchment (Skybrudsbassin) receives water via an inlet from the drainage basin (Indløb fra opland) and then releases it into the river (Vandløb) via a regulated discharge (Styret udløb til vandløb)[28].

Widening the river

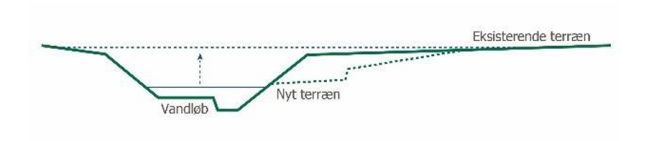


Figure A.3: Schematic representation of river widening(from [28].

The figure above shows a solution for widening the watercourse by changing the cross-section into a multilevel profile. The new terrain (dashed line) creates an additional space for water storage in the event of a flood, while maintaining a natural channel for ordinary flow (referred to as the "Vandløb") in the middle. This approach allows both lamination and rapid runoff during heavy rain events. Stabilising the banks with gentle slopes contributes to structural stability and improved water quality. Since widening increases the runoff capacity, the intervention must be carried out progressively from the point of

discharge upstream [28].

Removing bottlenecks



Figure A.4: Bridge over a river where the underpass must be widened to prevent bottlenecks during heavy rainfall [28].

Another solution is to adapt the crossing infrastructure, such as roads and railways. When the watercourse is widened, existing subways must also be widened to prevent them from becoming bottlenecks. Since widening subways increases the flow capacity, especially during extreme rainfall, both the river and the subways must be widened [28].

Centralised risk based management of reservoirs and pumps

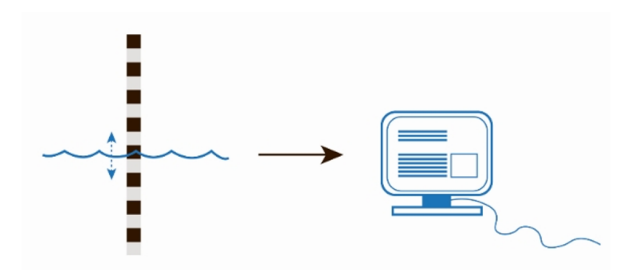


Figure A.5: Schematic figure showing water level monitoring and transmission to a central system for flood and storage management [28].

Rainfall events vary widely: sometimes heavy rainfall occurs in the upper part of the river basin, other times in the lower part. Consequently, the use of storage capacity must be optimized for each specific scenario through a centralized management system based on rainfall and flood forecasts. Coordinated management of this kind is crucial for the development of floodplains and reservoirs for heavy rainfall [28].

Sequence plan The table in Figure A.6 and the map in Figure A.7 show the priority subprojects included in the Capacity Plan, designed to handle a 100-year return time event within the next 30 years.

Expected period	Id	Sub-projects to be initiated	Municipality	Price, DKK million
	10.07	Control and monitoring	Common	20
	1.01	OV Harrestrup Mose	Albertslund	29
	1.02	OV Haraldsminde	Ballerup	15
	1.14	OV Vigerslevparken 2	Copenhagen/Hvidovre	72
	1.15	OV Vigerslevparken 3	Copenhagen/Hvidovre	See ID1.14
	1.16	OV Kagsmosen	Herlev/Rødovre/Copenhagen	25
	1.17	OV Kagsåparkens Rainwater project	Gladsaxe	160
	2.01	SB Haraldsminde	Ballerup	35
	6.03.1	L VU Vigerslevparken 2	Copenhagen, Denmark	See ID1.14
Period 1	6.04.1 VU Vigerslevparken 3		Copenhagen, Denmark	See ID1.14
	6.05	VU Kagsåen	Herlev/Gladsaxe/Copenhagen	4
2019-23	5.11	FH Underpass Vestkærs Alle	Copenhagen	5
	5.14	FH Cross tube Hvidovre Storcenter	Copenhagen, Denmark	5
	5.15	FH Intersection pipe Holmelundsvej	Copenhagen, Denmark	5
	5.17	FH Intersection pipe Sønderkær	Copenhagen, Denmark	5
	5.18	FH Sydkærsvej underpass	Copenhagen, Denmark	4
	5.21	FH Underpass Herlev Hovedgade	Herlev/Copenhagen	13
	5.22	FH Sonatevej underpass	Herley/Copenhagen	4
	5.23	FH S-train underpass	Herlev/Copenhagen	12
		•		
	5.24	FH Kagsmosestien underpass	Herlev/Copenhagen	4
	1.06	OV Ejbyvænge/Skovlunde Nature Park	Ballerup/Glostrup	26
	1.07	OV Ejby Mose	Glostrup	22
Period 2	1.09	OV Mileparken	Ballerup/Herlev	7
Period 2	1.10	OV Hanevad basin	Ballerup/Herlev	13
	1.18	OV Grøndalsparken	Copenhagen/Frederiksberg	79
2024-28	2.02	SB Skelgrøften/Ballerup Fritidslandskab	Ballerup	23
	2.05	SB Skovlunde Nature Park	Ballerup	12
	2.06	SB Ejby Mose	Glostrup	29
	2.07	SB Mileparken	Ballerup/Herlev	17
	1.03	OV Ballerup Leisure landscape	Ballerup	30
	1.04.2	2 OV Vestskoven	Albertslund	19
Period 3	1.11	OV Krogebjergparken/Stadionparken	Rødovre/Copenhagen	24
	1.12.1	L OV Damhusengen	Copenhagen, Denmark	64
2029-33	1.12.2	2 OV Damhussøen	Copenhagen, Denmark	30
	1.13	OV Vigerslevparken 1	Copenhagen, Denmark	55
	2.09	SB Stavnsbjerg Allé	Gladsaxe	12
	6.02	VU Vigerslev 1	Copenhagen, Denmark	See ID1.13
	1.04.1	L OV Bymoserenden	Ballerup/Glostrup	20
	1.05	OV Skovlunde Nature Park	Ballerup/Glostrup	11
Period 4	1.08	OV Sømosen	Ballerup/Herlev	33
	2.04	SB Bymosin ends	Albertslund/Ballerup	23
2034-38	6.01	VU New underpass along Roskildevej	Copenhagen, Denmark	114
_55- 56		VU Brink protection Ndr. Ringvej to Vestvoldens Voldgrav	Rødovre	10
	6.06			
	6.07	VU Brink protection Vestvoldens Voldgrav to Slotsherrensvej	Rødovre/Copenhagen	10

Figure A.6: Sequencing plan for the implementation of sub-projects across four periods. Abbreviations: OV = online floodplains, SB = cloudburst basins, VU = river widenings, FH = removal of bottlenecks [28].

The overall sequence of the plan is divided into four distinct phases. This subdivision is based on several factors, including the geographical distribution of projects, the need to maintain a constant investment rate to ensure stable rates, existing hydraulic interdependencies, the status of projects in progress or in the planning stage, and the priority given to subprojects that are already mature and ready for implementation [28].

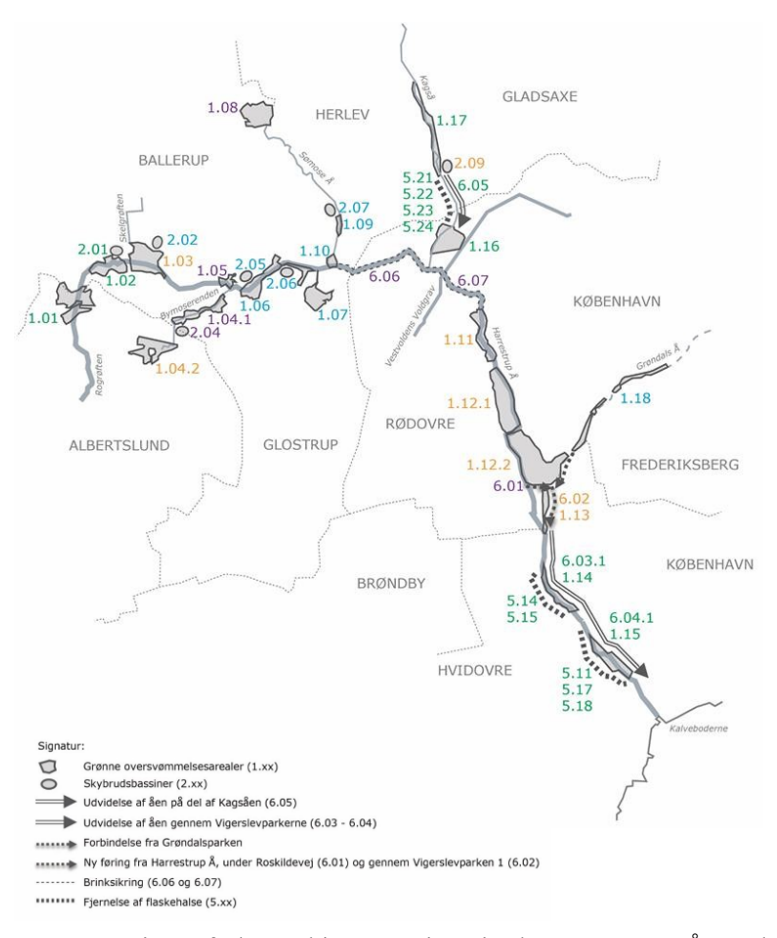


Figure A.7: Overview of planned interventions in the Harrestrup Å catchment area [28].

The map shows different types of measures related to stormwater and watercourse management in the Copenhagen area. These include: green overflow areas (Grønne oversvømmelsesarealer - 1.xx), heavy rainfall basins (Skybrudsbassiner - 2.xx), watercourse widening along part of the Kagsåen (Udvidelse af åen på del af Kagsåen - 6.05), watercourse widening through Vigerslev parks (Udvidelse af åen gennem Vigerslevparkerne - 6.03-6. 04), connection from the Grøndal park (Forbindelse fra Grøndalsparken), new route of Harrestrup Å under Roskildevej and through Vigerslevparken 1 (Ny føring fra Harrestrup Å, under Roskildevej og gennem Vigerslevparken 1 - 6. 01, 6.02), reinforcement of embankments (Brinksikring - 6.06 and 6.07), and removal of bottlenecks (Fjernelse af flaskehalse - 5.xx)[28]. Figure A.8 shows the current status of the project.



Figure A.8: Map of the Capacity Plan showing the status of the subprojects distributed within the catchment area. Light green = under development, green = under construction, dark green = completed [52].

Most of the subprojects are still in the planning phase, with only one completed and the others under construction.

The plan is expected to be completed by 2038.[28].

The cost of the project is estimated at around DKK 1.1 billion (about 148 million euros), spread over a period of 20 years [28]

A.1.2 Subproject-Sømose Å

.

Lowland restoration and biodiversity



Figure A.9: Green connections and lowland regions in nearby municipalities[29].

The Municipality of Ballerup has identified the Sømose Å watercourse as an area of ecological importance, useful for developing connections between existing natural areas, particularly between Hanevad basin and Sømosen. For this reason, the area is included in the Green Map of Denmark. These ecological connections (Økologisk forbindelse) are part of a national strategy to strengthen biodiversity and land-

scape continuity between different municipalities [29].

In addition to its ecological function, the area is classified as a low-lying area (Lavbundsareal), i.e. a natural area characterized by wet soils [29].

According to the map legend, this includes both areas that have already been set aside (low altitude area, adopted) and those that could be restored (low altitude area that could be restored). It is possible to restore natural water levels and create wetlands and meadows in these areas. This is useful for nature restoration, adaptation to climate change and water quality improvement[29].

Between Hanevad basin and Mileparken, the area has continuous green areas that include meadows and wooded areas. Further upstream, in the direction of Sømosen, the ecological corridor retains its structure due to the vegetation between the buildings, helping to form a coherent green connection in the urban area as well [29].

These designations represent an integrated and forward-looking approach to environmental planning, combining ecological connectivity with the restoration of natural hydrological conditions [29].

Bibliography

- [1] State of Green. *The cloudburst that changed Copenhagen and urban water management*. https://stateofgreen.com/en/news/the-cloudburst-that-changed-copenhagen-and-urban-water-management/. Accessed: 2025-06-14. 2023.
- [2] David Zetland. *Bad management and dry taps in Turin*. https://one-handed-economist.com/?p=4146, accessed June 14, 2025. 2023.
- [3] Ginevra Chelli. "Po river drought in 2022 was the worst of the last two centuries". In: *Nature* (2023).
- [4] S. I. Seneviratne et al. "Weather and Climate Extreme Events in a Changing Climate". In: *Climate Change 2021: The Physical Science Basis. Contribution of Working Group I to the Sixth Assessment Report of the Intergovernmental Panel on Climate Change.* Ed. by V. Masson-Delmotte et al. Cambridge University Press, 2021. DOI: 10.1017/9781009157896.013.
- [5] V. Masson-Delmotte et al., eds. *Climate Change 2021: The Physical Science Basis*. Contribution of Working Group I to the Sixth Assessment Report of the Intergovernmental Panel on Climate Change. Cambridge, United Kingdom and New York, NY, USA: Cambridge University Press, 2021. URL: https://www.ipcc.ch/report/ar6/wg1/.
- [6] IPCC. "Sections". In: Climate Change 2023: Synthesis Report. Contribution of Working Groups I, II and III to the Sixth Assessment Report of the Intergovernmental Panel on Climate Change. Ed. by Core Writing Team, H. Lee, and J. Romero. Geneva, Switzerland: IPCC, 2023. DOI: 10. 59327/IPCC/AR6-9789291691647.
- [7] European Environment Agency. What is the difference between adaptation and mitigation? https: //www.eea.europa.eu/en/about/contact-us/faqs/what-is-the-difference-between-adaptation-and-mitigation, accessed 14 June 2025. 2024.
- [8] State of Green, Hanne Kjær Jørgensen, and Ulrik Hindsberger. *Nature-Based Solutions: Using rainwater as a resource to create resilient and liveable cities*. 2021.
- [9] Deutsches Klimarechenzentrum (DKRZ). *The SSP Scenarios*. https://www.dkrz.de/en/communication/climate-simulations/cmip6-en/the-ssp-scenarios.
- [10] Haasnoot et al. *Dynamic adaptive policy pathways: a method for crafting robust decisions for a deeply uncertain world.* 2013. URL: https://doi.org/10.1016/j.gloenvcha.2012.12.006.
- [11] Vincent A. W. J. Marchau et al., eds. *Decision Making under Deep Uncertainty: From Theory to Practice*. Springer Nature Switzerland AG, 2019. DOI: 10.1007/978-3-030-05252-2.
- [12] B. C. O'Neill et al. "The roads ahead: Narratives for shared socioeconomic pathways describing world futures in the 21st century". In: *Global Environmental Change* 42 (2017), pp. 169–180. URL: https://doi.org/10.1016/j.gloenvcha.2015.01.004.
- [13] G. Langergraber et al. "Implementing nature-based solutions for creating a resourceful circular city". In: *Blue-Green Systems* (2020). DOI: https://iwaponline.com/bgs/article/2/1/173/72527/Implementing-nature-based-solutions-for-creating-a.

- [14] State of Green. *Urban Water Management: Creating climate* resilient cities. 2022. DOI: https://stateofgreen.com/en/publications/.
- [15] Network Nature. *Naure Based solutions*. DOI: https://networknature.eu/networknature/nature-based-solutions.
- [16] Amber Terton. *Building a Climate-Resilient City: Urban Ecosystems*. Tech. rep. Prairie Climate Centre, 2017. URL: https://www.prairieclimatecentre.ca.
- [17] Paul Taylor et al. *Nature-based Solutions for Water*. A collaborative publication by UN Environment-DHI Centre, UN Environment, and IUCN. Based on the UN World Water Development Report 2018. 2018.
- [18] Harald K. Gupta, ed. *Encyclopedia of Natural Hazards*. Encyclopedia of Earth Sciences Series. Springer, 2013. DOI: 10.1007/978-1-4020-4399-4.
- [19] Anna Biasin et al. *Nature-Based Solutions Modeling and Cost-Benefit Analysis to Face Climate Change Risks in an Urban Area: The Case of Turin (Italy)*. 2022. URL: https://doi.org/10.3390/land12020280.
- [20] Joseph Battiata et al. "The Runoff Reduction Method". In: *Journal of Contemporary Water Research & Education* 146 (2010). DOI: 10.1111/j.1936-704X.2010.00388.x. URL: http://dx.doi.org/10.1111/j.1936-704X.2010.00388.x.
- [21] *Sankt Kjeld's Square Bryggervangen*. DOI: https://www.sla.dk/cases/sankt-kjelds-square-and-bryggervangen/.
- [22] SCALGO. Whitepaper: Rainfall-Runoff Model for Flash Flood Map in SCALGO Live Denmark v.1.03. Tech. rep. SCALGO, 2023. URL: https://scalgo.com/uploads/documents/Whitepaper-RRM.pdf.
- [23] U.S. Army Corps of Engineers. *Curve Number*. https://www.hec.usace.army.mil/confluence/rasdocs/ras1dtechref/6.5/overview-of-optional-capabilities/modeling-precipitation-and-infiltration/curve-number. 2023.
- [24] Soil Conservation Service. *Urban Hydrology for Small Watersheds, Technical Release 55 (TR-55)*. Tech. rep. Revised edition. Washington, D.C.: U.S. Department of Agriculture, Soil Conservation Service, 1986.
- [25] Statistics Denmark. *Land Use accounts*. 2021. URL: https://www.dst.dk/en/Statistik/emner/miljoe-og-energi/areal/arealopgoerelser.
- [26] HOFOR. Områdeplan Herlev 2024, vandforsyning og spildevand. 2023. URL: https://www.hofor.dk/.
- [27] Herlev Municipality. *Grønne Byrum, Erhvervsområdet ved Marielundvej.* 2008. URL: https://herlev.dk/.
- [28] Harrestrup Å Kapacitetsprojektet. *Kapacitetsplan*. 2019. URL: https://harrestrupaa.dk/wp-content/uploads/2019/07/kapacitetsplan-2018.
- [29] NIRAS. Sømose Å, Ideoplæg/anlægsprogram. 2023. URL: https://www.niras.com/.

- [30] Y. Indriatmoko, R. D. Hapsari, and P. B. Santosa. *The infiltration capacity and rate at the grass, building yard and green open space areas of Universitas Gadjah Mada campus*. 2022. URL: https://iopscience.iop.org/article/10.1088/1755-1315/959/1/012046/meta.
- [31] Danish Meteorological Institute. *Data i Klimaatlas*. DMI. 2024. URL: https://www.dmi.dk/klima-atlas/data-i-klimaatlas.
- [32] D. Macdonald et al. "Groundwater flooding within an urbanised flood plain". In: *Flood risk management* (2011). URL: https://onlinelibrary.wiley.com/doi/epdf/10.1111/j.1753-318X.2011. 01127.x.
- [33] Sara Birkmose Andersen / Mads Harder Danielsen / Thor San- ner Adessa. *Harrestrup Å Ka-pacitetsplan, Fase 4 03 Projektkatalog 2018*. 2019. URL: https://harrestrupaa.dk/wp-content/uploads/2019/07/projektkatalog-03-2018.pdf.
- [34] SDFI Stefan Krebs Lange-Willman. *DVR90: Dansk Vertikal Reference 1990*. 2023. URL: https://sdfi.dk/Media/638325244589317645/010-DVR90.pdf.
- [35] NOVAFOS. Sømose Å-Dispositionsforslag. 2024.
- [36] UNaLab Project. *Nature-Based Solutions Technical Handbook. Part II*. 2019. URL: https://unalab.eu/system/files/2020-02/unalab-technical-handbook-nature-based-solutions2020-02-17.pdf.
- [37] Margit Koiv-Vainik et al. *Urban stormwater retention capacity of nature-based solutions at dif- ferent climatic conditions*. 2022. DOI: https://doi.org/10.1016/j.nbsj.2022.100038.
- [38] Bernd Eisenberg et al. UNaLab Urban Nature Labs. Layout: Jesús Martínez Zárate, Vishal Kumar, Alfred Palacios.
 Funded by the European Union's Horizon 2020 research and innovation programme under Grant Agreement No. 730052 (SCC-2-2016-2017: Smart Cities and Communities Nature-based Solutions). Stuttgart, Oct. 2022.
- [39] Rui Guo et al. "A Tool for Water Balance Analysis of Bioretention Cells". In: *Journal of Sustainable Water in the Built Environment* (2020). DOI: 10.1061/JSWBAY.0000920.
- [40] Capitol Region Watershed District. *Monitoring & Research*. URL: https://www.capitolregionwd.org/monitoring-research/.
- [41] Kaitlin Elfstrum. *All About Green Roofs*. 2022. URL: https://psci.princeton.edu/tips/2022/7/8/all-about-green-roofs.
- [42] ODU Green Roof. *Why an Intensive Green Roof.* 2025. URL: https://odu-green-roof.com/why-an-intensive-green-roof/.
- [43] Minnesota Pollution Control Agency. *Terminology for Swales*. Ultima modifica: 31 gennaio 2023. Minnesota Stormwater Manual. 2025.
- [44] Toke Emil Panduro, Doan Nainggolan, and Marianne Zandersen. *Cost-effectiveness analysis of urban nature-based solutions: A stepwise ranking approach*. 2024. DOI: 1https://doi.org/10.1016/j.nbsj.2024.100186.
- [45] Pioneer Valley Planning Commissio. *Porous asphalt*. DOI: https://www.pvpc.org/sites/default/files/files/PVPC-Porous%20Asphalt.pdf.

- [46] Danish Meteorological Institute. *Introduction to Klimaatlas*. Accessed: 2025-07-04. DMI Danish Meteorological Institute. 2024. URL: https://www.dmi.dk/klima-atlas/introduction-to-klimaatlas.
- [47] Technical University of Denmark. *Urban Drainage and Stormwater Management Course Notes*. https://www.env.dtu.dk/. Lecture material, formula for Climate Factor (CF) retrieved from course slides. 2023.
- [48] Peter Steen Mikkelsen, Morten Borup, and Karsten Arnbjerg-Nielsen. *SVK Paper No. 26: Design Storms for Urban Drainage*. Technical Report 26. Based on the method of Kiefer and Chu (1957). Copenhagen, Denmark: Spildevandskomiteen (Danish Wastewater Committee), 1999.
- [49] IDA. *Regionalregnraekke version 4.0.* https://ida.dk/media/3008/regionalregnraekke_ver_4_ 0.xls. Excel spreadsheet used to estimate rainfall values in the catchment area. 2020.
- [50] G. P. Smith. Expert Opinion: Stability of People, Vehicles and Buildings in Flood Water. Tech. rep. WRL Report 2015/11. Water Research Laboratory (WRL), University of New South Wales, 2015. URL: https://www.unsw.edu.au/content/dam/pdfs/engineering/civil-environmental/water-research-laboratory/publications/WRL-TR2015-11-Expert-Opinion-Stability-of-people-vehicles-and-buildings-in-flood-water.pdf.
- [51] Lilin Zhang et al. "The divergence of energy- and water-balance evapotranspiration estimates in humid regions". In: (2023). ISSN: 0022-1694. DOI: 10.1016/j.jhydrol.2023.129971.
- [52] Harrestrup Å-Kapacitetsplan. *Harrestrup Å Danmarks største projekt om klimatilpasning*. 2025. URL: https://harrestrupaa.dk/.